USE OF VIRAL FUSION PROTEINS TO DEVELOP TUMOUR - ANTIGEN PRESENTING CELL HYBRIDS LEADING TO CROSS-PRESENTATION OF TUMOUR ANTIGENS

Mahnoor

Wolfson College, University of Oxford

A thesis submitted for the degree of Doctor of Philosophy to the Department of Oncology, University of Oxford, Michaelmas Term 2024

Supervisors: Professor Len Seymour, Professor Kerry Fisher

Impact of COVID-19 on this Thesis

I began my DPhil in October 2019, and was only beginning to explore the project in depth when the COVID-19 pandemic hit and I lost access to the laboratory from March 2020 to August 2020. On return to the department, the access was extremely limited and there was no option of shadowing or learning new techniques which was crucial in the early stages of my PhD, and severely impacted the progress of my project. The limited and tightly regulated access continued well until June 2021, making it hard to make rigorous progress.

I was also severely impacted by the lockdowns and resulting challenges, causing severe mental health issues, long-term clinical depression which led to the University registering me as 'mentally disabled' and periods of hospitalization. All of this further slowed down my project work. Nevertheless, I persisted and pushed through despite extreme health challenges and continued to work on the project with the aim of completing the DPhil.

My financial situation means I can no longer afford to study and must now submit my thesis. I am conscious that the volume of experimental work is limited, nevertheless I hope the quality of work and significance of the findings are commensurate with the standards expected of a D,Phil.

Abstract

Cancer immunotherapy is a growing area of research with a great deal of potential yet to be explored. The development of therapeutic cancer vaccines is a technically challenging but highly desirable approach within the realm of immunotherapy. One approach, involving formation of tumour and dendritic cell fusions to improve immune presentation of tumour antigens has previously been shown to have a positive effect on tumour regression with no reported cytotoxicity. Building on this, the generation of tumour and antigen-presenting cell (APC) hybrids is a desirable approach that can be achieved through the use of viral fusion proteins. Viral fusion proteins have successfully been used in cancer research and shown to have good anti-tumour effects by creating giant syncytia which render the tumour cells unstable and lead to their killing. In this thesis we build on this knowledge by using the viral fusion proteins to generate heterocellular fusions of tumour cells with PBMC-derived macrophages. We used and compared the GALV fusion protein and the reovirus FAST p14 for generating tumour-APC hybrids. Our results show that both of these proteins are capable of leading to formation of heterocellular syncytia between cancer cells and APCs.

To further increase the interaction between cancer cells and APCs, and the subsequent activation of the APCs, a CD40 super agonist antibody was incorporated onto the tumour cell membrane. We have confirmed the feasibility of this approach by results showing a significant increase in heterocellular syncytia formation when p14 was used in combination with the anti-CD40. Intriguingly the same outcome was not achieved when using GALV in combination with the anti-CD40.

Leading from the successful formation of heterocellular syncytia, the potential of augmenting antigen cross-presentation from these cell hybrids was explored. The cellular fusions provide a strategy to increase presentation of tumour-associated antigens (TAA) in order to stimulate

an adaptive immune response. We used a model system of NY-ESO-expressing human HLA-A2 – DLD-1 colorectal cancer cells in combination with PBMC derived HLA-A2+ macrophages to allow direct measurement of cross presentation of tumour antigens. The readout for successful cross-presentation were nFAT reporter Jurkat cells recognizing HLA-A2-restricted presentation of NY-ESO. Our results show that the fusion between cancer cells and APCs leads to enhanced antigen cross-presentation which can be augmented by the presence of the antiCD40 superagonist. Although we exemplified this using NY-ESO, the strategy should apply to all cancer antigens simultaneously, and can be regarded as an 'antigen-agnostic' approach. These results provide an exciting direction for exploring the development of cancer vaccines based on the expression of fusion proteins and a CD40 super agonist from cancer cells to generate tumour-APC hybrids, leading to an antigen-agnostic anti-tumor immune response.

Declaration of Authentication

The work presented in this thesis was carried out under the supervision of Professor Leonard Seymour, at the Department of Oncology, Medical Sciences Division, University of Oxford. The work is entirely my own, with any contribution by others duly acknowledged. The work submitted here does not form part of another thesis in this or any other university.

Mahnoor

October 2024

Acknowledgements

All praise to the Almighty Allah for giving me the opportunity to begin and go through with a PhD program at Oxford of all places.

I am extremely grateful to Professor Leonard Seymour for all his support and guidance, and for his readiness to discuss science, his availability whenever needed for guidance, and the never-ending encouragement to do better. I would also like to thank Professor Kerry Fisher for his invaluable insights, experimental ideas, and his unique way of looking at things, which make complex science seem simple and more interesting. Thanks to Dr. Ahmet Hazini for being a crucial part of my PhD project and for all his help with experimental designs and setting up complex assays. Additionally, I am grateful to the Oxford Graduate Scholarship which enabled me to take my place at Oxford and fund my studies, the Oxford Pakistan Program for additional financial support, and my college; Wolfson (Dan Alred in particular) for all the support and pastoral care throughout my degree.

I could not have been any luckier than to work with all of Len's Angels, they have all been a delight to work with and the highlight of my PhD. I have so much to say for each one of them for all the support, scientific guidance, endless food, and much needed hugs on days of despair, of which there were many. My heartfelt gratitude to Amanda Chapman, Dr. Hena Khalique, Dr. Janet Lei, Dr. Egon Jacobas, Dr. Weiheng Su, Dr. Arthur Dyer, Dr. Richard Baugh (my voice of reason on my days of struggles and self-doubt), Dr. Sally Frost, Dr. Peter Wan, Emma Page, Kate Friesen, Fernando Gimenez Gallardo, and Henry Brigden. People from other labs; Alex Stephens, Yuqian Ou, Sichen, Constantinos, Amy Keating, Purusotha Thambiayah, and Rathi, who have all always been a source of support in what has been a crazy journey. And of course, my most favourite angel, Dr. Flurin Caviezel, this journey would not have been even remotely the same without you.

I would also like to extend thanks to my housemates, who have been my source of sanity and support. Getting home after a day of disappointments in the lab would have been even more shattering without them. To Danielle Watkis, Joshua Devaraj, Abdullah Riaz, and Yashvir Jugduth, thank you for being there, for listening to my laments, laughing at my lame jokes, and always being up for sharing a meal, and making the house more of a home.

I cannot do to forget my friends from back home, who have been an integral part of not only my PhD but also a number of transitions through life. Many thanks to Ammara Arif, Fatima Shahid, Fatima Tahir, Mariya Farooq, and Saria Bhutta from my life in Islamabad, who stayed with me beyond that journey. My people from the home town and my friends for the longest, thank you Yusra Riaz and Kiran Riaz for always keeping in touch, for all the love and prayers. Ushba Sohail, thank you for always being available to hear me out, and Rida Tariq, for supporting me in ways I could never even bring myself to properly thank you for, you have been an absolute hug of a person.

A great deal of thanks to the countless people who joined my PhD journey as sources of support, whether it be in the form of financial aids and bursaries, or supporting my mental health. I would particularly like to thank my uncle Amin Bilal for becoming an integral part of the final year of my PhD, and for supporting me endlessly. To my dearest friend Neha Gazder, who was not only a friend, but also my unpaid therapist, and always there for me in times of need. To my dearest and closest friend, Ahmed Usman, whose support has been extremely valuable always, and specially as I got immersed in thesis writing and winding up the PhD. From cheering me on to taking care of everything I could possibly need, it has been an absolute privilege to have such support.

Lastly, but most importantly, huge thanks to my parents and siblings for putting their trust in me, for allowing me to live life on my own terms and for always being there with prayers and words of support. I could not have come this far without support and prayers from my family.

Table of Contents

List of Figures

List of Tables

List of Abbreviations

ACT – Adoptive Cell Therapy

ADCC - Antibody-Dependent Cellular Cytotoxicity

APC – Antigen Presenting Cells

CAR – Chimeric Antigen Receptor

CD – Cluster of Differentiation

CFSE - Carboxyfluorescein succinimidyl ester

CMV – Cytomegalovirus

DC – Dendritic Cell

DMEM - Dulbecco's modified Eagle's medium

DMSO - Dimethyl sulfoxide

EpCAM - Epithelial cell adhesion molecule

EDTA - Ethylenediaminetetraacetic acid

FAST – Fusion Associated Small Transmembrane

FDA - Food and Drug Authority

FMG – Fusogenic Membrane Glycoprotein

GALV – Gibbon Ape Leukemia Virus

GFP – Green Fluorescent Protein

GM-CSF - granulocyte-macrophage colony-stimulating factor

HLA – Human Leukocyte Antigen

HSV – Herpes simplex virus

HS – Human Serum

IFN – Interferon

LPS – Lipopolysaccharide

MHC - Major histocompatibility complex

PBS – Phosphate Buffer Saline

PCR – Polymerase Chain Reaction

PEG – Polyethylene Glycol

RFP – Red Fluorescent Protein

TAA – Tumour Associated Antigen

TIL – Tumour Infiltrating Lymphocyte

TM - Transmembrane

TME – Tumour Microenvironment

v/v – volume by volume

1. Introduction

1.1 General Introduction

Cancer is among the leading causes of deaths worldwide. In the past decade, the incidence of cancer has increased from 14.1 million global new cases (Jacques Ferlay et al., 2015) to now roughly 20 million cases annually. As of 2022, the mortality burden owing to cancer was 9.7 million per year (Bray et al., 2024). The most frequently detected types of cancer include breast, lung, colorectal, and prostate cancer, with lung cancer being the global leader in terms of incidence and mortality (Jaques Ferlay et al., 2013; Kratzer et al., 2024). The high disease burden and mortality rates associated with cancer have led to a significant amount of research being dedicated to identifying potential cancer treatment.

Historically, cancer chemotherapy was focused around selective toxicity to proliferating cells, often influenced by the tissue of cancer origin (Zugazagoitia et al., 2016). However, with the passage of time, it became evident that treatments based on mutation-related molecular targets would be a better approach. The knowledge of molecular targets for different cancer types and the overlap between cancers of varying origins that could potentially be treated through focusing on the same molecular pathway or gene has brought the field of cancer therapy forward by huge leaps and bounds. However, the complexity of cancer makes the road to high potency treatments quite bumpy.

The traditional approaches to cancer treatment include surgery, radiotherapy and chemotherapy, generally to treat localised, locally disseminated and metastatic cancers, respectively. Each of these approaches has been used extensively and research in each of these areas continues due to the high disease burden and complexity of cancer. Radiotherapy and chemotherapy are each a two-edged sword, however, with side-effects to normal cells that hold

the potential of creating unwanted toxicities (Torrisi et al., 2011). For example, radiotherapy holds the potential of leading to an increase in the risk of more cancers later on (Cheng et al., 2017). Similarly, chemotherapy can be toxic to normal cells thereby leading to a general decline in health and well-being, along with other complications, such as damaging organs (Rix et al., 2020). The barriers to treatment also include the complex nature of cancers and the way that they interact with the immune system. The understanding of links between cancer and the immune system has led to efforts being directed towards understanding how tumours escape immune surveillance, and the possible targets to overcoming this escape. To this end, cancer immunotherapy has emerged as a promising approach that can sometimes lead to durable anti-tumour responses (Oliveira & Wu, 2023).

1.2 Immunotherapy

Cancer immunotherapy entails the use of strategies to boost the immune system to fight against cancer. The overall idea of immunotherapy is embedded in the immune cycle whereby cancer antigens are presented through the antigen presenting cells, used for priming and activating the T cells, and lead to antigen-specific killing of the cancer cells by the T cells. Under normal circumstances, the immune cycle runs continuously and effectively defends the body against the onset of cancer. However, immune cycling can change dramatically through the phenomenon of immune evasion, which is a characteristic of malignant tumours (Holmström et al., 2020). From basic principles it might be expected that the presence of T cells infiltrating tumours (tumour infiltrating lymphocytes (TILs) might suggest a better prognosis, however advanced tumours have acquired several mechanisms for evading the immune system, including but not limited to poor immunogenicity of the tumour antigen, defective T-cell trafficking, immunosuppressive APCs, and exhausted or impaired T cells. Through any of these

mechanisms, once the immune cycle has been interrupted or impaired, cancer then begins to establish and progress.

Several different types of immunotherapy approaches are used for cancer treatment, including immune checkpoint blockers, monoclonal antibodies recognising tumour surface antigens, immune modulators, T-cell therapies, and therapeutic vaccines. The immune checkpoints exist to regulate uncontrolled T cell mediated killing of cells due to strong immune responses. The blocking of these checkpoints, generally using monoclonal antibodies, restores T cell activity and allows the killing of cancer cells (Yan, Zhang, Zuo, Qian, & Liu, 2020). Monoclonal antibodies recognizing tumour surface antigens can either inhibit signaling pathways or activate ADCC (antibody-dependent cellular cytotoxicity) for targeted killing of cancer cells. T-cell therapy includes the adoptive cell-transfer therapy, where autologous T cells are modulated to target and kill cancer cells. A sub-type of T-cell therapy is the CAR-T (Chimeric Antigen Receptor- T) cell therapy, where the T cells are developed in-vitro such that they can recognize specific antigens on cancer cells, thereby becoming able to target and kill them (Narayan et al., 2022).

The use of oncolytic viruses is also a growing area of research that, although fundamental to gene therapy approaches, also has benefits in activating the immune system against cancer. Oncolytic viruses engineered to specifically replicate within tumour cells cause not only lysis of the cancer cells but can lead to activation of the immune system as a result (Marchini, Daeffler, Pozdeev, Angelova, & Rommelaere, 2019; Ramakrishna et al., 2009). Moreover, the use of different immune-modulating markers or proteins expressed through oncolytic viruses leads to activation of the immune system against cancer cells. The first Food and Drug Authority (FDA) approved oncolytic virus was T-VEC (talimogene laherparepvec), which is a modified herpesvirus expressing granulocyte-macrophage colony-stimulating factor (GM-CSF), and used for the treatment of advanced melanoma (Harrington et al., 2015). The

successful use of oncolytic viruses for cancer treatment in vitro, and in pre-clinical and clinical trials has led to an increasing amount of research efforts being dedicated to this particular type of cancer treatment.

1.2.1 Cancer Vaccines

Vaccines for the treatment and prevention of diseases are among the most incredible advances in the field of medical sciences. The concept of vaccines in the case of cancers is mainly embedded in the therapeutic advantage of such an approach. Cancer vaccines are aimed at priming and potentially enhancing the patient's immunity towards tumours. Among the different strategies involved in developing cancer vaccines, there is the use of the autologous cancer vaccines, developed from using the patient's own tumour cells, the use of autologous dendritic cell (DC) vaccines have also been explored by loading the DCs with the tumour associated antigens, TAA peptide-based vaccines, and DNA or RNA based vaccines that encode the TAAs.

The key behind successful vaccination against cancer lies in delivering a sizeable amount of antigens to DCs for activation of DCs, and subsequent induction of the T cells to mediate both, cytotoxic T cell based killing of tumours, and T helper cell activation for release of cytokines (Charles et al., 2020). The successful activation of the T cells leads to infiltration of the T cells into the tumour microenvironment, followed by generation and maintenance of an anti-tumour response. Such a response can be achieved by any of the cancer vaccine approaches discussed above. The use of autologous DCs loaded with tumour specific antigens has been explored to a certain extent previously. This approach is different from traditional vaccines in that the antigens are not purified or prepared selectively, rather they are sourced from the TME using the antigens released by dying cancer cells (Barbuto et al., 2004).

Among the DC vaccines, the use of DC-tumour hybrids has potential for generating a good immune response against cancer. This approach has proved better as compared to the use of co-culture of tumour cells and DCs (Phan et al., 2003). The fusion between DCs and tumour has been carried out using polyethylene glycol (PEG) or electrofusion in preclinical trials. The electrofusion approach for cell fusion is favoured over the use of PEG due to a better level of standardization that has been achieved in this approach when used *in vitro* and *in vivo* (Barbuto *et al., 2004)*. There is also evidence of this approach being successful in certain clinical trials. In the case of renal carcinoma, the use of autologous cancer cells from patients fused with DCs from healthy donors led to a certain level of immunity gained against tumour antigens. Although the results in this case were not overtly successful, the lack of any adverse reaction to this approach make the DC-tumour hybrids a desirable cancer vaccine approach for further investigation (Märten et al., 2003).

Evidences of DC-tumour hybrids leading to activation of immune responses in metastatic cancers (Neves et al., 2005) have increased the interest in this particular type of cancer vaccine. The use of fused cancer cells and APCs being an approach having the potential of enhancing anti-tumour immunity points towards the need to explore ways to create stable fusion between the two cells types. From a clinical perspective, achieving this in the patients is critical and one possible approach could be the delivery of fusion proteins to cancer cells with the aim of making them interact with the APCs present in the TME. Since viral fusion proteins have already successfully been explored as a measure of achieving tumour killing, combining that approach with methods for recruiting APCs into the fusing cells can potentially help create a cancer vaccine that elicits a pronounced immune response.

1.3 Viral Fusion Proteins

Fusion proteins are a common factor among the enveloped viruses for merging the viral membrane with the host cell-membrane to initiate internalization as the key step for establishing infection. The fusion of the virus with the host cell is most commonly achieved through the help of one or multiple viral glycoproteins, termed as fusogenic membrane glycoproteins (FMGs). The fusion proteins (FMGs) interact with the host cell membrane receptors and co-receptors and initiate the fusion process depending on their size, structure, and specific interacting pathways. Along with enabling virus entry into the host cell, fusion proteins are also useful for the virus life cycle in that they can induce cell to cell fusion and enable viral spread across cells more easily, thereby potentially increasing the virulence(De Leeuw, Koch, Hartog, Ravenshorst, & Peeters, 2005). Cell to cell fusion caused by viral fusion proteins leads to the production of giant multi-nucleated cells or syncytia, which eventually render the host cells non-viable.

Another class of viral fusion proteins include the fusion associated small transmembrane proteins (FAST), such that are found in the Reovirus. The FAST proteins are not associated with the entry of the virus into the cells, as the reoviruses are non-enveloped. The role of the FAST proteins has specifically been implicated in cell to cell fusion and viral spread (Brown et al., 2009).

The dual properties of the FMGs (enabling cell entry and viral spread) and FAST proteins (just enabling viral spread) make them both interesting candidates for inducing syncytia mediated death of cancer cells. Additionally, the field of oncolytic virotherapy stands to potentially explore the idea of enhancing the spread of viruses within tumours through arming them with fusion proteins.

1.3.1 GALV

The Gibbon Ape Leukemia Virus (GALV) fusion protein is an FMG, used by the virus for entry into the host cell and its subsequent spread from cell to cell. The GALV FMG is an 847 amino acid long protein, depending on the cellular receptor Pit-1 for interactions and cell entry, thereby making the virus entry and syncytia formation receptor-dependent (Lauring, Anderson, & Overbaugh, 2001).

Structure of the GALV protein

The structure of the GALV fusion protein is made up of three domains, the soluble unit (SU), the transmembrane domain (TM) and the fusion peptide (known as the R-peptide, which is a 16-amino acid peptide at the C-terminal of the fusion protein. The R-peptide is cleaved off through proteolytic cleavage during the viral life cycle and this enhances syncytia formation. The soluble unit binds to the cell surface Pit-1 receptor which is essential for inducing virus-to-cell or cell-to-cell fusion (Fielding et al., 2000). Figure 1.1 shows an overview of the structure of GALV fusion protein.

Various studies have used the GALV fusion protein encoded in an oncolytic virus to enhance viral spread within tumours and associated expression of any encoded therapeutic proteins. The use of fusogenic proteins in oncolytic viruses gives them the advantage of viral spread through syncytia as tumour cells begin fusing together following expression of the fusion protein. Moreover, the spread of virus through syncytia ensures less release of mature virions into the systemic circulation (Guedan et al., 2012). Additionally, it is likely that the fusion of tumour cells together leads to the death of multiple cells through single virions as more and more cells are pulled together into a giant cell or syncytium.

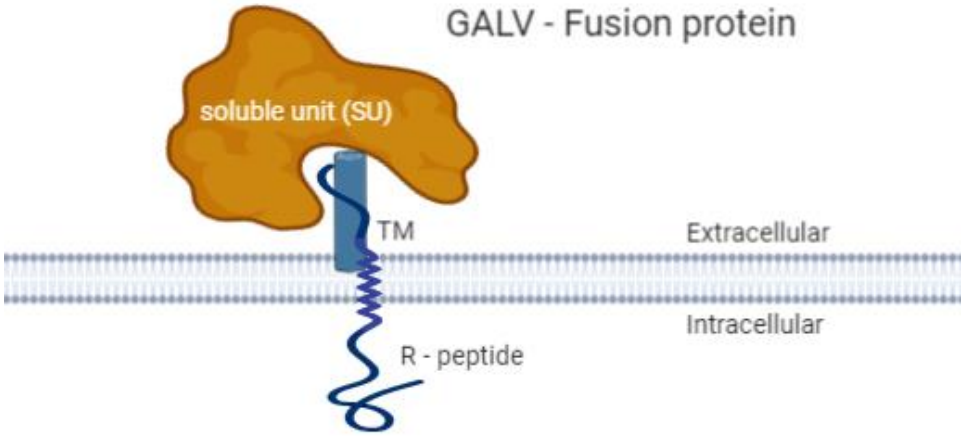

Figure 1.1: The structure of the GALV fusion protein. The fusion protein consists of an extracellular soluble subunit that interacts with the Pit-1 receptor on neighbouring cells, a region of transmembrane domains that imbed in the cell membrane, and an intracellular R-peptide that has to be cleaved off for during the viral life cycle for the fusion protein to be active.

GALV in cancer therapy

The GALV FMG has been extensively explored in the context of improving the efficacy of anti-tumour response. A number of studies using oncolytic viruses for cancer therapy have used GALV for improving the spread of the oncolytic virus. The expression of the GALV FMG in an oncolytic adenovirus (ICOVIR 16) was successful in significant cell death in several different cell lines as well as tumour killing in mice models having melanoma or pancreatic cancer. Within the *in vivo* models, ICOVIR 16 also showed a greater spread of the oncolytic virus within the tumour as compared to ICOVIR 15 (oncolytic adenovirus without the GALV FMG) (Guedan et al., 2012). The inclusion of GALV into the genome of an oncolytic herpes simplex virus 1 (HSV-1) has also been successful in achieving a high anti-tumour response when used in lung carcinoma xenograft mice (Zhu, Yang, Fu, & Jiang, 2014). There are a number of other similar studies showing the effectiveness of GALV in improving the efficacy of different oncolytic viruses.

1.3.2 FAST protein

The fusion-associated small transmembrane (FAST) protein encoded by reovirus is an unconventional fusion protein in that it is not among the structural proteins of the virus and is not essential for entry of virus in the cell. Among the different species within the family *Reoviradae*, only a few include the syncytium formation property. The *Mammalian orthoreovirus* and (MRV) and the *Piscine orthoreovirus* (PRV) which infects fish are both non-fusogenic. On the other hand, *the Reptilian orthoreovirus* (RRV), *Avian orthoreovirus* and the *Nelson Bay orthoreovirus* (NBV) are known to be fusogenic reoviruses. The additional (syncytia forming) protein has although not been found to be essential for virus replication, it is documented to aid the non-enveloped viruses in cell to cell spread due to syncytia formation (Duncan *et al.,* 1996). Theoretically, it is estimated that the fusogenic protein helps the reovirus establish local infection, followed by apoptotic cell death leading to the outburst of progeny virus causing systemic infection (Brown *et al.,* 2009). This theory has further been tested and proved to be true through subsequent studies. During the course of reovirus infection, syncytia have been found to maintain and regulate metabolic activities thereby providing a localized environment for the replication of virus. The rupture of syncytia once they become very large releases the viruses into the neighbouring environment, leading to dissemination of the infection (Duncan & Sullivan, 1998; Salsman *et al.,* 2005).

Structure of FAST proteins

Unlike the conventional fusion proteins which are part of the structural proteins of enveloped viruses, the FAST protein of reoviruses do not attach to specific receptors. The cell to cell contact is dependent upon the adherens junctions in cell membranes. Since the ectodomain of the FAST proteins is insufficient to span the length of cellular membranes, they localize the

adherens junction to bring cells closer and trigger a remodelling in the actin structure, resulting in fusion of cells (Helming & Gordon, 2009). The three distinct FAST proteins that have been so far been identified among the reoviruses include the p14 found in reptilian reovirus, p10 in the avian reovirus and p15 of the Nelson Bay reovirus. The naming of the proteins is based on their predicted molecular weights. All three FAST proteins are unrelated to each other in terms of sequence identity but have high resemblance in terms of their structures. Figure 1.2 shows an overview of two different FAST proteins

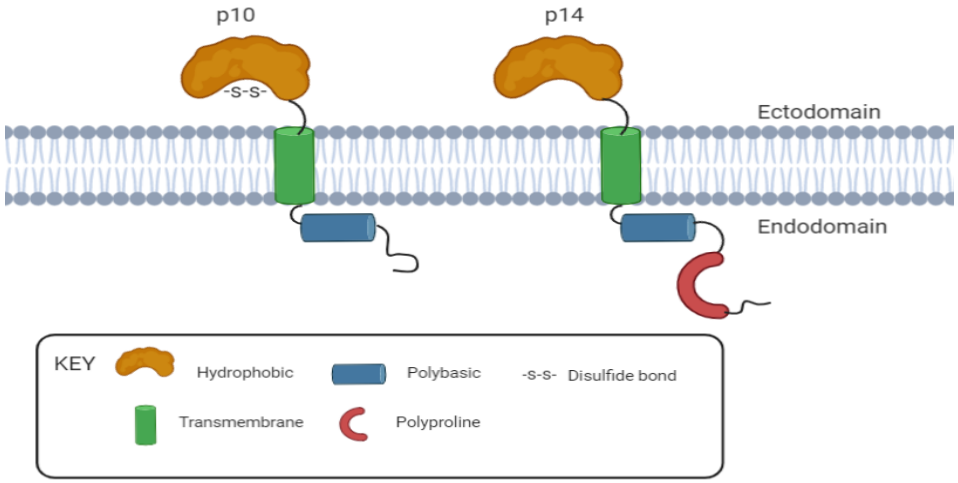

Figure 1.2: Structure of FAST protein. The structure of FAST p10 and p14. The basic structure of both is similar, with an ectodomain, a transmembrane domain, and an endodomain.

Each of the FAST proteins are small in size (approximately 100-200 amino acid residues), containing a transmembrane domain which serves as an anchor in the plasma membrane in the absence of a cleavable signal peptide. The ectodomain is small (20- 40 amino acid residues) while the C-terminal endodomains are longer (40-140 amino acid residues). This structural arrangement is reverse to that of structural proteins of enveloped viruses, which have larger ectodomains to traverse through cell membranes and form syncytia formation. The unusual structural topology of the FAST proteins leads to extensive structural remodelling of the ectodomain and cellular actin network during the syncytia formation (Cohen et al., 2004). Each

of the FAST proteins have specific motifs which are assumed to be essential for membrane interactions. The p10 and p14 FAST have a short hydrophobic patch in their ectodomain, while the same is found in the endodomain of the p15 FAST. These hydrophobic motifs are believed to confer functions analogous to the fusion peptides found in the fusion proteins of enveloped viruses. Additionally, fatty acylation modifies the FAST proteins; the p14 and -15 FAST have N-terminal myristate molecules (Corcoran & Duncan, 2004) while the p10 FAST comprises of a palmitoylated dicysteine patch in the endodomain, right next to the transmembrane domain (TMD) (Shmulevitz et al., 2003). The key features found to be common among the FAST protein endodomains include an intrinsic disorder in the cytoplasmic tails, a poly-basic motif, which possibly serves as a trans-Golgi export signal as observed in p14 (Parmar et al., 2014), and a hydrophobic patch which serves as an α helix model that promotes pore formation (Read et al., 2015). The N-terminal of the p14 and p15 FAST proteins are modified by fatty acylation (Corcoran & Duncan, 2004) while p10 FAST is modified at the endodomain next to the TMD with an essential palmitoylated dicysteine moiety. Mutational analysis has revealed that the palmitoylated dicysteine moiety is an essential modification for the syncytia forming ability of p10 (Shmulevitz et al., 2003). Similarly, the N-terminal myristylated amino acid residues in p14 are believed to be important for the positioning of the protein on the cytoplasmic membrane, leading to membrane fusion by interacting with the external portion of the bilayer membrane (Corcoran & Duncan, 2004).

Interestingly, each of the FAST proteins are different to each other in terms of the protein sequence but their function is similar; formation of syncytia between cells. The difference in the protein sequence is attributed to the evolution of the protein in different reoviruses at different time points. It is presumed, that the FAST proteins evolved from membrane-associated non-fusogenic pore-forming proteins (Nieto-Torres et al., 2015). Such proteins are encoded by a number of different viruses including Hepatitis C virus (HCV), influenza virus,

rotavirus, and human immunodeficiency virus (HIV). Such proteins are collectively known as viroporins and function to form pores in the cell membrane to channel ion flow in favour of viral infection (Lingwood & Simons, 2010). The similarity between the viroporins and the FAST proteins in their ability to use their transmembrane domain for remodelling the cellular membrane is the reason behind the presumed evolutionary path.

Despite the differences and the varying lengths of their endo and ectodomains, each of the FAST proteins contain a transmembrane domain that adheres to the plasma membrane as a reverse-single anchor protein directing the N-terminal (about 20 to 40 amino acids) outside the membrane and the longer C-terminal (40-140 amino acids) inside the cytoplasm. The N-terminal region is analogous to a fusion peptide and is amphiphilic in nature. The hallmark features of the endodomain of a FAST protein include: (i) intrinsically disordered cytoplasmic tails enabling interactions with multiple proteins (Uversky, 2011), (ii) A polybasic juxtamembrane motif, which acts a trans-golgi export signal in the case of p14 (Parmer *et al.,* 2014), and (iii) a region acting as an amphiphathic alpha helix. This alpha helix is generally known to be a hydrophobic domain that enabled the formation of pores within the cell membrane (Read et al., 2015). There is a slight difference in the above explained hallmarks within the p10 FAST protein since it has equal lengths of endo- and ecto-domains. This leads to the palmitoylation of the endodomain cysteine motif instead of the ectodomain myristylation essential for fusion activity (Shmulevitz et al., 2003).

FAST protein mediated fusion

The FAST proteins contain different motifs which are together responsible for bringing about membrane fusion. The process of FAST protein mediated fusion includes trafficking of proteins from the Golgi complex to the plasma membrane, localization of the protein in the membrane, multimerization and partitioning into the lipid rafts. The two crucial aspects of

FAST protein mediated membrane fusion are the formation of multimeric complexes and association of the FAST proteins with the membrane domains. The occurrence of these steps varies between the different FAST proteins. For example, the p14 first partitions into the liposome membrane microdomains which resemble thickened lipid rafts at the membrane. The multimeric complex assembly of p14 has been confirmed by treating the membrane with detergent, which did not disrupt the lipid rafts and it was seen that the multimers remained stable. However, treatment with chemicals that disrupt the ER-Golgi complex trafficking led to the disruption of the multimers, leading to the conclusion that the p14 multimers are formed and trafficked from the Golgi complex (Huttner & Zimmerberg, 2001). In contrast to the p14 FAST, the p10 FAST multimers have been found to be stable only in the lipid rafts indicating that the multimerization and microdomain formation steps are co-dependent in the case of the p10 FAST protein (Key & Duncan, 2014). The multimer formation in the p10 is dependent on a membrane proximal external region (MPER) of 13 amino acids within the protein. Within this MPER motif, there is a 9-residue long conserved motif (CM) which is known to be essential for the protein function (Yun *et al.,* 2014). Given the small size of the FAST proteins, it is quite likely that these proteins only serve as platforms for the formation of multimers in the cell membrane. This has although not been proven, the idea comes from studies on the influenza virus viroprotein (M2), which is highly similar in structure and function to the FAST proteins. The M2 protein uses the lipid raft regions for promoting membrane budding and fusion (Rossman & Lamb, 2011). The same region and pathway are likely to be used by the FAST proteins for cell fusion (Yang *et al.,* 2015).

The formation of the microdomains is believed to be based on the interactions of proteins and lipids. The close contact of lipids and membrane proteins is likely to provide a stearic advantage to the formation of the microdomains as it matches the transmembrane domain of the FAST protein. Once a microdomain is formed, it further promotes protein-lipid and protein-protein

interactions. This is due to a mismatch between the transmembrane domain length and the thickness of the cell-membrane. The ends of FAST protein TM domain adjacent to the MPER is thought to be crucial in fusion activity and in the p10, this region contains a conserved triglycine motif (Shmulevitz *et al.*, 2003). In the enveloped viruses, such motifs are found to be associated with fusion activity in conjunction with the TM (Yang et al., 2015), but the same has not yet been established for the FAST proteins. While the FAST protein TM is essential for initiating the fusion activity, the actual cell-cell fusion occurs through the involvement of cellular adhesions and the remodelling of the actin network which mediate a pre-fusion state. The short stretch of amino acids in the ecto-domain of the FAST protein fails to span the gap between two cells. This leads to the use of adheren junctions on the cell membrane, to which the FAST proteins localize. The adheren junctions form cell-cell junction which is stabilized by cadherins, which are in turn dependent on calcium ions (Koch et al., 2004). The formation of stabilized junctions is followed by actin remodelling within the cells (Hartsock & Nelson, 2008). Blocking cadherins or the adheren junction complex formation stopped the fusion activity, thus confirming that it is the adheren junctions bring the cells in close proximity leading to syncytia formation (Salsman et al., 2008). There is also evidence of other cell junctions being utilized by the FAST proteins for carrying out their fusogenic activities (Salsman et al., 2008), indicating that the FAST proteins are opportunistic fusogens which use the cellular junctions for their own benefit.

The initial fusion reaction leads to the development of a pore in the cell membrane which is only a few nanometers in diameter. Syncytia formation requires a larger pore, which is achieved by means of expansion of the minipores initially formed. The annexin (AX1) protein has been found to be responsible for expansion of the pore by altering membrane curvature and promoting membrane aggregation (Ciechonska et al., 2014). This is possibly a general cellular activity, where cell fusion occurs by means of increase in pore size (Hayes et al., 2004).

Normally, the membrane sculpting activity occurs within cells for fulfilling a variety of cellular functions including endocytosis, exocytosis and control of the actin dynamics (Richard et al., 2011). Thus, the cellular proteins play a crucial role in the post-fusion expansion of pores.

FAST proteins as promiscuous fusogens

FAST proteins have been shown to be bonafide fusogens. These proteins can promote cell-cell fusion between almost all cell types under neutral pH conditions. These proteins can also induce liposome-cell fusion and liposome-liposome fusion (Top et al., 2005). In consistency with their promiscuous nature, the FAST proteins lack receptor binding activity. In the absence of the necessity to bind to a receptor, the fusion activity of FAST proteins depends on the level of their accumulation within the plasma membrane, which in turn depends on the translation of the protein within the cells (Salsman et al., 2008). This property of the FAST protein ensures that they do not need specific pH for their action and syncytia formation is regulated by translation through sub-optimal start codons and the Endoplasmic Reticulum mediated degradation pathway (Shmulevitz et al., 2004).

FAST proteins in Oncolytic Immunotherapy

FAST proteins have been engineered into oncolytic viruses as a measure of causing syncytia formation between tumour cells, leading to immunogenic cell death. The use of FAST proteins in oncolytic viruses has been shown to increase intra-tumoral spread of the virus, causing apoptotic cell death and activation of anti-tumour immune response (Le Boeuf et al., 2017).

1.4 Tet-Regulatory System

The tetracycline (Tet) resistance regulatory system confers tetracycline resistance in bacteria. In the bacterial cell, the Tet resistance (TetR) binds to the tetracyline operator (TetO) to confer

antibiotic resistance. The regulatory mechanism of this operon system is widely used for regulating gene expression in eukaryotic cells (Baron & Bujard, 2000). The system works by binding of a transcription activator derived from herpesvirus (Vp16) which is co-expressed with TetR onto the Tet Operon for the activation of the gene present downstream of the operon (Ogueta, Yao, & Marasco, 2001). This circuit plays a regulatory role in the levels of gene expression when used in a eukaryotic system.

Briefly, the tet operator system works positively on the absence of tetracycline in the system. Meaning, that the gene present downstream of the TetO is activated when the TetR-Vp16 binds to the operon. The opposite of this phenomenon occurs in the presence of tetracyline; the TetR-Vp16 fails to bind to the TetO, thereby leading transcriptional silencing of the gene present beyond the operator region. The use of such a system is critical in studying levels of expression of a gene of interest by controlling the interaction between TetO and TetR-Vp16 (Krueger et al., 2006). In our project, this system is useful in that the regulatory elements (TetR-Vp16 and TetO) could be expressed through different plasmids and their interaction would rely on fusion of cells expressing a viral fusion protein. This could possibly lead to the activation of a marker gene (EGFP) present in the TetO plasmid, thereby providing a means of quantifying syncytia formation.

1.5 Antigen Cross Presentation

Cross-presentation is the process by which APCs (Dendritic cells and Macrophages) internalize antigens and present them through the MHC-I molecules. Successful antigen cross-presentation is a crucial step towards triggering and potentially establishing the adaptive immune response against viral infections and tumours (Baron & Bujard, 2000). Although the process of cross-presentation is believed to occur through a wide population of APCs, it is

reported that the dendritic cells are the most potent candidates of antigen cross-presentation (Di Pucchio et al., 2008).

The mechanism of cross presentation has been explored through a wide variety of studies to determine how antigens can successfully be loaded onto the MHC-I molecule. There are two major pathways which have been deemed as central to cross-presentation; a) vacuolar pathway, and b) cytosolic pathway.

The vacuolar pathway involves internalization of the antigens into the endo-lysosomal compartment, which is followed by degradation of the antigen into antigen-derived peptides through the lysosomal proteases. One the antigen has been processed, the peptides are then loaded onto the MHC class I molecules located within the endosomal compartment of the APC. The key player in this pathway is reported to be Cathepsin S, which is a lysosomal protease. In contrast the Cytosolic pathway involves the degradation of the antigens by the proteasome rather than the lysosome. The peptides degraded by the proteasome are reported to follow the normal TAP-mediated MHC-I loading of proteasomal peptides (Monu & Trombetta, 2007).

Although there have been some reports about the loading of antigens onto the MHC-I irrespective of the proteasomal degradation, the arguments and evidences in favour of the proteasomal degradation pathway being the key to cross-presentation seem to be more compelling. Arguably the proteasomal route is a logical premise since the outcome of antigen cross-presentation is the activation of the cytotoxic T cells, which are antigen-specific, and thereby equipped for killing the target cells (Sengupta, Graham, Liu, & Cresswell, 2019).

1.5.1 Regulation of cross-presentation

The process of antigen cross-presentation is not fully understood, although it is clear that the pathway is critically regulated and highly sophisticated. Though there are different pathways of antigen cross-presentation that have been under study, it has become clear over the years

that the stability of the antigens within the lysosomes is critical to successful cross-presentation (Chatterjee et al., 2012). This implies that a rapid degradation of the antigens within the endosomal compartments leads to a decrease in the cross-presentation efficiency. Rapid degradation of the antigen is likely to cause a destruction of multiple epitopes before they could be loaded onto the MHC class I molecules, thereby reducing the chance of priming the T cells. Moreover, pre-loaded MHC I molecules have a short life span. The success of T cell activation relies on prolonged cross-presentation (Shen & Rock, 2006). Hence, it seems that limiting antigen degradation and creating an internal antigen depository is crucial for enhancing the overall antigen cross-presentation process. Having antigens available for a prolonged period of time can ensure that the right epitopes are presented over time for priming the cytotoxic T cells.

The ability to keep antigens internalized and present them to T cells over time, has been associated with human monocytes and dendritic cells. It has been established that the DCs are best suited to antigen cross-presentation and that they possess more than one method of preventing rapid lysosomal degradation of the antigens. In comparative studies between DCs and macrophages, it has been found that the levels of lysosomal proteases expressed by DCs is less. Moreover, endopeptidase and Cathepsin, which are both involved in peptide degradation have also been found to be much lower in concentration in DCs as compared to macrophages, resulting in making DCs managing to maintaining higher antigen stability within the endo-lysosomal system after antigen internalization. Additionally, DCs are equipped with receptors that direct the endocytosed molecule towards the non-degradative endosomal compartments.

It has been shown through previous studies that the endocytosis receptor used for antigen internalization is the key to determining the antigen processing pathway. Poor cross-presentation has been reported for antigens that have been internalized through either pinocytosis or the scavenger receptors (Burgdorf, Kautz, Böhnert, Knolle, & Kurts, 2007). The use of the mannose receptor for antigen receptor has been found to target antigens towards

early endosomes, which have a delayed fusion with the lysosome, thereby retaining the antigen for a longer period of time, thereby causing improved antigen cross-presentation (Burgdorf et al., 2010). Studies on cell markers and antigen uptake receptors in human DCs have revealed that the CD103+ DCs in the liver and lungs use the mannose receptor for the internalization of viral antigens. It has also been confirmed that the targeting of antigens into early endosomes leads to efficient cross-presentation. Poor cross-presentation has been reported for antigens that are uptaken by DEC205, as this directs the antigens towards the lysosomes directly, leading to rapid degradation and no time for proper cross-presentation (Chatterjee et al., 2012). However, blocking the lysosomal degradation of antigens was reported to rescue the cross-presentation efficiency even if antigens were internalized through DEC-205 (Tacken et al., 2011). This points towards the importance of intra-endosomal stability of antigens for efficacious cross-presentation. Other targets for efficient cross-presentation include the carbohydrate recognizing domain on the APCs, the DC-SIGN, which directly delivers antigens to the lysosomal compartments, resulting in quick degradation and thereby causing inefficient or weak cross-presentation.

1.6 Phagocytosis

Phagocytosis is a cell-eating process used by eukaryotic cells for engulfing particles, other cells, and antigens. Professional phagocytic cells like macrophages, dendritic cells, and neutrophils achieve phagocytosis with great efficiency. These cells are mainly responsible for removing microorganisms and infected cells to then present the antigens to the lymphocytes for cell-mediated immunity. Phagocytosis is deemed a critical process in the context of cancer therapy, in that engulfment of cancer cells can lead to their clearance and release of cancer-associated antigens for activating the adaptive immune responses against cancer. Cancer cells

uptaken by APCs brings the TAAs into the same cytoplasm as the APCs, thereby providing a way for antigen presentation on the surface of the APCs (Tseng et al., 2013).

The role of macrophages has been found to be quite important in the phagocytosis of cancer cells. The polarization of macrophages is also important in this regard. The M1 and M2 polarization of the tumour-associated macrophages determines the overall effect these phagocytic cells have on the tumour (Yunna, Mengru, Lei, & Weidong, 2020). Both, the M1 and M2 macrophages are capable of carrying out phagocytosis, with the M1 being more apt at the process (Liu et al., 2021). The M1 polarized TAMs are pro-inflammatory in nature and prove anti-tumour in their action. While the M2 polarized TAMs are anti-inflammatory and maintain an immuno-suppressive microenvironment, thereby promoting tumour growth and resistance to treatment (Jayasingam et al., 2020). The phagocytosis carried out by macrophages is deemed important clinically. There is evidence of monoclonal antibodies that successfully bridge the innate and adaptive immune responses together and enhance their targeted response towards cancer.

1.7 CD40 Stimulation

CD40 is a transmembrane protein present on the surface of a variety of normal cells, including macrophages, B cells, dendritic cells, endothelial cells, epithelial cells, and platelets. The CD40 molecule belong to the Tumour Necrosis Factor (TNF) superfamily and is activated by the CD40 ligand which is present on T cells as well as platelets. There is also evidence of CD40 receptor being present on a number of cancer cells such as melanomas and carcinomas of breast, lung, colon, kidney, pancreas, prostate, head and neck, and ovaries, along with all B cell malignancies (Pang et al., 2017).

The interaction of the CD40 ligand to the CD40 receptor on the APCs leads to an increase in the MHC expression and the upregulation of the costimulatory molecules, such as the CD86, and a stimulation of IL-12, which is a pro-inflammatory cytokine and causes T cell activation (Leifeld et al., 1999). Each of these events play a role in the cell-mediated immune responses. The critical role of CD40 has been recognised through analysis of patients with germline mutations in the CD40, which revealed high tendency of immunosuppression, increased susceptibility to infections, and impaired T cell- dependent immune reactions. The CD40-CD40 ligand interaction has been deemed critical in the activation of the B and T cell immune responses, maturation of B cells and dendritic cells, as well as their antigen presentation capabilities. The improved antigen presentation capacity of DCs leads to an expansion in the cytotoxic T cells specific for tumour antigens, which can potentially lead to tumour eradication (Marigo et al., 2016).

1.8 Thesis Hypothesis

Overall hypothesis: The use of fusion proteins and CD40 agonists enhance the interactions between tumour cells and APCs, leading to APC activation and a shared cytoplasm that will allow direct processing of cancer antigens by the immunoproteasome of the APC, allowing increased cross-presentation of tumour antigens.

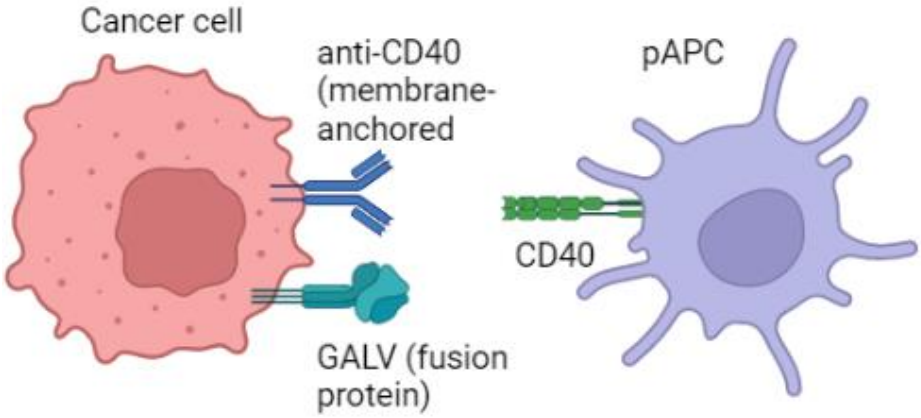

Figure 1.3: The expression of a CD40 superagonist and a viral fusion protein from cancer cells leading to binding and fusion with an APC

2. Materials and Methods

2.1 Cell Culture

Cell lines and the culture media used for them are summarized in table 2.1. Briefly, the cell lines used were sourced from the American Type Culture Collection (ATCC). The cells were cultured and maintained in an incubator set at 37˚C and 5% CO2. Each of the cell lines were passaged every 3 to 4 days. The adherent cell lines were cultured in Dulbecco's Modified Eagle Medium (DMEM from Sigma-Aldrich, USA) containing 10%FBS (FBS from Gibco) (v/v). These cells were passaged by removing the media, followed by washing the cells with Dulbecco's phosphate buffer saline (1x DPBS; #14190250, Gibco™), then trypsin was added to the flask for dissociating the cells. This was followed by neutralizing the action of trypsin by adding media containing FBS, the cell splitting ratios are shown in the table below. The non-adherent cells used in our experiments were cultured every 2 to 3 days and the Roswell Park Memorial Institute 1640 (RPMI-1640) medium was used for culturing these cells. The non-adherent cell line, Jurkats were subcultured every 2 to 3 days in RPMI media, supplemented with 10% FBS, 1% Penstrap, 1% glutamine, and 1% sodium pyruvate. The cells were passaged by first collecting the media from the flask intro falcon tubes and spinning it in a centrifuge to collect cells into a pellet. The pellet was then resuspended into fresh media, split and seeded into a new flask.

Table 2.1: Cell types and culture conditions

Cell Line/Type	Medium	Additional Supplements	Subculture time
DLD-1	DMEM + 10% FBS		3-4 days
A549	DMEM + 10% FBS		3-4 days
Jurkats	RPMI + 10% FBS	1% Penstrap, 1% Glutamine, 1% sodium pyruvate	2-3 days

PBMC derived macrophages	XVIVO + 2% HS		Monocyte to Macrophage induction – 6 days

2.1.1 Storage and long-term maintenance of cell lines

The cell lines were stored through cryopreservation. The cells were dissociated using trypsin, centrifuged to collect cells into a pellet, and then resuspended in freezing medium (FBS with 10% v/v dimethyl sulphate). The cells were then aliquoted into cryogenic tubes and then placed into cooling containers (Mr. Frosty) at - 80˚C. Long term storage was achieved by keeping these cells in a liquid nitrogen tank (-196˚C).

The revival of cells was carried out by thawing the frozen cells at 37˚C, resuspending the cells into warm medium. Once the cells were thawed, they were centrifuged (5 minutes at 400 x g), and then resuspended into fresh medium for culturing.

2.1.2 Cell Seeding

Cell seeding into flasks or plates was carried out at desired densities depending on the plates used. The seeding densities were achieved by counting of cells in a haemocytometer, and adjusting the cell numbers as per the requirement of the experimental conditions.

2.2 Cell Staining

2.2.1 Cell Tracker Dyes

Cells were labelled using cell tracker dyes Red or Green (Thermofisher # C34552 and # C7025). The cells to be labelled were dissociated by trypsin, collected in falcon tubes, centrifuged to collect cell pellets, which were washed with PBS to remove media completely, and then resuspended in the cell tracker dye (diluted at 1:1000 in PBS). The cells were incubated at 37˚C for 30 minutes with the dye, and then again centrifuged, washed, and seeded at desired densities in the black, flat bottom plates (Greiner #655090).

2.2.2 Antibody staining

The cell medium was removed, followed by washing of cells with PBS, dissociation of the cells from the flasks, and then collecting the cells into 96-well v-bottomed flasks (Corning #3894) for staining. All the staining steps were carried out in the same 96-well plate. After collection, the plate was centrifuged (5 minutes at 400 x g), media was removed, and the cells were washed with PBS. After washing, the cells were resuspended in 50 μL FcR blocking reagent (a 1/100 dilution in MACS buffer), and kept at 4˚C for 10 minutes. After blocking, the cells were topped up with MACS buffer to make a total of 200 μL volume per well. The plate was then centrifuged and the supernatant was removed. Cells were again resuspended in 50 μL MACS buffer containing a mix of antibodies for staining different cell surface markers. A list of the antibodies used for staining is provided in table 2.2. Following the addition of the staining cocktail, the cells were incubated at 4˚C for 30 minutes, by covering the plate in tin foil to protect the cells from light. After staining, the cells were washed again with PBS, and then fixed using formalin and incubated for 15 minutes at room temperature. The cells were again centrifuged, washed, and resuspended in 200 μL MACS buffer per well. These cells were then analysed by flow cytometry.

Table 2.2: List of antibodies used for cell staining

Antibody	**Fluorophore**	**Dilution**	**Manufacturer**	**Catalogue Number**
CD8a	APC	1:200	Biolegend	300912
EpCAM	FITC, BV605	1:200, 1:100	Biolegend	324304, 310938

CD11b	BV421, BV605	1:200, 1:100	Biolegend	301324, 301331
HLA-A2	PE	1:200	Biolegend	343305
LIVE/DEAD ™ Fixable Near-IR dead cell stain	Near IR	1:5000	Thermofisher Scientific	L10119

2.3 Flow Cytometry

The data acquisition for flow cytometry was carried out using the Attune NxT flow Cytometer (ThermoFisher Scientific). A sample of 160 μL (out of 200 μL) was collected per well at a flow rate of 500 μL per minute maximum. The data was processed using the FlowJo v10.8.1 software (BD Biosciences).

2.4 Cell Cytometry using CELIGO

The Nexcelom CELIGO image cytometer was used for analysing GFP expression by cells following fusion. Cells were seeded in 96-well plates after transfection with GALV and TetR-Vp16 plasmids, and cocultured with cells transfected with the TetO-EGFP plasmid. Following coculture, the cells were incubated at 37˚C for 48 hours before analysis on the cytometer. The expression analysis package of the software was used to calculate the total number of cells per

well, along with measuring the integrated fluorescence in each well. The final integrated intensity of the EGFP expression was calculated as follows

Integrated Intensity of EGFP Expression: Mean integrated intensity (for single cell) x number of cells per well.

2.5 Monocyte Isolation from Human PBMCs

Ethical approval for the study was obtained from the Health Research Authority (REC reference 19/LO/1848; IRAS ID 253836). PBMC derived Monocytes were obtained through isolation from a 10 mL blood leukocyte cone (provided by NHSBT Oxford). Firstly, the blood was collected in a 50 mL Falcon Tube and diluted with PBS to make up to 30 mL volume in total. The diluted blood was then transferred to a SepMate PBMC isolation tube (Stem Cell Technologies), containing Ficoll-paque as the density gradient medium. A total of 15 mL of the blood sample was added gradually to a single SepMate tube, by carefully overlaying the blood on top of the Ficoll layer. The tubes were then centrifuged at 400 x g for 10 minutes to separate PBMCs at the top as a cloudy buffy layer in the tube. In total the tube contained four layers separated by gradient, with the top layer being plasma, followed by the cloudy PBMC layer, then the separation medium, and finally the red blood cells and granulocytes as the bottom layer. The cloudy layer of cells was then collected in a fresh 50 mL falcon tube and washed thrice (see table 2.3 for details of washing steps).

The washed PBMCs were then resuspended in 20 mL RPMI 1640 (with 10% FBS). A total of 5 mL of this PBMC solution was then overlayed onto 6 mL of a Percoll Plus Solution in a 15 mL falcon tube (making a total of 4 tubes to isolate cells from the total 20 mL PBMC solution). These tubes were then centrifuged (see table 2.3) to achieve 4 layers; top layer being the RPMI,

an interphase of monocytes, Percoll, and then lymphocytes as the pellet. The monocyte interphase was collected, washed, and seeded into low adherence T-175 flasks for culturing.

Table 2.3: Centrifugation steps for isolation and washing of PBMCs

Step	Speed	Time	Acceleration	Break
1. Isolation	950g	30 minutes	Half maximal	Off
2. Wash	950g	10 minutes	Maximal	Maximal
3. Wash	600g	10 minutes	Maximal	Maximal
4. Wash	400g	10 minutes	Maximal	Maximal

2.3.1 Macrophage Differentiation and Polarization

The PBMC-derived monocytes cultured using the X-VIVO media (containing 2% HS) in low-adherence T-175 flasks for 6 days were polarized into macrophages. On day of culturing, the macrophages were treated with 10 ng/mL LPS and 25 ng/mL IFN-γ for polarization of cells into M1 macrophages. The cells were allowed to grow for a further 48 hours before dissociation. The dissociation step was carried out by removing the media, washing the cells with PBS, and then addition of 8 mL of 20 mM EDTA and keeping the flask at 37 ˚C for 10 mins. The macrophages harvested thus were then seeded into plates as per cell densities desired for the experiment being carried out.

2.4 Molecular Cloning

2.4.1 Linearization by Polymerase Chain Reaction (PCR)

The plasmid backbones (pSF or pCR3.1) were linearized and the DNA fragments of interest were subjected to PCR amplifications. The Phusion polymerase was used in a total of 20 μL

reactions. The DNA template used was 1ng, and 0.5 μM of each, the forward and reverse primers were used (list of primers present in Appendix). The thermocycling conditions used were as follows:

1. Initial Denaturation: 95°C for 30 seconds
2. Denaturation: 95°C for 30 seconds
3. Annealing: Primer-specific temperature for 30 seconds
4. Extension: 72°C for 1 minute
5. Cycle Repeats: starting from step 2 (30 cycles)
6. Final Extension: 72°C for 10 minutes

These steps were followed by storing at 4°C forever (until further use and processing). The PCR reactions were performed in the Peltier Thermal Cycler DNA Engine Tetrad.

Agarose Gel Electrophoresis

The PCR products were visualized on an agarose gel. A 1% (w/v) agarose gel was prepared in a 1 x TAE buffer. The samples were loaded onto the gel after mixing with 5x loading dye (NEB) for DNA visualization, and ran alongside 1 kb DNA ladder (NEB) in TAE buffer at 100 V for about 60 minutes. The gels were visualized using the UV light on the BioRad gel imager.

For Gibson Assembly, the DNA bands were excised from the gel and purified using a DNA Gel Extraction Kit (NEB).

2.4.2 Gibson Assembly

The addition of DNA fragments into a bacterial plasmid backbone can be achieved through the Gibson Assembly cloning method, which relies on a single reaction to carry out joining of DNA fragments using their complimentary overlapping regions. The overlapping regions were generated through PCR and the Gibson assembly was performed using the HiFI DNA assembly

master mix (NEB E2621L). The assembly of 2 to 3 fragments was carried out using 50 ng vector, and a 1:3 ratio of vector to insert was used. This was followed by incubation of the reaction tube at 50°C for 1 hour. The product thus achieved was used for bacterial transformation.

2.4.3 Bacterial Transformation

Competent XL 10 *Escherichia coli* (E. coli) cells were used for transformation with the DNA plasmids. The DNA assembly product was incubated with competent cells (2 µL of DNA in 50 µL of cell mixture) on ice for 30 minutes. The cells were treated to a heat shock at 42°C for 45 seconds, followed by incubation on ice for a further 10 minutes. 950 µL of SOC growth media was then added to the bacterial cell tubes, which were then incubated at 37°C for 1 hour in a shaking incubator. The cells were then spread on agar plates (containing the appropriate antibiotic) and then incubated overnight at 37°C.

2.4.4 Plasmid Preparation

Bacterial colonies grown on the agar plates were selected and grown in Lysogeny Broth (LB) medium at 37°C overnight in a shaking incubator. The next day, plasmid purification was carried out using the bacterial culture and processing it using either the Qiagen Miniprep kit (27106) or the Qiagen Maxiprep kit (12945), as appropriate using the manufacturer's instructions.

2.4.5 Sequencing

Successful cloning and correct sequence of the plasmid were confirmed by sequencing the plasmids though Sanger Sequencing by Eurofins and the sequencing results were analysed using the Snapgene software.

2.4.6 Anti-CD40 cloning

A membrane-anchored anti-CD40 construct was cloned into the bacterial plasmid PCR3.1, which contained the CMV promoter. The same construct was also cloned into the pCR3.1 containing the GALV fusion protein construct. The gene cassette was designed to have a P2A site between the anti-CD40 and GALV to achieve co-expression of both the proteins once they were transfected in cell lines. The cloning was achieved through the use of the Gibson Assembly protocol. Briefly, the plasmid was linearized by PCR, then the anto-CD40 gblock was added alongside the pCR3.1 plasmid backbone (or the pCR3.1 GALV) with the Gibson Assembly mastermix. The insertion of the anti-CD40 into the respective plasmid was confirmed through sequencing of the plasmid. An overview of the cloning process is shown in figure 2.1.

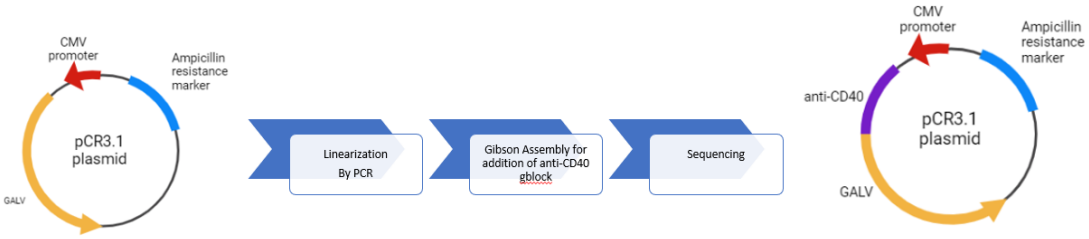

Figure 2.1: Cloning of the anti-CD40 membrane anchored gene into the pCR3.1 plasmid having the GALV construct.

2.5 Transient Transfections

0.7 x 10^6 cells were seeded in a T-25 flask. The next day, 8 µg of DNA per reaction was added by diluting in 500 µL of OptiMem (Thermo Fisher Scientific #13778150). 10 µL Lipofectamine2000 was used by diluting in 500 µL OptiMem. The two solutions were then combined and mixed properly by shaking, followed by a 20-minute incubation at room temperature. The total of 1 mL OptiMem solution containing the DNA and Lipofectamine2000

mixture was then added to the cell complexes. After 6 hours of incubation with the transfection mixture, the medium was changed in the flasks to add complete media and replace the OptiMem.

2.6 Syncytia Formation Assay

2.6.1 Homocellular Syncytia

The homocellular syncytia studies were carried out in black 96 well plated (Greiner #655090). Briefly, cells were stained with cell tracker red and transfected with the desired plasmid, 6 hours after transfection, the cells were cocultured with cells stained with cell tracker green and then allowed to grow for either 24 or 48 hours before analysing through microscopy or flow cytometry depending on the readout desired from the assay.

2.6.2 Heterocellular Syncytia

The homocellular syncytia studies were carried out in black 96 well plates (Greiner #655090). Briefly, cancer cells were transfected with the desired plasmid, 6 hours after transfection, the cells were cocultured with PBMC derived macrophages cells and then allowed to grow for either 24 or 48 hours before staining with fluorescent antibodies and analysing through microscopy or flow cytometry depending on the readout desired from the assay

2.7 Cross-Presentation Assay

50,000 cancer cells (transfected with desired plasmid or untransfected cells for negative control) were seeded per well in a 96-well plate (Day 0). The cancer cells were cocultured with 50,000 PMBC-derived macrophages (M1 polarized) per well (Day 1). 48-hours after coculturing of the two cell types, 150,000 Jurkats cells were added per well (Day 4). The cells

were then incubated at 37°C for 4 days before staining with appropriate fluorescent antibodies (day 8). The optimization steps for this method are discussed along with the effect of those optimizations in the results section (chapter 4).

2.8 Microscopy

Cells were stained and seeded in black flat bottom 96-well plates (Greiner #655090) as explained in the above sections, and imaged using the Zeiss LSM 710 microscope.

3. Formation of Multicellular Syncytia using Viral Fusion Proteins

3.1 Introduction

Multicellular syncytia formation involves plasma membrane fusion between more than one cell to produce a tissue with more than one nucleus contained in a shared cytoplasm. The basic process of cell fusion includes the fusing of cell membranes, cytoplasmic mixing, sometimes followed by fusion of the nuclear membranes (Pötgens et al., 2002). Cell fusion occurs in both physiological and pathological conditions, and can be either homotypic or heterotypic, depending on the types of cells involved (Wiener, Klein, & Harris, 1971). For example, fusion of cancer cells with stromal cells, macrophages, or stem-like cells can result in either tumour promotion, dormancy, or tumour reduction (Wang et al., 2021).

Homotypic fusion occurs between cells of the same type/origin, while heterotypic fusion occurs between cells of different types. Homotypic or homocellular fusion induced by viral proteins is a phenomenon that often occurs following infection with a virus expressing a syncytium forming protein. The fusion of cells or syncytia aids viral intercellular spread in that the virus can simply pass between cells that have been fused together instead of having to exit through a cell membrane and re-enter a new one through the normal attachment, and entry pathways (Gaudin, Ruigrok, & Brunner, 1995; White, Kielian, & Helenius, 1983). This process increases the speed and extent of spread of virus within the host cells, thereby enhancing their overall lifecycle (Shmulevitz, Corcoran, Salsman, & Duncan, 2004).

Heterocellular or heterotypic syncytia formation is the fusion between two different types of cells; epithelial cells with endothelial cells, or cancer cells with immune cells, as is the case explored in this study.

In the context of cancer therapy, viral fusion proteins have been explored for their potential to induce anti-tumour activity, partially due to the fact that syncytium are not stable structures and become unviable after a short stretch of time leading to immunogenic cell death. Cell death following the expression of a fusion protein can take several hours to days (Wong et al., 2016). As a first step the formation of multinucleated syncytia can begin in as little as 24 hours, which then goes on to recruit more cells in the growing syncytium before eventually becoming an unstable structure and dying in up to 5 days. There is considerable ambiguity in terms of the mechanism that leads to syncytium related cell-death. However, evidences in the literature point towards ATP depletion, mitochondrial failure, and autophagic degeneration, which indicate that necrosis might be a potential mechanism involved in FMG-induced cell death (Lin et al., 2010). Since necrosis results in the release of cellular components into the extracellular spaces, the resulting inflammatory response and bystander effect can lead to an overall heightened immune response (Higuchi et al., 2000).

The exploitation of syncytiaforming ability of fusion proteins has led to a leap in the usage of different viral fusogenic membrane glycoproteins (FMGs) within tumour models. Moreover, a number of studies have also explored the use of FMGs in oncolytic viruses, demonstrating successful enhancement in the anti-tumour activity and replication of oncolytic HSV, adenovirus, and vesicular stomatitis virus (VSV). The use of FMGs either on their own or their delivery into tumours through oncolytic viruses are generally aimed at both enhancing virus spread and possibly improving cancer vaccine effects.

There are two broadly different types of fusion proteins naturally present in viruses. The first and more well-studied type of fusion protein is the FMG, which is a part of the structural proteins of the virus. The FMGs are critical for the initial entry of viruses into the cell, hence often depend on particular receptors on the target cell membrane for successful infection. The Gibbon Ape Leukaemia Virus (GALV) fusogenic protein uses the Pit-1 receptor present on the cell membrane for cell entry of the virus and also for fusing different cells together. The Pit-1 (SLC20) receptor is part of the symporter membrane proteins that transport phosphate by using either sodium or protons to develop a gradient based movement of ions across the cell membrane (Liu & Eiden, 2011).

The second category of fusion protein is the non-structural fusion protein, better known as the fusion associated small transmembrane proteins (FAST), currently only reported to be found in the reovirus family (Boutilier & Duncan, 2011). Since the FAST proteins are part of the non-structural proteins of the virus, and do not play a role in the entry of virus into the cell, these fusion proteins are generally regarded as possibly having a role in enhancing the virulence and improving spread of viruses between cells. The FAST proteins have a receptor-independent method of causing cell-fusion, in that they do not require or depend on particular cellular receptors, as is common with the FMGs, rather the FAST proteins utilize the cell adhesion molecules or tight junctions which are used for cellular communication, and embed in the cell membrane near these junctions to cause cell fusion.

3.2 Chapter Aims

1. Analyse and compare the homocellular syncytia forming potential of GALV and FAST p14

2. Investigate and quantify the homocellular syncytia forming potential of the selected viral proteins using the Tet Repressor system
3. Analyse and compare the heterocellular syncytia forming potential of GALV and FAST p14

3.3 Results

3.3.1 Transfection Efficiency in different cell-lines explored for the fusion assays

In order to decide which cell lines could be used for testing fusion protein expression and assay development in later stages of the project, the transfection efficiency of Lipofectamine 2000 was evaluated in a range of different cell lines in vitro using a CMV promoter driven GFP-expressing bacterial plasmid. The highest level of GFP expression after 24 hours of transfection was observed by confocal fluorescence microscopy in HEK-293A cells, followed by A549 human lung adenocarcinoma, DLD-1 human colorectal carcinoma and the lowest expression was seen in PSN-1 cells (figure 3.1). In all subsequent experiments, including assays or tests for all further transfections, the same CMV-GFP plasmid was used as a transfection control.

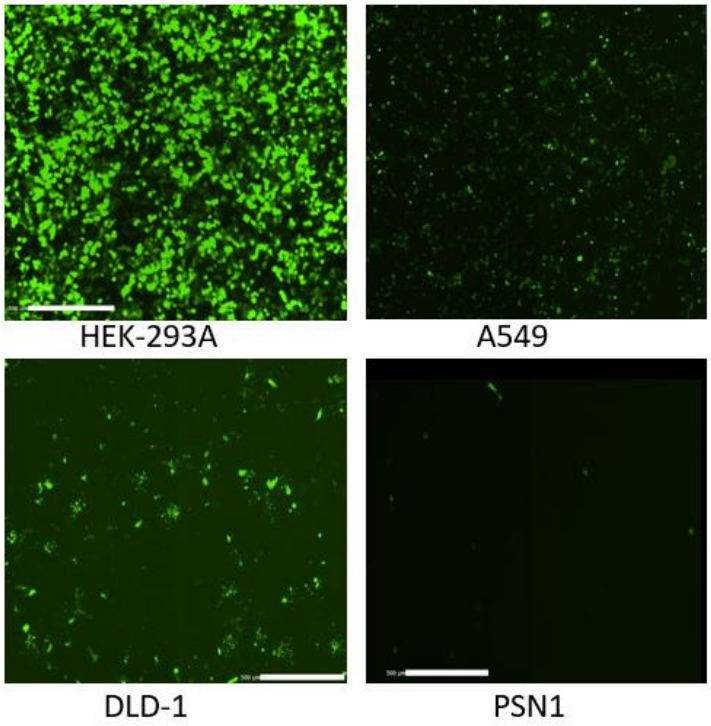

Figure 3.1: GFP expression in different cell-lines following transfection with a CMV-GFP plasmid. A pSF plasmid expressing GFP under the CMV promoter was transfected in different cell-lines. The cells were imaged 24-hours after transfection using a confocal microscope (Zeiss 710).

3.3.2 Homocellular syncytia formation by GALV

Syncytia formation is a highly ordered process that depends on the cell to cell contact such that the membranes of two different cells can interact and merge to become multinucleated cells with their cytoplasm becoming combined. Such a fusion is enabled through membrane proteins present on two different cells.

In the case of FMG the viral fusion proteins tend to embed in the cell membrane and interact with receptors on neighbouring cells to grow into a multi-cellular body. The mechanism of fusion by the GALV fusion protein for example, depends on the interaction of the fusion peptide of this viral protein to the PiT1 receptor (Slc20a1 – sodium-phosphate co-transporter)

present on the neighbouring cell. As per literature, the pit-1 receptor is ubiquitously present on all human cells, making it possible for the GALV fusion protein to form syncytia with cells that it comes in contact with.

We explored the syncytia forming ability of GALV and p14 FAST proteins. The study design involved transfection of cancer cells (A549) with fusion proteins and observing their fusion with neighbouring cells. Untransfected cells and/or cells transfected with CMV-GFP were used as negative controls for all syncytia formation tests and experiments. Firstly, as we designed the study, CMV-GALV (the pCR3.1 CMV-GALV plasmid was a kind gift from Professor Richard Vile, Mayo Clinic, Minnesota, USA) was used for initial tests and studies. As a first test, we used human lung adenocarcinoma A549 cells stained with cell tracker Red Dye, and transfected them with CMV-GALV. Syncytia were observed in these cells after 48 hours of transfection (Figure 3.2).

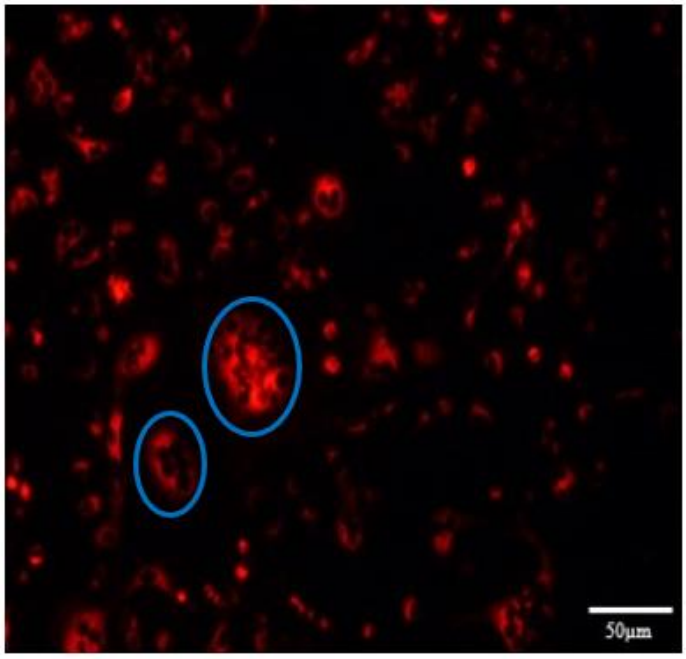

Figure 3.2*: A549 cells transfected with CMV-GALV. A549 cells were stained with cell tracker Red, and then transfected with the GALV fusion protein. The cells were observed under a fluorescent microscope, 48 hours after transfection. The blue circles include structures that are characteristic of syncytia; multiple nuclei surrounded by stained cytoplasm.*

3.3.3 Cell tracker Dyes for analysing syncytia formation

Labelling cell-lines with cell-tracker dyes was chosen as a method for observing fusion of differently labelled cell populations and confirming formation of multicellular syncytia. Cell-tracker dyes are designed to diffuse through cell membranes and become transformed into cell-impermeant reaction products when a constituent thiol-reactive chloromethyl or bromomethyl is activated by cytoplasmic glutathione-S-transferase, leading to durable labelling of the cell.

Cell-tracker Red was used to label a population of DLD-1 cells, which were then transfected with the GALV fusion protein. These transfected cells were then cocultured with untransfected DLD-1 cells stained using Cell-Tracker Green. DAPI was used for staining the nuclei after 48 hours coculture, just prior to observing the cells under a confocal fluorescence microscope (ZEISS-710). As can be seen in Figure 3, GALV transfection led to syncytia or giant cell formation. The structures encircled in red represent syncytia or fused cells. A syncytium typically entails multiple nuclei in the centre of what appears a united pool of cytoplasmic content. In the image here, the cytoplasmic dye has more or less leached out but the cell remains intact. The cells were analysed through a Z-stack in the Zeiss-710 software, which enables analysing different sections or slices of a particular field under the microscope, this enabled us to ensure that the fields imaged contained cells that were merged and not just lying on top of each other.

The orange cells encircled in Figure 3 are possibly early stage syncytia and represent the ideal case of red and green cytoplasmic dyes mixing to give an orange appearance to the cytoplasm. At the same time, some cells appeared dead and floating, which is reported in the literature to be the case in late stage of syncytia formation where the giant cell becomes unstable and undergoes cell death. One of the issues encountered with using two different cell tracking dyes was the difficulty in maintaining the cell stains after co-culture. Despite multiple optimizations of dye concentration used and time points of co-culturing stained cells together, it appeared

technically quite challenging to have cells stably showing a combination of red and green (ideally orange) upon fusion. It was very rare that any orange cells were observed (see figure 3.3). When the orange cells did appear, it was typically in a frame where most other surrounding cells had lost the dye. In the representative image used here, the field observed only included single cells that were green, while the cells stained red and transfected with GALV appeared to have more or less lost the red stain, evidenced by the lack of any red cells. It is possible that growing syncytia lose the dye due to the nature of cell fusions where the nuclei become pushed closely together and cytoplasmic content is gradually lost as the giant cell moves towards instability and eventually cell death.

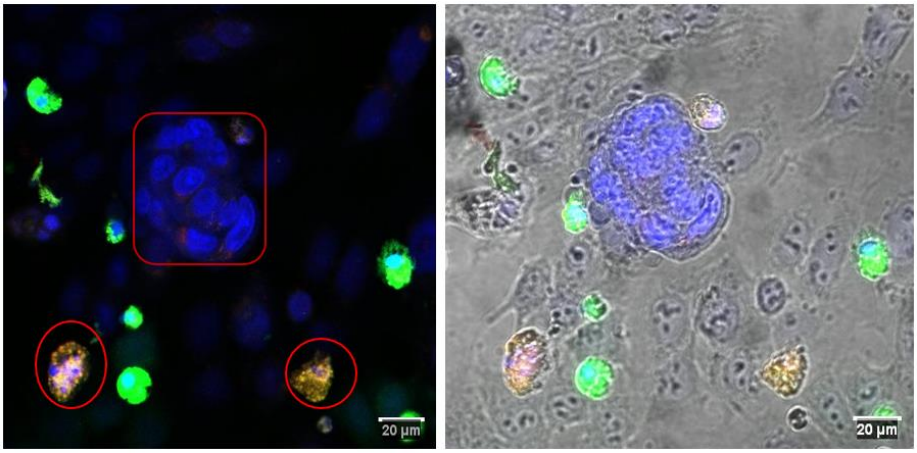

Figure 3.3: Syncytia formation in DLD-1 cells following transfection with GALV fusion protein. DLD-1 cells were stained with cell tracker Red and then transfected with GALV fusion protein. 6 hours after transfection, these cells were mixed with a population of green DLD-1 cells (stained with cell tracker Green), which were untransfected. The cells were stained with DAPI 48 hours after co-culture and observed under a confocal microscope. The red circles represent giant cells or syncytia.

3.3.4 Stable cell lines for analysing syncytia formation

To circumvent the issue of dyes leaching out upon syncytia formation, DLD-1 human colorectal carcinoma cells stably expressing either the ZsGreen or mBe-RFP (kindly gifted by Dr. Egon Jacobus) were used for studying syncytia formation. These cells while stably expressing the dyes and overcoming the issue of dyes leaching out posed rather challenging emission ranges when observed using the available confocal microscope. The ZsGreen cells

could be detected with the Zeiss 710 confocal microscope package with the use of a reasonable wavelength detection range (a range similar to what detects GFP using the same system), therefore these cells could reliably be used. However, in the case of the mBe-RFP, the range of emission seemed undetectable unless an extremely high gain was set on the emission channels, making it hard to detect the colour without making the image grainy and difficult to clearly observe. As can be seen in the different fields shown in figure 3.4, the green cells appear sharp and clear, while the red mostly appears as a haze and there is more fluorescence in the background when the red emission channel was selected for observation. This made it difficult to detect any syncytia successfully as the cell outlines were hard to pick in this system. The possibility of using a stable cell line was tough appealing, it appeared that moving forward, a combination of stably stained cells and cell tracker dyes might possibly be a more successful approach.

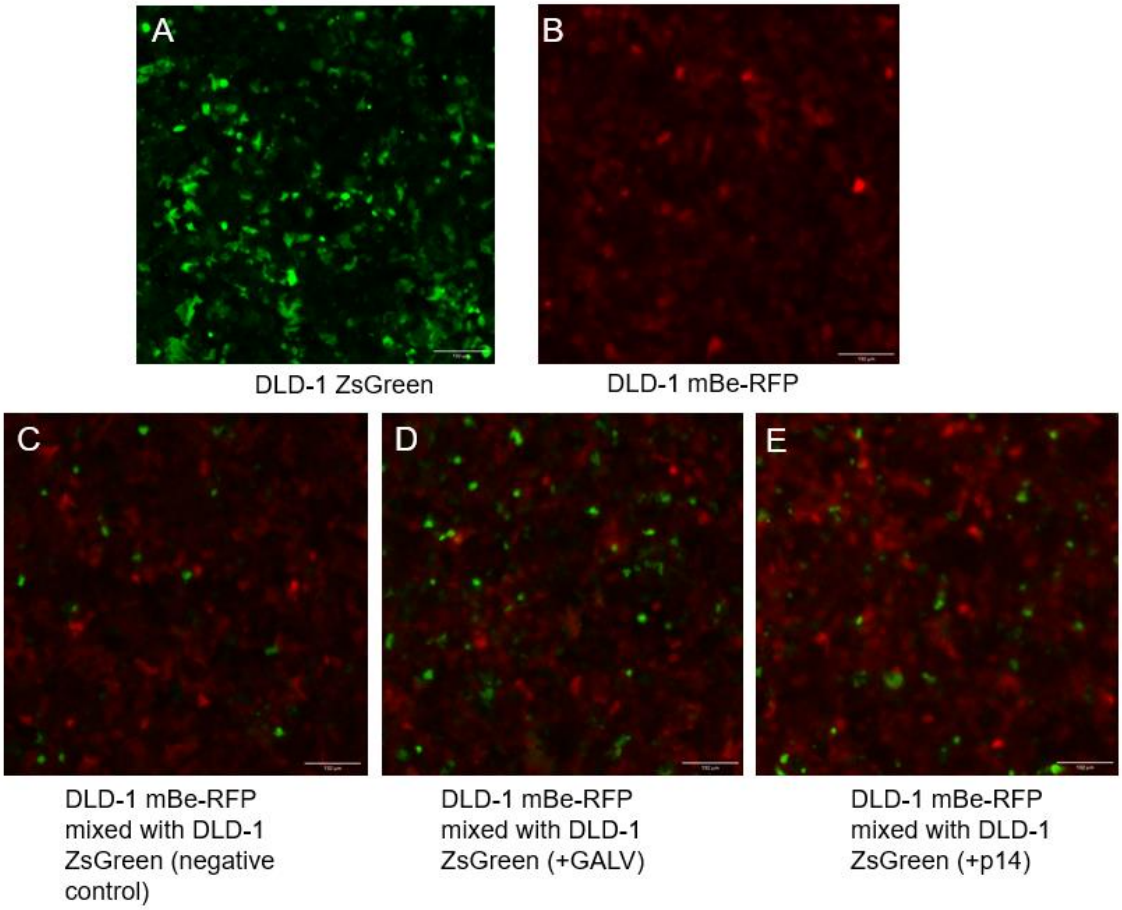

Figure 3.4: DLD-1 cells stably expressing ZsGreen or mBe-RFP for analysing syncytia formation. The DLD-1 mBe-RFP cells were transfected with GALV, and cocultured with DLD-1 ZsGreen (untransfected). The cells were observed under a confocal microscope 24 hours after transfection

3.3.5 Combination of stable cells and Cell Tracker dyes

After exploring cell tracker dyes and cell stably expressing fluorescent proteins, we decided to use a combination of the two approaches to study syncytia. DLD-1 ZsGreen cells were transfected with GALV fusion protein and then cocultured with DLD-1 cells that were stained with cell tracker red and not transfected. The cells were observed under a confocal microscope, 48 hours after co-culture. Figure 3.5 shows representative images of sections where syncytia were observed. The yellow circles in the figure highlight multiple nuclei (stained blue with DAPI) encased in a state of fused cytoplasm, which is typical of a syncytium. The giant orange cell represents red and green cells fused together to emit a mixed signal, hence the change in colour.

The use of a combination of cells stably expressing a fluorescent protein, and cells stained with a cell tracker dye appeared to be stable and reliable, such that fused cells could be observed along with a visible mixing of the two fluorescent labels, making it easy to detect syncytia, and overcoming the problem of dyes leaching out as was occurring in the previous set of experiments.

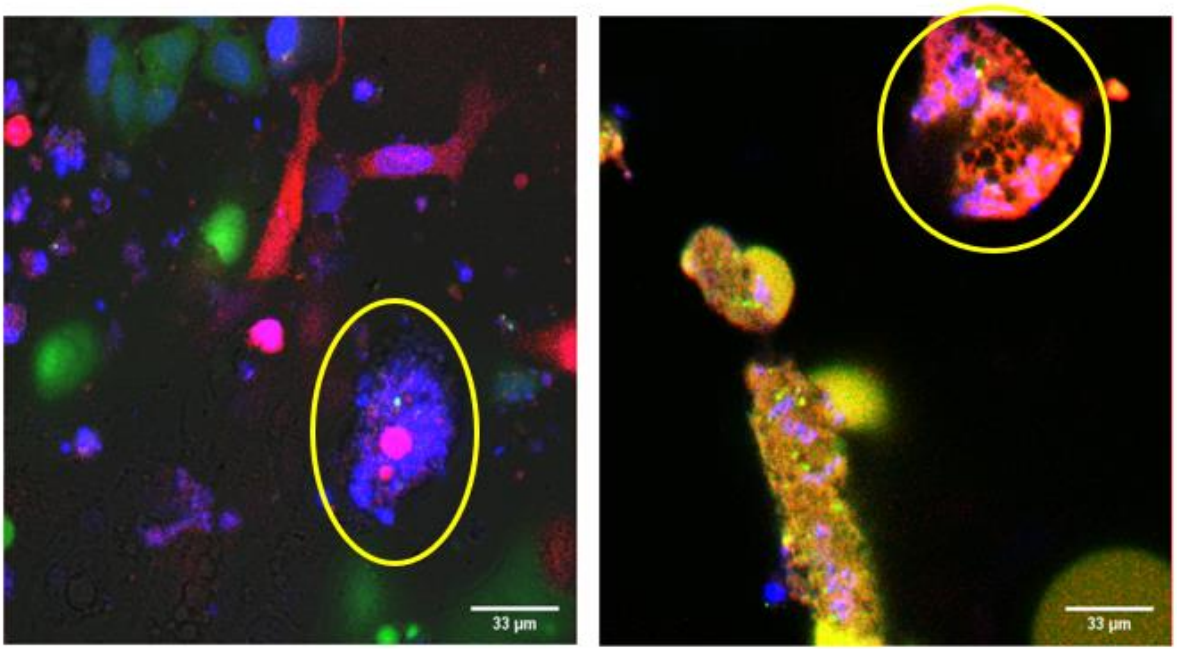

Figure 3.5: GALV mediated syncytia formation in DLD-1 cells. DLD-1 cells expressing ZsGreen were transfected with GALV, and 6 hours later they were cocultured with DLD-1 cells stained with cell tracker Red and untransfected. Two different frames of observation are shown here where syncytia (yellow encircled) were observed, 48 hours after co-culture.

3.3.6 Cell Cytometry for quantifying Fused cells

Quantification of syncytia was a critical step in our study, to achieve a consistent and reliable method of estimating the extent of cells recruited into syncytia following transient transfection with fusion proteins. To this end, we used the cell cytometry platform CELIGO. The cell cytometry through CELIGO works by imaging entire well, plates, and flasks, and gives an automated count of the number of cells per well. Using the cell count feature after scanning wells, allowed for viewing images of different sections of a well and select the different

parameters for analysing the contents of a well. In the experimental setup, DLD-1 cells were stained with cell-tracker red dye and transfected with GALV, and analysed for syncytia formation at 24 hours and 48 hours time point. At each time-point, cells were stained with the nuclear stain DAPI. The idea was to count the total number of cells present per well, using untransfected DLD-1 cells as control. The imager settings allowed for marking the area occupied by a cell, making it possible to visually locate, and mark what was to be counted as a single cell.

In this case, we visually located single cells by focusing on the nuclei (DAPI stained), and then masked the cells based on the Cell Tracker Red that stains the cytoplasm. Any instance where multiple nuclei were present merged together with little to no cytoplasm visibly distancing or separating them, this was masked as a larger/fused or merged cell. Once the setting was applied, the analysis then allowed for observing the overall number of single cells, and calculated anything bigger than that size ratio as a merged cell. This allowed to gain an overall cell count and percentage per well, and helped identify how many single or merged cells were present per well, with the readout being percentage of merged cells (Figure 3.6).

The calculation of percentage of fused cells was carried out through using the numeric values generated by the CELIGO software, which provides the total number of cells per well, and once the cells were masked or single or merged/fused cells, the software also provides a total count and percentages of each of the conditions set for the different wells. In this experiment, we used untransfected DLD-1 cells as control, so the wells that were untransfected could be used as a basis for the total number of cells present per well. In relation to the negative control, the cells appearing fused in the imager setting were then counted and a count and percentage was generated for the percentage of fused cells in the cells transfected with GALV. The yellow circle in figure 6(A) represents a syncytium masked by a green outline. Similarly, the red dots represent single cells. Along with the imaging and masking of cells, the total count and

percentages were generated by the software, the results of which are plotted and represented in figure 6(B). As can be seen in the graph, at 24-hour time point, the percentage of merged cells remained below 10%, which was similar to the baseline as counted for the negative control, implying that possibly no syncytia were detected at the 24-hour time point. At the 48-hours time point, the percentage of fused cells in the wells transfected will GALV went up to nearly 40%, as compared to a 10% in the negative control, indicating that fusion was successfully detected and accounted for at this time point. The cell cytometry approach that provided a means to be able to successfully count and calculate the number of cells that successfully went under syncytia formation following transfection with GALV.

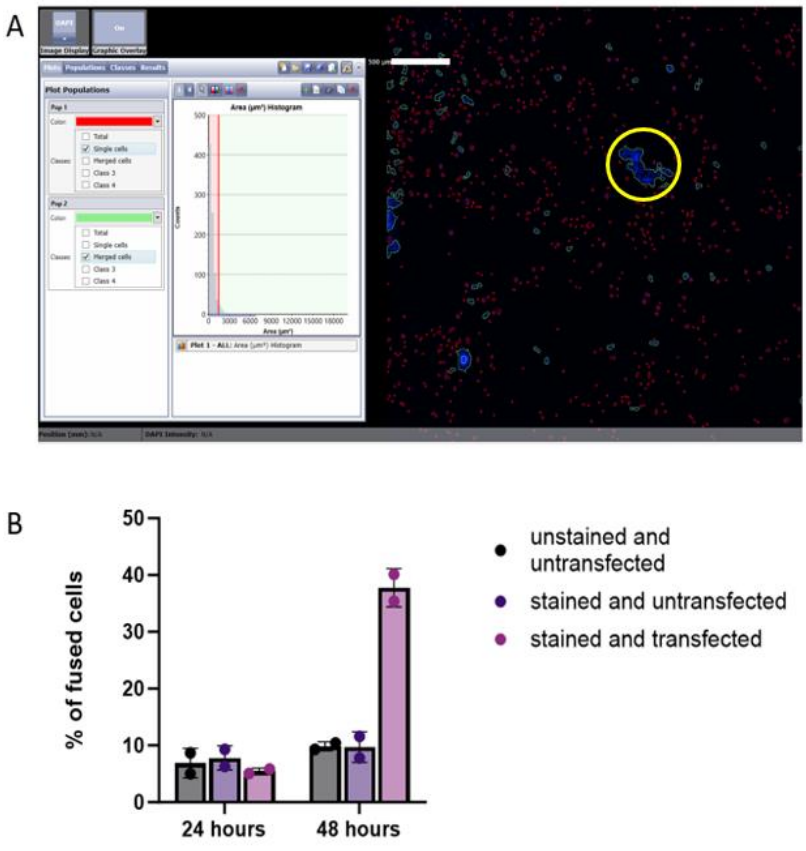

Figure 3.6: Homocellular syncytia formed in DLD-1 cells following. (A) Imaging and masking of cells to assign cell diameters to the system for consistently analysing and counting cells as single or fused cells as per the parameters set while scanning the different wells. The parameters once set are applied to all the wells, making the calculations normalized for all wells. The data points in the graph represent 3 technical repeats and the bars show the mean percentage of fused cells. Error bars represent +/- Standard Deviation

3.3.7 Homocellular syncytia formation by FAST p14

DLD-1 cells, stained with CFSE (green) were transfected with CMV-p14 FAST protein (a kind gift from Professor Roy Duncan, Dalhousie University, Canada). After 48-hours of transfection, the cells were stained with DAPI and observed under a confocal microscope. The characteristic features of fused cells were observed (figure 3.7); large, multinucleated cells with little to no cytoplasm (green stain) around them, as annotated through the red circle in the figure. This is in line with how syncytia have been previously observed and defined in literature pertaining to the use of fusion proteins. Briefly, syncytia formation is an orderly process, with the first step being the fusion of cell membranes, followed by mixing of cytoplasm of the fused cells, leading to the nuclei from these fused cells coming close together. The larger a syncytium gets, the more unstable it becomes, and the nuclei become fused, with cell death occurring by means of bursting of the syncytium or leakage of cytoplasm from the large, unstable cell.

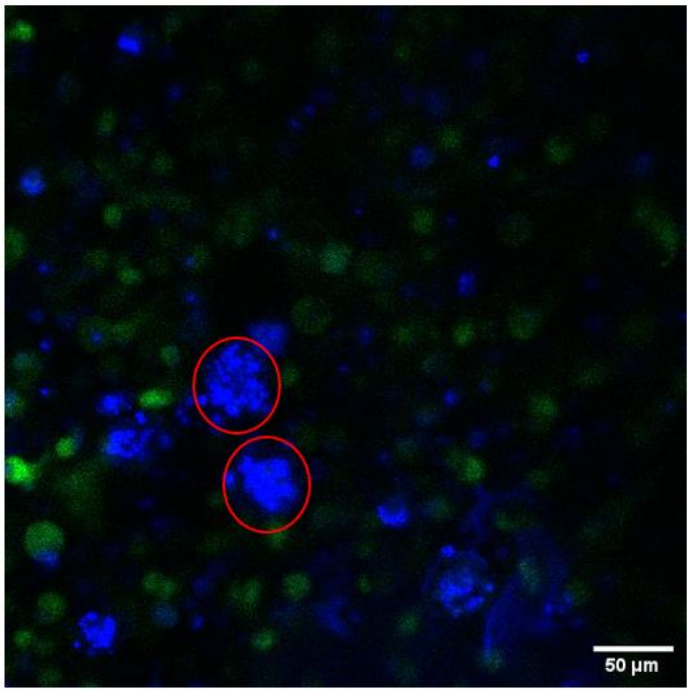

Figure 3.7: DLD-1 ZsGreen cells transfected with CMV-p14 observed under a confocal microscope, 48 hours after transfection.

Having confirmed the syncytia forming abilities of the CMV-GALV and the CMV-p14 FAST constructs, we used these plasmids for further refining and testing methods that we could subsequently use for potentially analysing and quantifying syncytia formation.

3.3.8 Flow cytometry for confirming syncytia formation

While microscopy provided insights about the fusion of cells, further analysis of the extent of fusion and potentially quantifying the syncytia formation potential of the fusion protein remained an aim we wished to explore. To this end, developing and refining a method studying syncytia formation led us to the use of flow cytometry. The set up for syncytia formation analysis used the same basic experiment set up as for imaging; staining and transfection of cells, followed by coculturing different populations. Briefly, DLD-1 cells stained with cell tracker Red were transfected with either GALV or p14, and then mixed with untransected DLD-1 ZsGreen cells. A coculture of untransfected red and green cell populations was used as a negative control. Following coculture, cells were collected and run through the Attune for flow cytometry. The strategy for counting syncytia involved gating for single cell population of green or red cells, and then exploring those populations that were positive for both; the red and the green signal, implying a fusion of cells stained with the two different colours. As can be seen from figure 3.8, the use of GALV led to around 40% of cell population appearing positive for both the colours, while the use of p14 led to around 50% cells expressing a double positive signal. As compared to the untransfected negative control, where 10% of the cells expressed the dual signal, it was estimated that the higher percentages of dual positive cells in the transfected cells was due to syncytia formation in those populations.

This method provided a basis for quantifying syncytia formation reliably. However, a critical point in this case is the fact that these analyses were using co-incident stains as markers of fusion. So, while the comparison to the negative control is stably representing an estimate of a

percentage that could be used as a baseline for data normalizing or cutting out any chance dual positive and the percentage of double positive cells is higher in the transfected cells, we have not carried out any real-time molecular analysis to be a 100% sure that the percentages are absolutely truly representing syncytia with mixed cytoplasms. In any case, the comparison and the successful use of the negative control provide some direction and reliability in the data set and indicate that this method could give at least an estimate for quantifying syncytia.

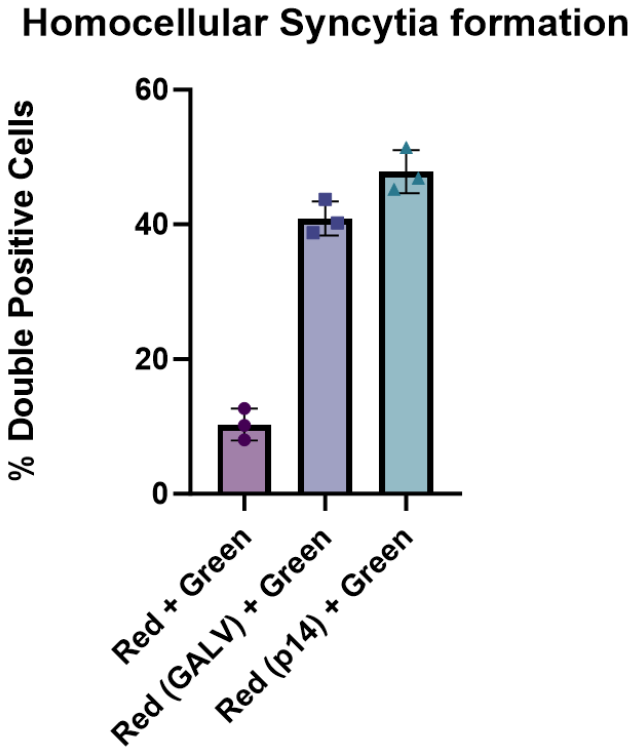

Figure 3.8: DLD-1 cells stained with cell tracked red and transfected with a fusion protein (GALV or p14) were mixed with a population of DLD-1 cells stained with CSFE (green) 6 hours after transfection. The cells in coculture were allowed to grow for 48 hours before fixing and running them on the flow cytometer (ATTUNE). The data points in the graph represent 3 technical repeats and the bars show the mean percentage of double positive cells. Error bars represent +/- Standard Deviation.

3.3.9 Homocellular Syncytia formation analysis using Tet-Repressor System

In an attempt to further refine the process of quantification of syncytia formation, we utilized the Tet-Repressor System (the plasmids used in these studies were a kind gift from Dr.

Weihang Su). The Tet systems are operon-based technologies where the interaction or fusion of different proteins on the operator or repressor regions impart an effect on the expression or repression of the downstream gene on the operator system. Figure 3.9 provides an overview of the Tet-Repressor system and how we utilized it in our study. Briefly, the Tet-repressor system we used entailed the use of two plasmids; pSF-CMV-TetR-Vp16, which was the plasmid containing the Tet Repressor in combination with the Vp16, the expression of which is essential for the activation of the Tet operon. The second plasmid was the pSF-7xTetO-CMV-EGFP, which was the plasmid expression the Tet Operon, and an EGFP which would only be activated if the Tet Operon was activated (following binding of the Vp16 protein to the Tet Operon). In order to utilize this system for quantifying syncytia formation, we developed an assay where one set of cells were cotransfected with the CMV-TetR-Vp16 and GALV, and then cocultured with another set of cells transfected with the pSF-7xTetO-CMV-EGFP (no GALV was transfected to these cells). The idea behind this setup was that cells will only express EGFP once syncytia formation had occurred since the Vp16, which is essential for Tet-Operon activation was present in cells expressing GALV. A crucial aspect of this assay is that a positive fluorescence readout is dependent on a physical interaction of molecules from the different cells within the fused syncytial cytoplasm, removing any possibility of imaging artefacts from apparently coincident stains.

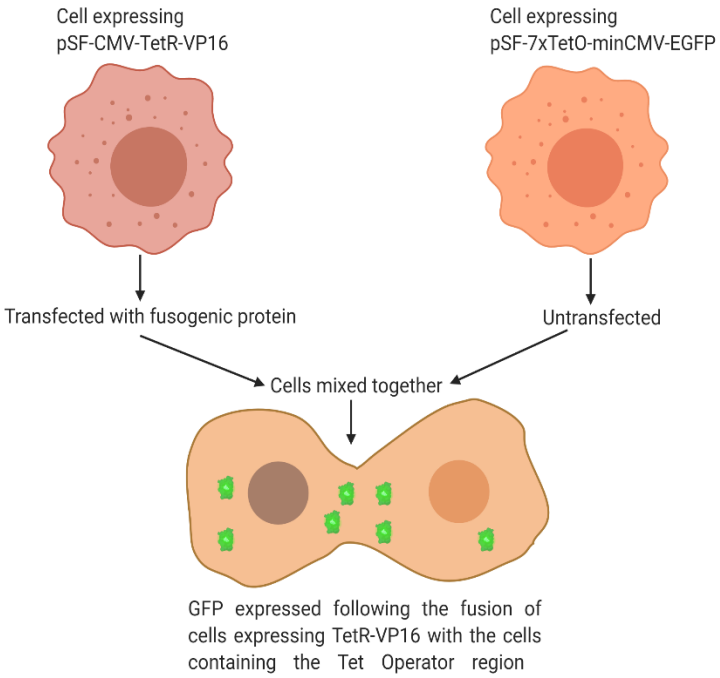

Figure 3.9: Tet-Repressor System. The assay was developed such that cells were transfected with the TetR-Vp16 and GALV, and then cocultured with cells expressing the TetO-CMV-EGFP. The expression of EGFP in the coculture represents cells that have successfully undergone cell fusion, enabling the interaction of Vp16 with the Tet Operon.

The use of this system in the context of syncytia formation enabled us to explore the extent of fusion caused by GALV. The setup for these experiments included co-transfection of GALV with the Tet-Repressor construct, and the transfection of the Tet-operator-EGFP construct in separate wells/set of cells. Following these transfections, the two different cell populations were cocultured 6 hours later, and allowed to grow for 48 hours before being analysed through CELIGO (cell cytometry). Figure 3.10 shows the results for using the experimental system explained in the above section. Cell imaging showed expression of the EGFP following fusion of cells (3.10C and D). The positive control was the pSF-GFP for checking successful transfection (3.10A), and the negative control was a coculture of cells expressing the TetR-Vp16 and cells expressing TetO-EGFP without any fusion protein involved (3.10B). A background level of EGFP expression was observed in the negative control, which could be due to autofluorescence.

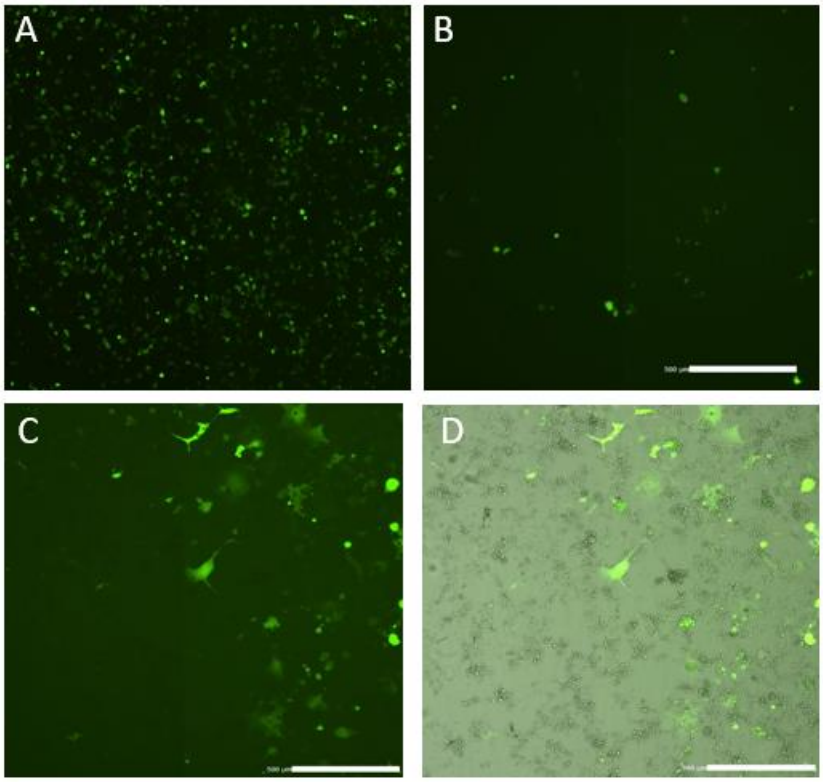

Figure 3.10:GALV mediated fusion of DLD-1 cells and activation of TetO-EGFP post fusion. (A) positive control of pSF- GFP, (B) negative control, coculture of cells expressing TetR-Vp16 and cells expressing TetO-EGFP without any fusion protein involved. (C-D) coculture of cells expressing TetR-Vp16 and cells expressing TetO-EGFP and GALV. The cells were imaged through CELIGO imaging 48 hours after coculture.

Since imaging of the experimental setup was carried out using the CELIGO cytometer, we also utilized the software package of the said system to carry out EGFP expression quantification. The expression analysis option in the software was used to measure the integrated intensity of EGFP expression. The calculation for achieving the estimate of EGFP expression per well was carried out as follows:

Integrated Intensity of EGFP Expression: Mean integrated intensity (for single cell) x number of cells per well.

The formula provided the total expression of EGFP per well, accounting for overall EGFP expression from all the cells in a single well. Having calculated the integrated intensity, we could quantify syncytia formation, and thereby represent it graphically, as shown in figure 3.11.

Using a co-transfection of the Tet-Repressor and Tet-Operator successfully led to EGFP expression of upto 5-10^6 while the use of the GALV fusion protein to fuse cell populations containing the different components of the Tet-Repressor system led to an EGFP expression rate of around $1.5x10^7$, indicating that fusion had occurred and possibly led to much better interactions of the Tet-Operator and Vp16 protein as compared to when the two plasmids were co-transfected in the same cell population. The Tet-O EGFP plasmid on its own was used to estimate for any auto-fluorescence in the system, the total number of cells expressing EGFP in these wells accounting to negligible levels of integrated intensity of EGFP expression. The use of this experimental setup not only helped in quantifying the syncytia formation but also provided the dual advantage of imaging and graphically representing the fusion data, thereby leading to a real-time analysis of the imaging data for studying syncytia formation.

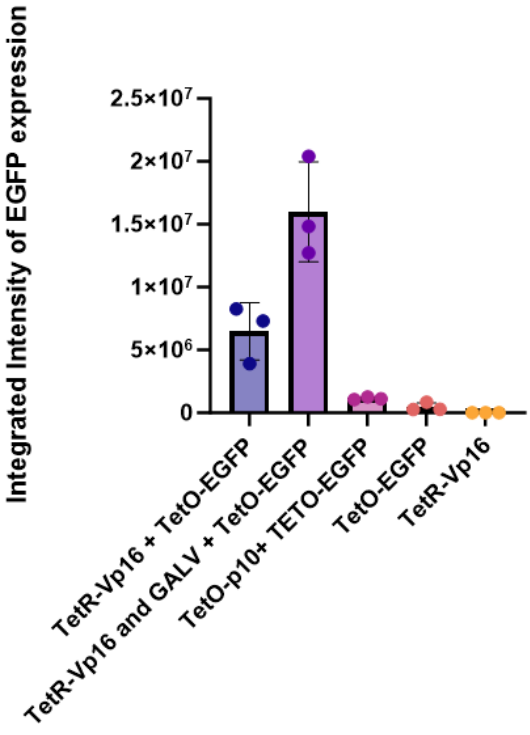

Figure 3.11: Quantification of GALV mediated syncytia using the Tet-Repressor system. An estimate of the integrated intensity of EGFP expression was calculated using the 'Expression Analysis' method in the CELIGO cell cytometer software package. The data points in the graph represent 3 technical repeats and the bars show the mean integrated intensity of EGFP expression. Error bars represent +/- Standard Deviation

3.3.10 Promoting phagocytosis of cancer cells by APC

Phagocytosis in the context of cancer treatment has is important for achieving tumour immunity. The engulfment of cancer cells by APCs leads to their degradation, followed by processing, and presentation of tumour associated antigens to T cells through the MHC molecules present on the APC surface. Tumour cells can evade phagocytosis by APCs by expressing anti-phagocytic signals on their surface, such as the CD47 ligand, or PD-L1. From a treatment perspective, identifying the phagocytic potential of APCs is an approach that could lead to developing therapeutic strategies targeting the APCs. The phagocytic potential of macrophages towards cancer cells was studied using macrophages (M1 polarized) derived from healthy peripheral blood mononuclear cells (PBMCs). Figures 12 and 13 represent the results for phagocytosis of A549 cells and DLD-1 cells respectively, by M1 macrophages. The experiment was carried out using cancer cells cocultured with macrophages for 48 hours before being stained with fluorescent antibodies; anti-EpCAM for cancer cells, and anti-CD11b for macrophages. Following staining, the cells were run through a flow cytometer (ATTUNE) and gated for detecting those cell populations that had become positive for both markers (anti-EpCAM and anti-CD11b). These double positive populations were accounted as phagocytosed cancer cells. In the case of A549 cells (figure 3.12), at the 3-hour time point (3.12 A), there was no significant phagocytosis detected, with a maximum of about 8% cells appearing double positive for cancer and APC markers. Interestingly, after 48 hours of coculture (3.12 B), the same percentages of double positive cells was detected, indicating the phagoctysis had not occurred to a significant level. The anti-CD47 antibody was used as a positive control for detecting phagoctysis, and significant phagoctysis was detected in the wells containing the antibody, at both, 3 hours and 48 hours' time points.

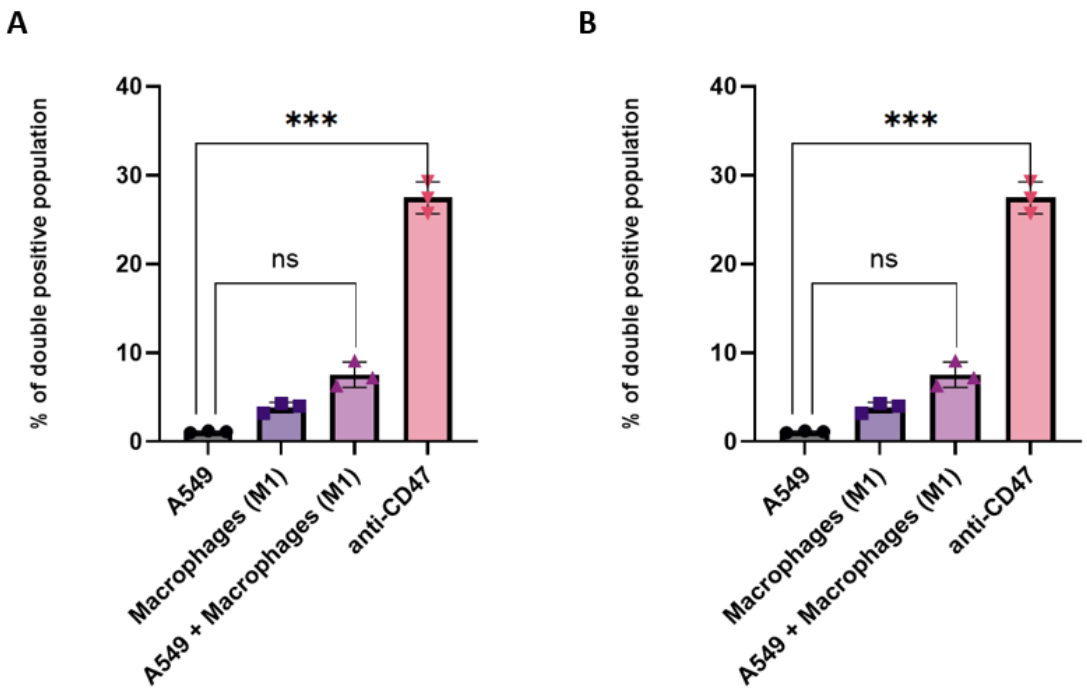

Figure 3.12*:* Phagocytosis in A549 cells. A549 cells were cultured with M1 polarized macrophages and stained with fluorescent antibodies specific for the different cell types at a (A) 3-hour time point and the (B) 48-hour time point. The anti-CD47 antibody was used as a positive control. The data points in the graph represent 3 technical repeats and the bars show the mean percentage of fused cells. Error bars represent +/- Standard Deviation Statistical significance was assessed using the two-way ANOVA test. Significance was assessed versus A549 cells cultured alone as a negative control (ns $p>0.05$, and ***$p\leq0.001$).

While using the DLD-1 cells for estimating the extent of phagocytosis by APCs (figure 3.13), at the 3-hour time point (3.13 A), there was no significant phagocytosis detected, with a maximum of about 7% cells appearing double positive for cancer and APC markers. However, after 48 hours of coculture (3.13 B), the percentages of double positive cells was found to be increased slightly and reaching a maximum of about 10%, indicating the phagoctysis had not occurred to a slightly significant level (*$p\leq0.05$). The anti-CD47 antibody was used as a positive control for detecting phagoctysis, and significant phagoctysis was detected in the wells containing the antibody, at both, 3 hours and 48 hours' time points.

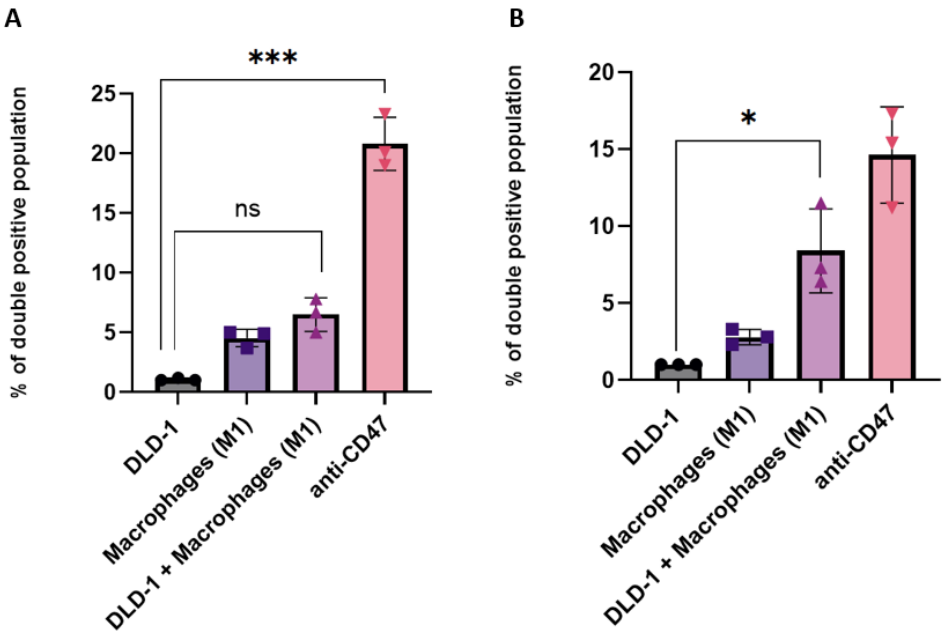

Figure 3.13: Phagocytosis in DLD-1 cells. Phagocytosis in DLD-1 cells. DLD-1 cells were cultured with M1 polarized macrophages and stained with fluorescent antibodies specific for the different cell types at a (A) 3-hour time point and the (B) 48-hour time point. The anti-CD47 antibody was used as a positive control. The data points in the graph represent 3 technical repeats and the bars show the mean percentage of fused cells. Error bars represent +/- Standard Deviation Statistical significance was assessed using the two-way ANOVA test. Significance was assessed versus A549 cells cultured alone as a negative control (ns $p>0.05$, *$p\leq0.05$, **$p\leq0.01$, and ***$p\leq0.001$).

These data indicate that the occurrence of phagocytosis upon the interaction of cancer cells with macrophages either occurred at a very slow rate, which could not be truly significant at the 48-hours' time point or that the phagocytic potential of APCs towards the cancer cells used was quite low. Arguably, the APCs performed slightly better towards phagocytosing the DLD-1 cells as compared to the A549s but the significance of these results are not high enough to be truly conclusive. Our results are in line with the existing data on phagocytosis in cancers, which indicate that tumour cells develop resistance towards the action of APCs due to the gain of immune modulating markers on their surface.

3.3.11 Heterocellular Syncytia formation by GALV and p14

After successfully testing the syncytia forming potential of GALV and FAST p14, we next moved on to identifying the potential of these fusion proteins in a heterotypic setting. The aim here was to enable fusion between cancer cells and APCs with the idea that such a fusion would

lead to killing of the tumour cells along with possibly leading to improved antigen presentation through such cell fusions. The experimental design for studying heterocellular syncytia was similar to that explained in the earlier sections for homocellular syncytia. DLD-1 cells were stained with CFSE green, transfected with either GALV or p14, and then co-cultured with PBMC derived macrophages that were stained with Cell Tracker Red. The coculture was then observed under a confocal microscope at 24 hours and 48 hours, after staining with the nuclear stain DAPI right before imaging. Figure 3.14 shows the representative images of heterocellular syncytia formed between cancer cells and macrophages at 24 hours (3.14 A and C), and 48 hours (3.14 B and D). The fused cells are annotated by yellow circles in each of these images. As observed in the images, p14 appeared to be quicker and more advanced at heterocellular syncytia formation as compared to GALV. At the 24 hour time point, GALV (14A) had extremely few and small sized syncytia. The number of syncytia found in the wells transfected with GALV increased at the 48 hours time point (3.14B), the yellow circle in the image represents a giant cell representing fused macrophages and cancer cells, appearing pink due to the combination of red, green, and blue dyes following fusion. The presence of multiple nuclei (blue), surrounding by little to no cytoplasm pointed towards a giant cell structure. However, at the same time, there were still more single cells in the wells transfected with GALV than there were syncytia. On the contrary, the use of p14 led to rapid syncytia formation, multiple giant structures were observed at the 24 hour time point (3.14C), and the overall cell size seemed to increase remarkably at the 48-hour time point (3.14D). These data point towards p14 having a higher potential for heterocellular syncytia formation as compared to the GALV, which is in line with our hypothesis as the FAST proteins are receptor-independent in their fusion pathway, and therefore are likely to be more promiscuous in the way they lead to heteroypic cell fusions.

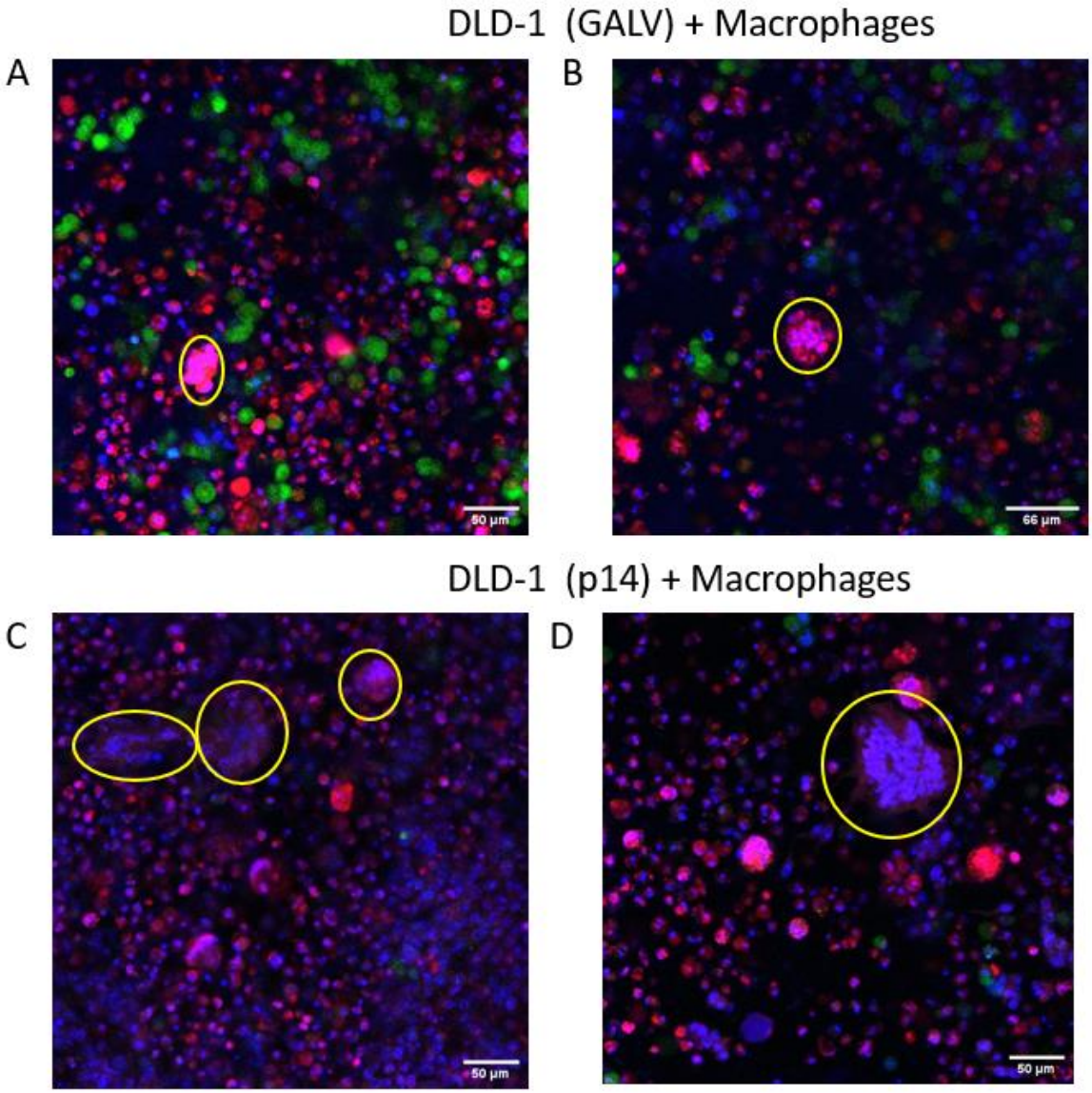

Figure 3.14: Confocal Microscopy for Heterocellular syncytia, Cancer cells stained with CSFE green and transfected with either GALV (A-B) or p14 (C-D) were cocultured with Macrophages that were stained with cell tracker Red. The cells were then analysed under a confocal microscope at 24-hours and 48-hour time points. (A) heterocellular syncytia by GALV in 24 hours (B) heterocellular syncytia by GALV in 48 hours, (C) heterocellular syncytia by p14 in 24 hours, and (D) heterocellular syncytia by p14 in 48 hours.

Having confirmed heterocellular syncytia formation through imaging, we next used flow cytometry to analyse and possibly compare the syncytia formation potential of the two fusion proteins in a more quantified manner. DLD-1 cells were transfected with GALV or p14, untransfected DLD-1 cells were used as negative control, 6 hours after transfection, these cells were cocultured with PBMC-derived macrophages. The cells were stained with fluorescent

anti-bodies; anti-EpCAM for cancer cells, and anti-CD11b for macrophages. The gating was applied to account for cells that appeared for both antibodies (double positives), indicating that fusion had occurred between the two types of cells. Figure 3.15 shows the heterocellular syncytia formed using GALV and p14, the percentage of double positive cells was significantly higher as compared to the negative control (no fusion protein used) when using the fusion proteins, indicating the formation of syncytia. Both GALV and p14 had similarly significant levels of double positives in comparison to the negative control, with p14 being slightly higher in terms of percentage (30%), as compared to GALV (22%). These results are again, in line with our hypothesis that p14 is more promiscuous and efficient in its potential for heterocellular syncytia formation as compared to GALV, which is a receptor dependent fusion protein.

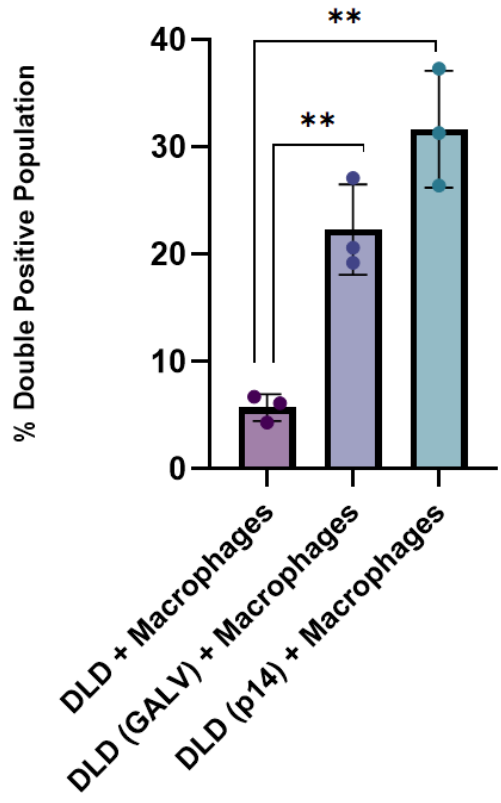

Figure 3.15: Flow cytometry for heterocellular syncytia. DLD-1 cells were transfected with either GALV or p14, and then cocultured with macrophages, untransfected cancer cells were used a negative control. The cells were stained with anti-EpCAM, and antiCD11b, and then gated for double positive cells during flow cytometry (ATTUNE), to look for fused cells. The data points in the graph represent 3 technical repeats and the bars show the mean percentage of fused cells. Error bars represent +/- Standard Deviation Statistical significance was assessed using the two-way ANOVA test. Significance was assessed versus A549 cells cultured alone as a negative control (ns $p>0.05$, *$p\leq0.05$, and **$p\leq0.01$).

3.3.12 Anti-CD40 in heterotypic cell fusions

The role of an anti-CD40 molecule in facilitating the interactions between cancer cells and APCs is known to lead to activation of the APCs. Using a super agonist, membrane anchored anti-CD40 molecule expressed from cancer cells was explored in this study to check if using such a molecule could possibly cause an increase in the syncytia formation of cancer cells and APCs. The anti-CD40 molecule was therefore used either on its own, or in combination with either GALV or p14 to test the extent of syncytia formation in each of these cases. Figure 3.16 shows the results for heterocellular syncytia in A549 (3.16A) and DLD-1 (3.16B) cells. In both the cell lines, it was observed that the heterocellular syncytia caused by GALV and p14 were significant as had been established in the prior section. The point of interest in this experimental setup was the use of the membrane anchored anti-CD40, which seemed to cause cell interactions between cancer cells and APCs to a similar level as that achieved by the fusion proteins even when used on its own. In both the cell lines used, the combination of GALV and anti-CD40 did not seem to bring any observable change in the cell fusions as compared to using each of these proteins their own. However, the combination of p14 and anti-CD40 seemed to have a highly significant ($p \leq 0.0001$) effect on syncytia formation as compared to the negative control, and even when compared with the use of anti-CD40 alone, the combination of anti-CD40 and p14 was significant ($p \leq 0.0001$). These data point towards the usability of the p14 in combination with the anti-CD40 in that this combination seems to lead to significantly higher cell fusions then with any other case scenario explored.

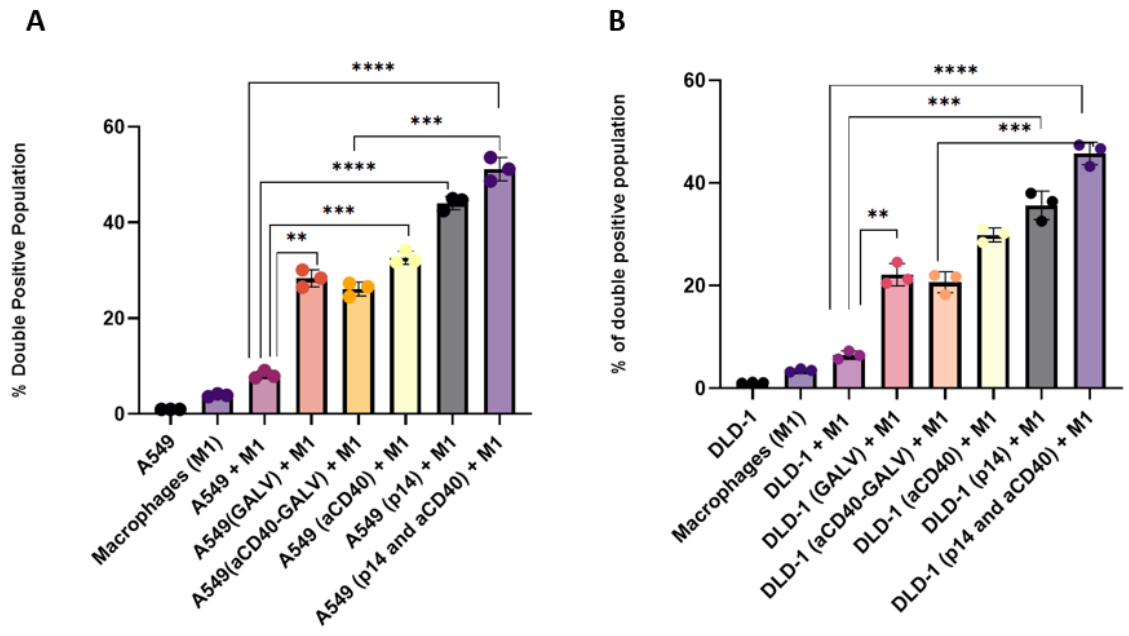

Figure 3.16: Membrane anchored anti-CD40 in combination with fusion proteins for estimating heterocellular interactions and subsequent fusion. Cancer cells (A) A549 and (B) DLD-1 were transfected with different combinations of fusion protein and anti-CD40, and then cocultured with macrophages. The cells were stained with fluorescent antibodies (anti-EpCAM and anti-CD11b) and then analysed through flow cytometry. The data points in the graph represent 3 technical repeats and the bars show the mean percentage of fused cells. Error bars represent +/- Standard Deviation Statistical significance was assessed using the two-way ANOVA test. Significance was assessed versus A549 cells cultured alone as a negative control (ns $p>0.05$, *$p\leq0.05$, **$p\leq0.01$, *** $p\leq0.0001$and ****$p\leq0.0001$).

These findings provide insights into the comparison of GALV and p14 with a deeper aspect, as the use of a super agonist anti-CD40 with these fusion proteins seems to be quite different in each case. While the fusion potential of p14 remarkably increased with the use of the anti-CD40 agonist, there seemed to be no effect on the GALV mediated fusions when it was paired with anti-CD40. This could be due to the fusion pathways of the two proteins, and the different in their sizes, which could lead to a starking stearic difference in their placement within the cell membrane, and hence the potential of leading to fusion with neighbouring cells. GALV is a large protein (2000 basepairs), with 7 transmembrane domains in its structure, and depends on the presence of the PiT-1 receptor on the neighbouring cells for mediating fusion. The use of a large protein in combination with the membrane anchored anti-CD40, which also embeds in the cell membrane could possibly be causing a stearic hindrance in the interaction and action of these proteins with their respective receptors due to the complex structures of each. On the

other hand, the p14 is relatively small (200 base pairs), and has a promiscuous binding pattern in that it does not depends on receptor for fusion, and uses the cell-adhesion proteins for initiating fusion. The use of such a protein with the membrane anchored anti-CD40 is possibly better in terms of physical interactions of these proteins when expressed together, thereby causing a significant increase in the formation of heterocellular fusions.

3.4 Discussion

The experiments and results in this chapter explored the syncytia forming potential of GALV and p14, which are different types of viral fusion proteins. The overall aim was to identify if these proteins could be utilized for killing of cancer cells when expressed in those cancer cells. Moreover, the potential of heterocellular syncytia formation from these cells was also explored by co-culturing cancer cells with APCs. The role of syncytia in the lysis of cancer cells is evident from literature, and GALV in particular has been used in a number of different studies for causing fusion of cancer cells and subsequent cell death. The key mechanism of killing by fusion is the instability caused by merging of multiple cells such that the cytoplasm of multiple cells becomes enclosed inside a single membrane and the nuclei is pushed to the center, as has been shown through our results as well. A large cell with multiple nuclei and bulking cytoplasm eventually becomes unstable and cell death occurs due to loss of nuclear control over the giant cell, and leakage of cytoplasm due to membrane instability. Such cell death occurs even when the same types of cells merge, thereby making cell fusions an interesting approach for killing cancer cells. The use of FAST proteins has also been explored and found to have similar killing effects on cancer cell. The comparison of the two types of fusion protein is important from the point of their mechanism of recruiting cells into a fused state. The FAST proteins are among non-structural proteins of the reovirus and are used during the viral life cycle for increasing their virulence and spreading to nearby cells through cell fusions. An interesting point in this

type of a fusion protein is that it utilizes the cell adhesion molecules and thereby potentially could have a higher rate and wider range of fusion as compared to GALV. Our data confirm this hypothesis through the quicker homocellular and heterocellular syncytia formed when using p14 as compared to GALV. While GALV is definitely capable of forming heterocellular syncytia between cancer cells and APCs, the rate of fusion appeared to be better and quicker when p14 was used.

The data for heterocellular syncytia indicates that both GALV and p14 significantly lead to heterfusions. The use of antibodies against cancer cells and APCs make the detection of fusion quite reliable in that, the presence of both these antibodies detected in the same cell points towards their fusion. The use of flow cytometry in this case was therefore provided insights about the fusion of cancer cells and APCs in the presence of fusion proteins. These data sets are also to be compared with the phagocytosis data present in this chapter, where the absence of any fusion protein also shows a small level of double positive outcome, indicating interaction of the cancer cells and APCs. This is not surprising since macrophages are potent phagocytic cells and can lead to engulfment of cancer cells even in the absence of any aiding factor. However, the key here is to look at the extremely low levels of phagocytosis, which could indicate that the cancer cells have resistance towards the action of macrophages. The presence of anti-phagoctyic markers on cancer cells is a known factor and could be one of the reasons that we saw low levels of double positives when checking for cell interactions without any fusion proteins involved.

The use of a super agonist anti-CD40 molecule covered the aim of exploring ways to enhance the interactions between cancer cells and APCs when cultured together. Since the tumour microenvironment does have APCs surrounding the tumour, the goal was to explore if an anti-CD40 molecule expressed on the surface of cancer cells led to increased interactions with the APCs. To this end, we did observe the anti-CD40 having a significant effect on the interactions

of the two cell types, as is shown through the levels of double positive cells seen through flow cytometry when cancer cells expressing the anti-CD40 were co-cultured with the APCs. We also used the anti-CD40 in combination with GALV and p14, with the aim of exploring if the presence of fusion proteins along with the APC specific anti-body could lead to a further increase in cell interactions. The results showed that there was no significant effect of using the anti-CD40 with GALV. However, when used in combination with p14, the heterocellular fusions were pronouncedly higher than seen while using any other conditions. This could possibly reflect on the differences of fusion mechanism used by the two fusion proteins used. The two proteins are not only different in their mechanisms of action, but also in their structure, which could be one of the reasons that they have different effects when used with another membrane anchored molecule. The multiple transmembrane domains in GALV possibly take up more space and lead to slower interactions with nearby cells, especially when another membrane anchored molecule is expressed from the same cell. On the other hand, the p14 has a single transmembrane domain and might be physically placed on the cell membrane in a manner that causes no barrier to the expression and action of the anti-CD40. While we have not explored these interactions through any molecular anlaysis, the effects of these proteins on heterocellular fusions remains interesting and provide a direction for exploring more cellular interactions. In particular, the extent of fusion of cancer cells and APCs while using different fusion proteins or antibodies is of great importance as we next set to explore what effect this process has on the antigen presentation once APCs interact with the tumour.

4. Cross-Presentation of Tumour Antigens

4.1 Introduction

Antigen -presenting cells (APC) take up antigens from the environment and usually process them for presentation on MHC-II molecules for stimulation of CD4 helper cells, which can then play a role in confirming activation of B cell clones to produce antibodies. However, some APC also have the ability to present antigens on MHC-I molecules to promote activation of CD8 cytotoxic T cells. This process is called 'cross presentation' (Bevan, 1976; Rock & Shen, 2005). In more detail, cross-presentation is the ability of professional APCs to uptake antigens from other cells or from the environment, process and present them on MHC-1 molecules for recognition by the TCR expressed on CD8+ T cells. For successful stimulation of new T cell clones this process requires two other components – simultaneous presentation of MHC-2 epitopes on the same APC leading to activation of a cognate CD4 helper T cell coupled with cytokines (including CD40) produced either by the APC or the T helper cell that can stimulate the CD8 cell (Hoffmann, Meidenbauer, Müller-Berghaus, Storkus, & Whiteside, 2001). Stimulation of the cytotoxic T cells in this way leads to their proliferation and activation of the cytotoxic activities of these T cells. The process of cross-presentation is central to the activation of new cellular immune responses, and provides not only a key aspect of vaccination against infectious diseases but also constitutes an essential feature of any cancer vaccine approach.

In the classic sense, dendritic cells are known for being the major cell-type capable of cross-presentation. Within the dendritic cell populations, there exist the specific sub-type, the cDC1 (conventional DCs) which are known to be specialized antigen cross-presenting cells. Other DC populations, and macrophages can also cross-present antigens, depending on the development and maturation stages of these APCs (Le Gall et al., 2021). The role of cytokines,

such as granulocyte–macrophage colony-stimulating factor (GM-CSF), is important in the development of cross-presenting APCs.

Studies exploring antigen cross-presentation and the pathways involved in the phenomenon have looked at the signals and markers that possibly activate DCs to cross-present antigens. Although there are still a lot of unanswered questions, and gaps in the understanding on what makes an APC present antigen to the MHC-I over the MHC-II, there is agreement on the cDC1s being the most efficient subclass of APCs that can cross-present antigens. A minority group of cDC1s are $CD8^+$ and $CD103^+$(in mice), and are found to be particularly capable of cross-presenting antigens from dying cells (Sathe et al., 2011). The human counterpart of the mouse $CD8^+$ cDC1s include the expression of the CD141 marker, and are capable of efficiently cross-presenting antigens (Poulin et al., 2007).

There are many macrophages and few dendritic cells within most solid tumours, hence formation of hybrid syncytia between tumour cells and myeloid cells within solid tumours will likely involve macrophages. There is some evidence that proinflammatory macrophages can be involved in cross-presentation of antigens from virally infected cells, leading to the activation of cytotoxic T cells, and antiviral actions (Bernhard, Ried, Kochanek, & Brocker, 2015). Whether the same occurs in the context of a tumour is not truly established. In context of this study, since we were using fusion proteins, we hypothesised that cross presentation by macrophages might be substantially improved by formation of heterotypic syncytia. The presence of tumour antigens in the same cytoplasm as that of the macrophage immunoproteasome (after fusion of the two cell types) could lead to antigen presentation through the MHC-I pathway, thereby bypassing the need for endosomal escape and promoting cross-presentation. Accordingly the role of the proinflammatory macrophages in priming anti-tumour responses make them an interesting candidate in this area of cancer vaccine research.

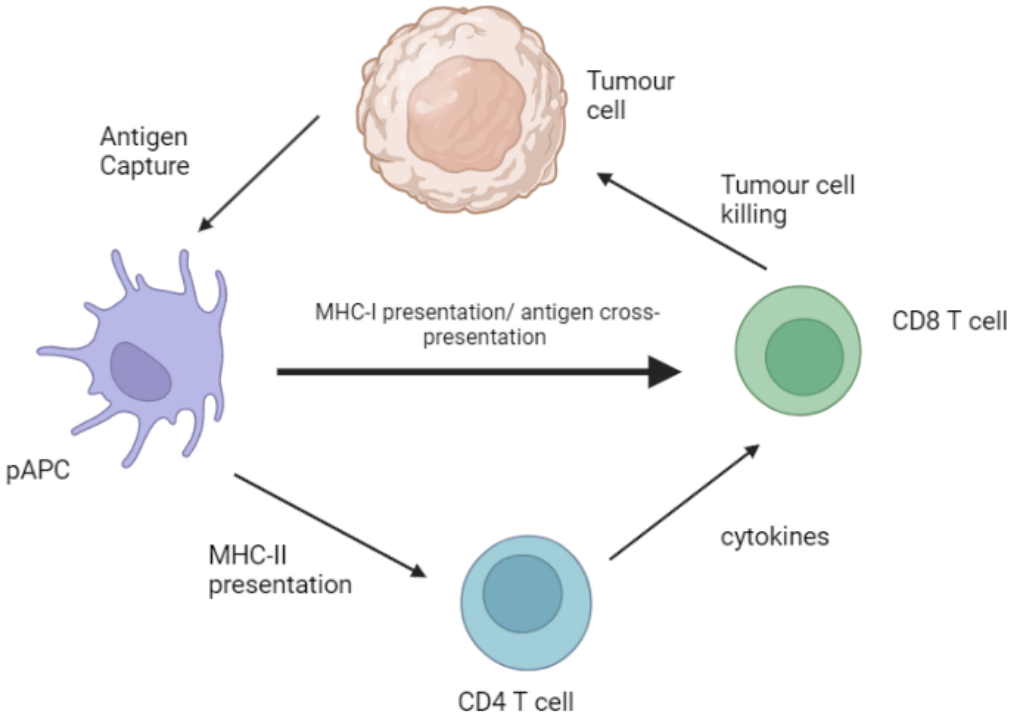

Figure 4.1: Schematic of Antigen Cross Presentation – the tumour antigens once successfully captured by APCs, are presented via MHC-I molecules to the CD8+ T (cytotoxic) cells. This presentation and activation of the CD8 T cells makes up the phenomenon of antigen cross-presentation. The successful activation of cytotoxic T cells also requires support from cytokines which are released by the CD4+ (helper) T cells. The CD4+ T cell activation is also caused by the APCs that process the tumour antigens and present it to the helper T cells via MHC-II presentation pathway.

4.2 The roles of CD40 in antigen presentation and antigen cross presentation

CD40 super agonist antibodies are designed to mimic the CD40 ligand whilst avoiding the need for antibody trimerization, and are highly potent at activating the APCs (Uno et al., 2006). The key role of CD40 in licensing APCs for T cell priming is critical for achieving an immune response against TAAs (Pilon et al., 2009). In this study, along with the use of fusion proteins, the use of a super agonist anti-CD40 antibody anchored to the cancer cell membrane was explored with the aim of achieving higher chances of greater binding between cancer cells and APCs with simultaneous activation of the APC through CD40. The use of a membrane anchored anti-CD40 expressed from the cancer cells, along with a fusion protein could potentially make the cancer cell much more likely to interact and fuse with APC whilst simultaneously activating them.

4.3 Model System

The model system proposed for studying the phenomenon of cross-presentation in vitro was developed to analyse the uptake and processing of tumour antigens by APCs, and their subsequent presentation to cytotoxic T cells. The model system that was employed and further developed as part of this project included NY-ESO-1 peptide expressing cancer cells (DLD-1), PBMC-derived macrophages (M1 polarized) as the professional APCs, and reporter Jurkat cells (having the NFAT reporter comprised of GFP controlled by the NFAT promoter) specific for the recognition of NYESO-1 in the context of MHC-1 only. The concept behind the assay is that the Jurkat reporter cells will express GFP following stimulation of the NFAT promoter when they recognize the NY-ESO-1 peptide on the APCs. This is a simple measure of CD8 T cell stimulation, and allows study of the TCR activation mediated on the Jurkat cell by antigen-reocognition, without involvement of CD4 helper cells. Although this is arguably not full 'cross-presentation', since some studies reported below include stimulation of CD40 on the APC the definition is rather blurred. For simplicity we have referred to the assay as a cross-presentation assay, since that is the biological process it seeks to elucidate.

Essential to this model is that the cancer cells are HLA-A*02-negative, the APCs are HLA-A*02-positive, and the reporter cells only recognize HLA-A*02-restricted peptides, thereby ensuring that any fluorescence activity by the Jurkat reporter cells will be due to the cross-presentation of the tumour antigen (NYESO-1 in this case) by the APC, and not by Jurkat cells recognising NY-ESO-1 presented on the surface of the cancer cells.

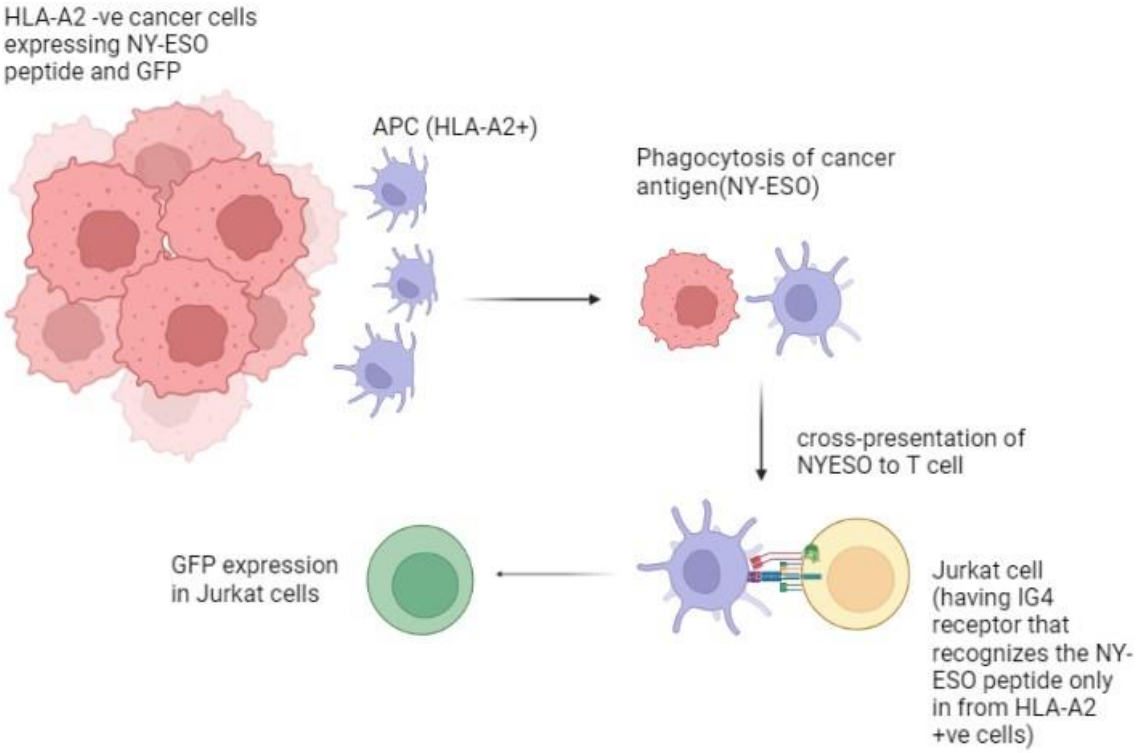

Figure 4.2: Model system for the cross-presentation assay – the cross-priming/cross-presentation assay was designed such that an HLA-A*02 negative cancer cell line expressing NYESO-1 peptide was cocultured with HLA-A*02 positive APCs. The reporter cells in this system were the Jurkat cells having the IG4 receptor that recognizes NYESO-1 only in the context of HLA-A*02 positive cells, thereby ensuring that any Jurkat activation (GFP signal in Jurkats) would reflect presentation of the NYESO-1 through the APCs (meaning they were cross-presented), and not through the HLA-A*02 negative cancer cells.

4.4 Chapter Hypothesis:

Using syncytium-forming proteins to make tumour cell-macrophage hybrids combined with activation of CD40 will bypass the need for endosomal escape and allow cross presentation of tumour cell antigens

4.4.1 Component Aims

1. To develop and validate an in vitro macrophage model system for studying the cross-presentation of tumour antigens
2. To identify the effects of using fusion protein in cross-presentation of tumour antigens
3. To improve cross-presentation through the use of an anti-CD40 agonist expressed on the surface of cancer cells

4.5 Results

4.5.1 Developing the cross-presentation assay

An *in vitro* cross-priming/cross-presentation assay using cancer cell lines and primary macrophages and T cells (originally developed by Dr Ahmet Hazini in our laboratory with early work performed by Vivian Lau) was developed for studying the potential of syncytium-forming and CD40-agonising proteins in promoting successful cross-presentation of cancer antigens. HLA-mismatched cancer and macrophage cells were used to determine whether antigens were cross-presented, and to allow quantification of CD8 T cell stimulation.

As shown through the model system in Figure 1, a stable HLA-A2 negative human cancer cell line (DLD1 colorectal carcinoma) expressing an NYESO-1 peptide was used (a kind gift from Dr Margareta Rei and referred to hereinafter as DLD-$1_{NYESO-1}$ cells). The cancer cells were transfected with a plasmid encoding the fusion protein (and/or the anti-CD40) and then co-cultured with HLA-A2 positive human APCs (M1 macrophages in this set of experiments) with the aim of increasing antigen uptake and subsequent cross-presentation. The syncytium-forming proteins were intended to promote heterocellular syncytia formation between cancer cells and macrophages, aiming to allow direct processing of cancer antigens for loading onto the macrophage class I MHC molecules. In contrast the membrane-bound CD40 agonist was intended both to activate the macrophages and also to increase physical association between tumour cells and macrophages to promote either phagocytosis or syncytium formation. All of these mechanisms could have the effect of enhancing the efficiency of cross presentation.

The reporter cell line in this system were Jurkat cells (engineered to express the NFAT reporter, a kind gift from Dr Margareta Rei), that would express GFP only if they recognized the NYESO-1 peptide in the context of MHC-1. The readout for this assay was therefore the GFP expression, measured mainly through the use of flow cytometry. Briefly, the assay started with transfection of cancer cells to express syncytium-forming proteins and/or CD40 agonist, then

co-culturing them with M1 macrophages 6 hours after transfection to allow cross presentation to occur. Addition of the Jurkat cells 24-hours after the coculture would allow them to recognise any cross-presentation of NYESO-1. The combination of these three cell-lines was then allowed to grow and interact together for a total of 4 days (96 hours) before staining with antibodies and analysing through flow-cytometry. The antibody staining involved the use of an anti-EpCAM (for cancer cells), anti-CD11b (for macrophages), and anti-CD8 (for Jurkats). The gating of cells in the flow cytometry involved identifying the total number of CD8+ cells per well, and then looking for how many of those cells expressed GFP (green signal). The percentage of GFP expression was then taken as the final estimate of cross-presentation of the NYESO-1 peptide to the Jurkats, starting from the cancer cells through macrophages.

Figure 4.3 represents the initial run of this assay in A549 human long adenocarcinoma cells expressing NYESO-1 peptide. The controls used in this setup included the HLA-A2 negative M1 macrophage population as the negative control for cross-presentation. The free NYESO-1 peptide was used as the positive control, intended to load directly onto macrophage class I and leading to over 60% of Jurkat cells expressing high levels of GFP. Controls such as cancer cells with Jurkats but no macrophages gave far lower levels of expression, typically 6-8%, while adding HLA-A2-negative macrophages gave an increased basal level of about 20%. Exactly why this occurred was unclear, but suggests perhaps NY-ESO-1 peptides presented by other MHC isotypes can be recognised, to some extent, by these Jurkat cells. Transfection of cancer cells with increasing amounts of GALV, with HLA-A2-negative macrophages also showed a small enhancement of Jurkat stimulation, although this barely exceeded 20%. In contrast, in the presence of HLA-A2-positive macrophages, substantially more Jurkat stimulation was achieved, with GALV showing a dose-dependent enhancement that led to over 40% of Jurkats being activated at the highest dose of GALV. These are encouraging data that suggest the formation of syncytia may for a useful strategy to promote antigen cross presentation.

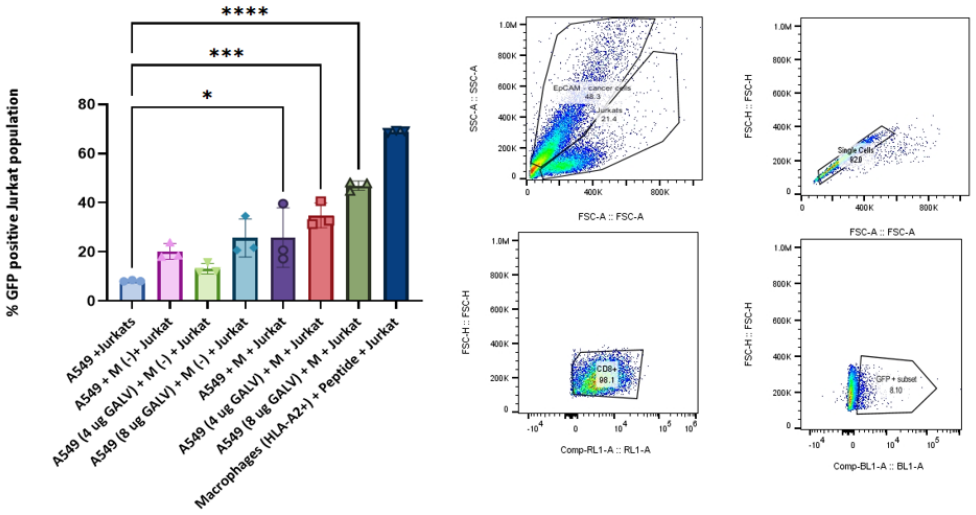

Figure 4.3: **Antigen Cross-Presentation using A549 cells** – The extent of cross-presentation of the NYESO-1 peptide was studied using the model system explained in the section above. The readout for the assay was the percentage of GFP positive Jurkats, analysed through flow cytometry. The cells were gated to select single cells (lymphocytes), followed by gating for the CD8+ T cells, and then among that population, the GFP positive cells. The graph represents the overall GFP positive percentage achieved using different conditions. The data points on the graph represent three biological repeats

As we set up and conducted the assay in the initial development stages, a number of inconsistencies were encountered, mainly in the viability of cells following the coculture steps and the incubation over a number of days. The transfection of GALV in different concentrations was also explored in order to identify which concentration of DNA led to syncytia formation and subsequent optimum antigen cross-presentation. The assay set-up was therefore optimized through a series of steps involving changing the timepoints for co-coculturing, switching cell-lines in favour of DLD-1 cells which appeared more stable post coculture and transfections as compared to A549s, and changing or topping up media at specific time-points during the assay to ensure continued supply of fresh nutrients to the cells, without disturbing the coculture setup.

4.5.2 Anti-CD40 expression

The construct containing membrane-linked antiCD40 was engineered as described in Materials

& Methods, using Gibson assembly. Having verified the correct sequence of the anti-CD40 gene in the bacterial plasmid, we assessed the level of expression of the constructs in the DLD-$1_{NYESO-1}$ cells. The anti-CD40 transgene contained a His-tag, which allowed simple measurement of transgene expression levels. As shown in Figure 4.4, following transfection, the cell lines were stained with an anti-His antibody, and then analysed through flow cytometry. Both the constructs, the anti-CD40-GALV construct, and the anti-CD40 construct showed around 40% expression within 24 hours of being transfected into the DLD-1 cells. Upon confirming that the anti-CD40 constructs were successfully expressed, we included these in the subsequent assays to explore the hypothesis that having an anti-CD40 molecule expressed and anchored onto a cancer cell would increase cancer cell association with macrophages and also activate them, leading to enhanced antigen cross-presentation.

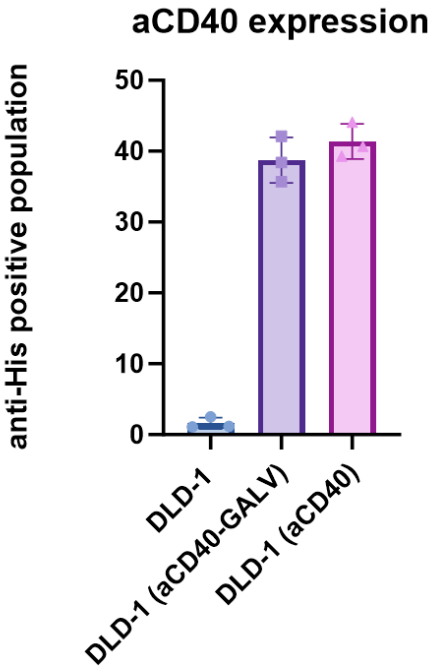

Figure 4.4: Level of expression of the membrane-anchored anti-CD40 on the DLD-1 (NYESO) cells. DLD-1 cells were transfected with the anti-CD40-GALV construct, or the anti-CD40 construct, untransfected cells were used as a negative

control. The data points in the graph represent 3 technical repeats and the bars show the mean percentage of GFP activation. Error bars represent +/- Standard Deviation .

4.5.3 Assay Optimization

The initial study (Figure 3, above) although promising highlighted several technical challenges with the experimental system. For example, there was a very high level of Jurkat cell death, and the percentages of positive cells recorded in Figure 3 actually relate to small numbers of cells. As a first step towards optimizing the assay we introduced a medium change to remove waste products and provide more nutrition, important for optimal Jurkat cell viability. Figure 4.5 represents the results for the step where the culture media was changed 3 days into the assay – where day 1 was co-culturing of cancer cells (A549) with HLA-A2 positive M1 macrophages, Jurkats were added on day 2, and on day 3, the plate was spun down (by centrifugation), the media was removed and fresh culture media (RPMI-10%) was added to the wells. This led to improved cell viability as well as a high percentage of GFP positive cells. The change in viability was not only seen in the overall cancer cell population, but also the Jurkats, which reflected in the overall GFP readout. For example the overall GFP-positive population, which reached a maximum of 30% without media change, was reflective of only a surviving population of 15 to 20% of the original population of Jurkats. However, on changing media, the Jurkat cell population that was alive by the endpoint of the assay increased to 40%, and the total GFP readout was more steadily around 4%. Although it may seem that the GFP expression decreased, it is important to note that this effect was reproducible and associated with the total live population, whereas the 30% readout was associated with a smaller population of cells with very high apoptosis and possible intrinsic autofluorescence.

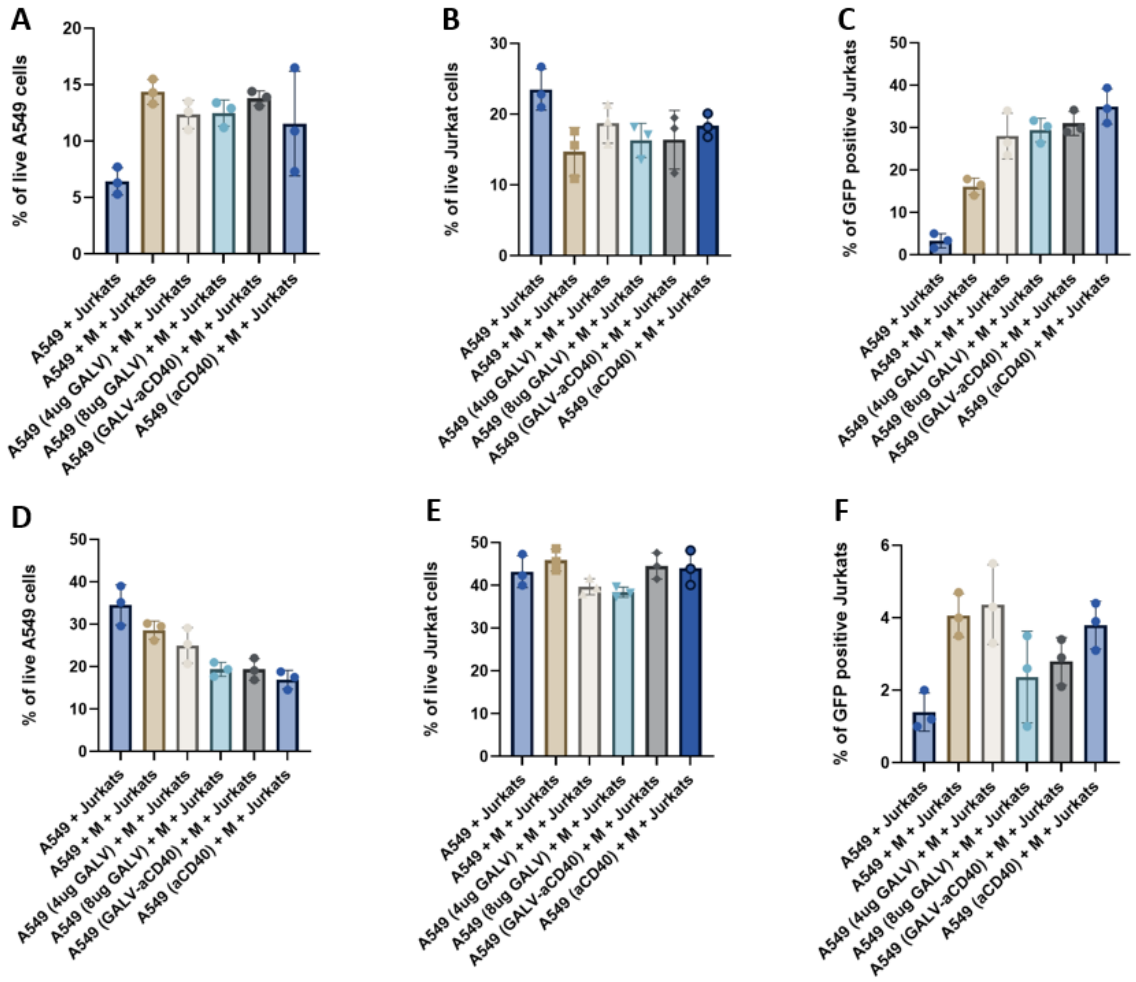

Figure 4.5*: Optimization of the antigen cross-presentation assay in A549 cells* – The cross-presentation assay was refined by comparing the effects of changing the media in the plate on day 3 of the assay. **(A-C) Without media change** – (A) percentage of live A549 cells at the end of the assay, (B) percentage of live Jurkat cells at the end of the assay, (C) Percentage of GFP positive Jurkat cells **(D-F) with media change** - (D) percentage of live A549 cells at the end of the assay, (E) percentage of live Jurkat cells at the end of the assay, (F) Percentage of GFP positive Jurkat cells. The data points in the graph represent 3 technical repeats and the bars show the mean percentage of GFP activation. Error bars represent +/- Standard Deviation.

We also explored the cross-presentation assay using DLD-1$_{NYESO-1}$ (mitochondrial NYESO-1 expressing) human colorectal cancer cells instead of A549 cells. The change in cell viability and overall readout improvement following the introduction of a medium change with DLD-1 cell lines (Figure 4.6) was similar to that seen in A549 cells, above. The percentage of live cancer cells receiving any treatment increased from maximum 40% (Figure 4.6A) to around 70% (Figure 4.6D). The percentage of live Jurkats went from about 18% (Figure 4.6B), to 70% (Figure 4.6E), and the GFP expression remained more or less around 4% of live Jurkats with or without media change (Figures 4.6C and 4.6F). Although it seems that the overall GFP

readout percentage of live Jurkats did not increase in the assay using DLD-1 cells, it is crucial to note that the Jurkat cell viability increased at least 2-fold and this is considered to lead to a truer reflection of the assay readout. This medium-change optimization step led to ensuring that at the end of the assay, the cell populations were more viable, the readouts were more reproducible, and the end result (% GFP positive viable Jurkats) was a truer reflection of the level of cross-presentation that truly occurred without most cells being dead.

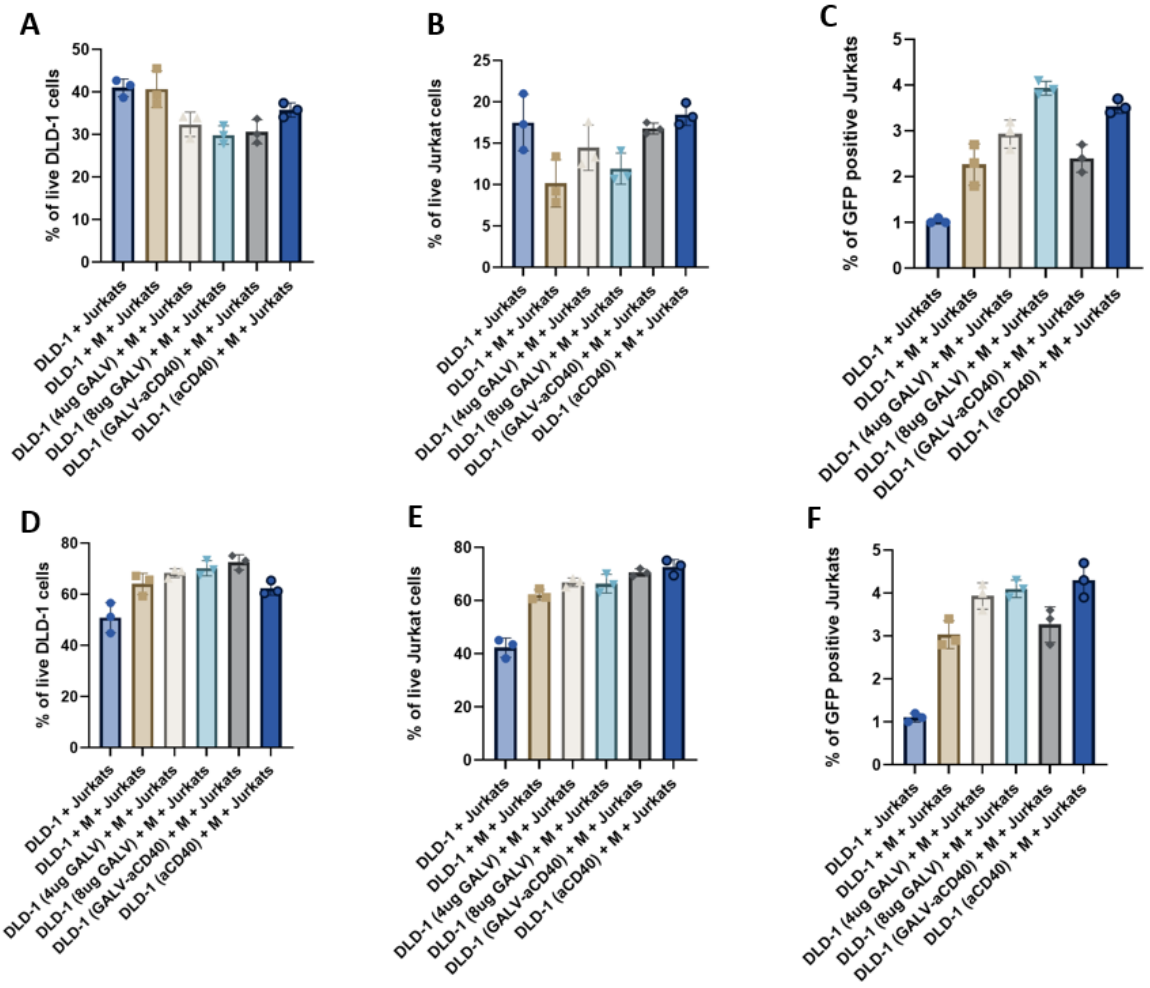

Figure 4.6: Optimization of the antigen cross-presentation assay in DLD-1 cells – The cross-presentation assay was refined by comparing the effects of changing the media in the plate on day 3 of the assay. **(A-C) Without media change** – (A) percentage of live DLD-1 cells at the end of the assay, (B) percentage of live Jurkat cells at the end of the assay, (C) Percentage of GFP positive Jurkat cells **(D-F) with media change** - (D) percentage of live DLD-1 cells at the end of the assay, (E) percentage of live Jurkat cells at the end of the assay, (F) Percentage of GFP positive Jurkat cells. The data points in the graph represent 3 technical repeats and the bars show the mean percentage of GFP activation. Error bars represent +/- Standard Deviation

Overall, as can be seen through figure 5 and 6, in both the cell lines used, not only did the total percentage of viable cancer cells and Jurkat cells at the end of the assay (day 5) increase following introduction of a medium change step, there was also a more stable readout for the GFP positive Jurkat population. The overall percentage of Jurkat cells that were alive by the end of the assay was much higher as compared to the ones we were dealing with prior to media change, where the dead cell percentage was usually too high to get a reliable read-out from the assay through flow-cytometry. Given that the Jurkat cells were largely dead in the previous cases, and the readout was GFP positive Jurkats, there was little to no signal for the desired read-out. In addition, comparing the assay using two different cancer cell lines revealed that the DLD-1 cells remained more stable and the percentages of live cells were much better than when using A549 cells. Having tested and compared the viability and readout feasibility through assay optimization, we moved on to using DLD-1 cells for the assessment of antigen cross-presentation.

Once we had selected DLD-1 cells as the baseline for further assays, there was a choice to be made between two types of NYESO-expressing DLD-1 cells available; one cell line expressing NYESO-1 in the cytoplasm, and another with NYESO-1 expressed through the mitochondria. Among the two cell lines, it appeared that the mitochondrial NYESO-1 expression led to a slightly greater percentage of Jurkat activation (GFP expression) as can be seen in Figure 4.7. The cytoplasmic NYESO-1 peptide led to a maximum of 2.5% GFP expression, while the mitochondrial NYESO-1 cell line led to a GFP positive population of about 4%. Though this difference is small and may be considered insignificant, the consistently better rates of Jurkat activation (tested through technical 3 repeats of the assay) in the mitochondrial cell-line pointed towards that being a better choice when trying to further optimize and improve on the assay, and test the hypothesis of different fusion proteins or membrane anchored markers having an impact on the rate of antigen cross-presentation. Our results also fit with published data that

mitochondrial expression of the antigen has been found to promote greater antigenicity (Prota et al., 2020). Therefore, the mitochondrial cell line appeared as a superior choice for testing different strategies to promote antigen cross-presentation.

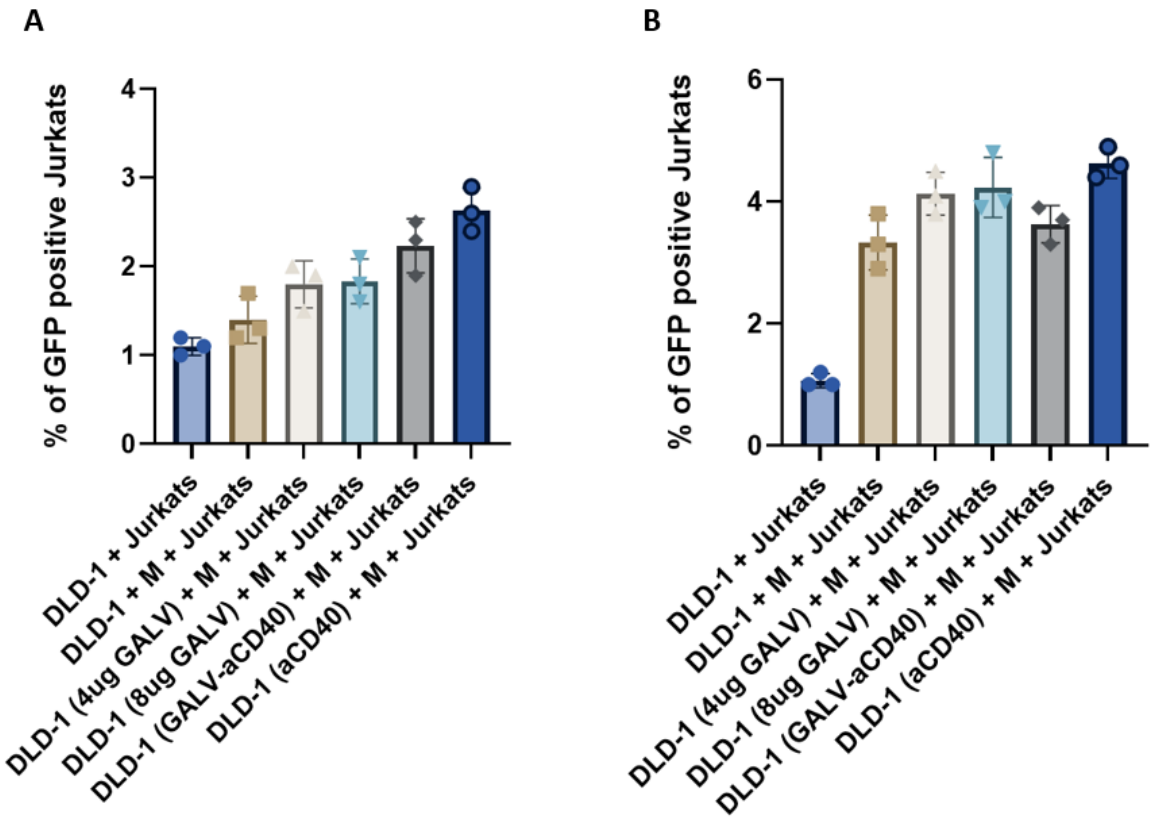

Figure 4.7: Cross-Presentation in DLD-1 cells. The extent of cross-presentation was compared in two different types of DLD-1 cell lines *A) cyt-NYESO DLD*-1: expressing NYESO-1 in the cytoplasm, and *B) mt-NYESO DLD*-1: expressing NYESO-1 through the mitochondria. The data points in the graph represent 3 technical repeats and the bars show the mean percentage of GFP activation. Error bars represent +/- Standard Deviation.

Further optimization steps involved the consideration of timeline in terms of adding the Jurkat cells to the combination of cancer cells and antigen-presenting cells (APCs, in this case M1 macrophages). Figure 4.8 shows the contrasting results gained through coculturing cancer cells with M1s for 24 hours before adding Jurkat cells versus co-culturing them for 48 hours before

adding Jurkat cells. This led to a noticeable improvement in the total percentage of GFP-positive Jurkat cells. A 24-hour delay before addition of Jurkats led to a maximum of 4% of cross-presentation detected in DLD-1 cells, whereas, having a gap of 48-hours before adding the Jurkats led to antigen cross-presentation increasing up to 10%, and even above 15% with the use of GALV. This could be due to the time taken by the cancer cells and macrophages to develop sufficient contact and engage in a fused state/syncytium. The subsequent antigen processing and presentation may have therefore proved better for antigen presentation to the Jurkats, thereby increasing the GFP positive readout.

As can be seen in figure 8, the change in time points of adding the Jurkats also created a difference in the overall effect of different fusion proteins, making the effects more easily differentiated and clear. For example, in Figure 8A, the effect of different concentrations of GALV, presence or absence of the anti-CD40 did not seem to have major differences, and the absence of any such proteins also achieved 4% GFP cross-presentation consistently, suggesting that the use of fusion proteins or CD40 agonist does not impact antigen presentation. However, changing the time point of adding the reporter cells (Jurkats), led to a change in percentages of GFP expression, indicating that addition of fusion proteins had some effect on the antigen cross-presentation. For example, in Figure 8B, the percentage of GFP positive cells was around 7 percent when no fusion protein or additional condition was added. However, the addition of GALV in different concentrations (4 micrograms or 8 micrograms), led to the percentage of GFP positive cells being nearly 15% (with 8 micrograms of DNA), or even higher (with 4 micrograms of DNA), while the presence of the anti-CD40 did not seem to dramatically influence the rate of cross-presentation.

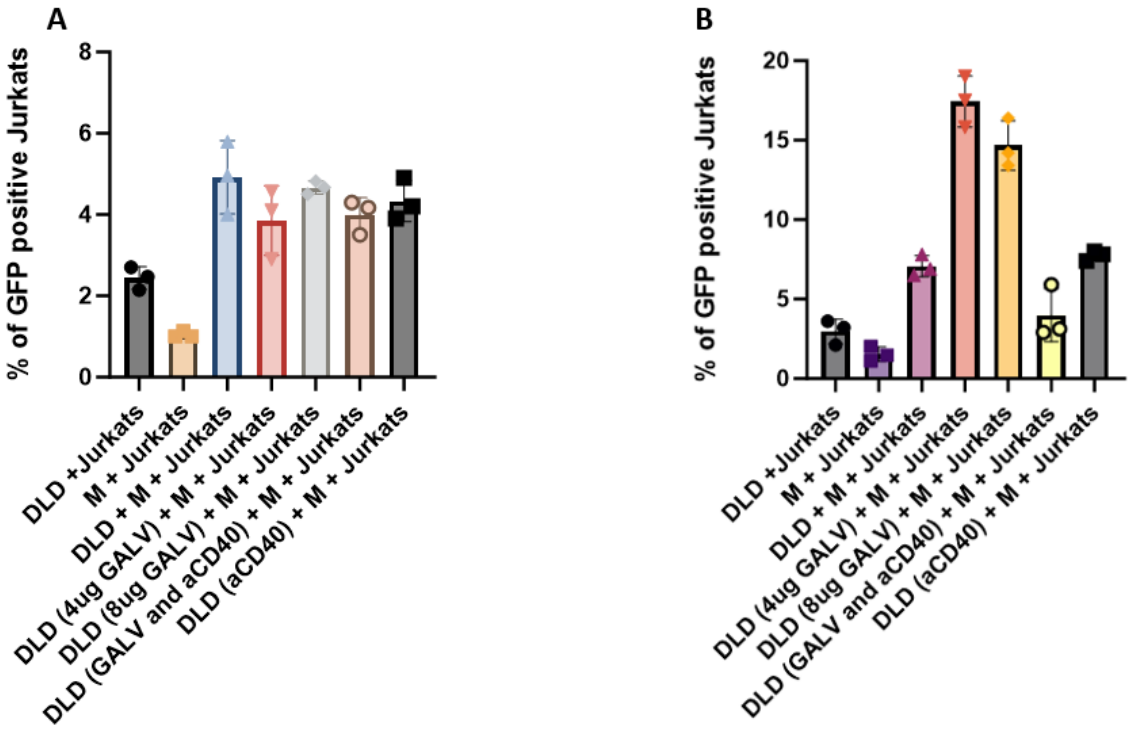

Figure 4.8: Effect of assay time points on the Jurkat activation. (A) Jurkats added to the cancer cells and APC co-culture after 24 hours. (B) Jurkats added to the cancer cells and APCs co-culture after 48 hours. The data points in the graph represent 3 technical repeats and the bars show the mean percentage of GFP activation. Error bars represent +/- Standard Deviation.

Once the optimizations were locked in the overall assay design was finalized to include a 48-hour delay in adding Jurkats after coculturing cancer cells and macrophages. Moreover, the media was refreshed on the day after addition of Jurkats. The final staining and readout of the assay was analysed through flow cytometry on day 8 (4 days after adding Jurkats). Figure 4.9 shows the percentage of GFP activation achieved in the Jurkats after all the optimizations and inclusion of the fusion proteins (GALV and FAST p14), along with the anti-CD40 constructs. The basic control conditions using cancer cells plus macrophages plus Jurkat cells, to establish basal levels of cross presentation, gave an activation of about 6% of the Jurkats, and this was the target for improvement. As far as the use of the fusion proteins is concerned, it can be seen that the FAST p14 appears to have a more pronounced effect (10%) on Jurkat activation as compared to GALV (6% GFP positive Jurkats). Meanwhile, the use of anti-CD40 either on its

own or in combination with GALV caused a more or less steady level of Jurkat activation, with around 10% of the cells being GFP positive. However, the combination of p14 and anti-CD40 appeared to be the best among all conditions, as it led to around 12% of GFP positive Jurkats cells.

While the differences between the effects of the varying constructs appear small and insignificant in comparison to each other, the major comparison lies against the levels of antigen cross-presentation in the absence of any fusion protein or APC agonist (about 6%). Therefore, it is plausible to conclude that the use of fusion proteins and/or APC agonist leads to higher levels of antigen cross-presentation, as can be seen by the increased levels of GFP expressing Jurkats when these different proteins are used.

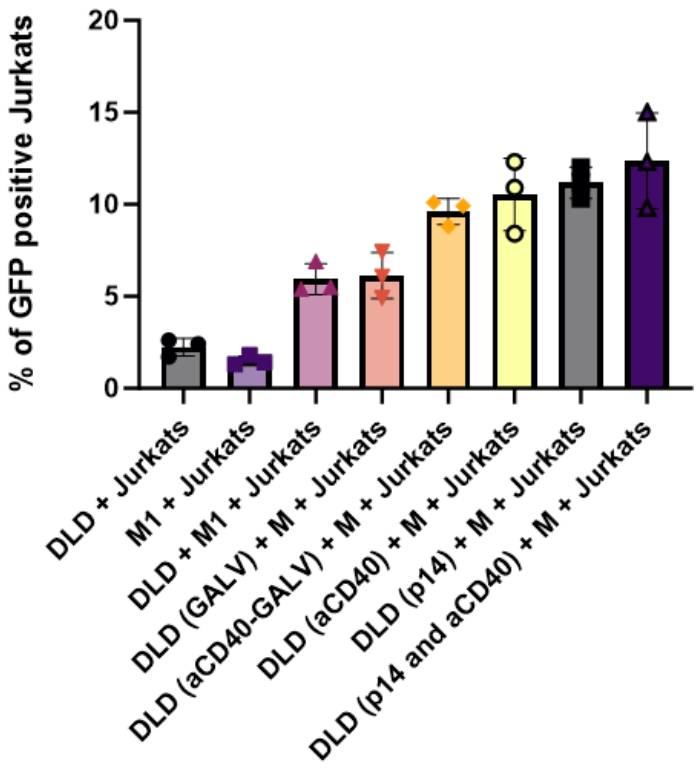

Figure 4.9: Antigen cross-presentation. The percentage of GFP positive cells in the optimized cross-presentation assay, where Jurkats were added after 48 hours of co-culture and media was topped up on the following day. The final version of the assay included comparison of different conditions (fusion proteins, and anti-CD40). The data points in the graph represent 3 technical repeats and the bars show the mean percentage of GFP activation. Error bars represent +/- Standard Deviation.

4.6 Discussion

This chapter aimed to explore the possibility of analysing antigen cross-presentation *in vitro,* along with identifying ways to possibly improve the rate of cross-presentation from tumour cells. To this extent, we set out to firstly develop, refine, and optimize a model system that could be used as a reliable assay method for studying the phenomenon of antigen cross-presentation. This aim was achieved by using an HLA mismatched system, which enabled us to ensure that any activation of the T cells (Jurkats) was strictly due to antigens being cross-presented and not being picked up directly from the cancer cells. Having established basic functionality of the model system as explained above, we then set out to refine the system such that it would give us the most reliable results as we cocultured different cell types and transfected cancer cells with different protein constructs. The technical challenges in establishing this system ranged from high levels of cell death, auto-fluorescence, optimising time-points to coculture different cells together, and suitable strategies to manage the viability and good health of cells as the assay progressed. The optimization steps led to identifying the best possible times for adding the Jurkat reporter cells. It also led us to the conclusion that topping up media halfway through the assay (day 4) helped improve cell viability as the assay progressed.

The presence of different molecules expressed in the cancer cells to test the hypotheses relating to their possible roles in or effects on antigen cross-presentation was also explored in this chapter. Firstly, the use of GALV fusion protein, which has been used by a number of research studies exploring cancer therapy (Roulstone et al., 2021), to evaluate the idea that successful fusion between cancer cells and APCs through this protein could lead to a higher rate of cross-presentation than is normally achieved in the absence of any syncytia forming agent. However,

while the heterocellular syncytia formation potential of GALV has successfully been shown in the previous chapter, it did not appear to have any significant effect on the cross-presentation of tumour antigen (NYESO-1). Meanwhile, the use an alternative syncytium-forming protein, FAST p14 led to noticeable positive changes in the rate of antigen cross-presentation, as seen by the heightened percentage of GFP expression by the Jurkats when p14 was used, as compared to GFP expression in the absence of p14 expressed from cancer cells.

One of the reasons that GALV might have been slower or less efficient at leading to cross-presentation could be the slower rate of syncytia formation of GALV in comparison to p14. As has been shown in the previous chapter, while GALV does lead to heterocellular syncytia formation, it is much slower in action as compared to the p14. In particular, the imaging data for heterocellular syncytia formation clearly highlights that large syncytia detected while using p14 as within 24 hours, as compared to GALV that had minimum fusion at the same time point. The rate of fusion also remained the same at 48 hours with the p14 appearing to be causing more widespread heterocellular fusions as compared to GALV. Moreover, p14 is promiscuous in its binding patterns in that it does not need a specific receptor on the neighbouring cells for initiating fusion. This could possibly be the key reason that p14 appeared to be better at inducing cross-presentation, and also seemed to further improve when used in combination with the anti-CD40 super agonist.

The use of an anti-CD40 agonist was aimed at potentially increasing antigen cross-presentation, as there are evidences of anti-CD40 antibodies leading to antigen presentation to dendritic cells, and increasing the expansion of the cytotoxic T cells (Deronic et al., 2021). To this end, our results align with the existing data, and we have shown that the use of a membrane anchored anti-CD40 agonist leads to increased antigen cross-presentation. When the anti-CD40 was used in conjunction with GALV, the effect was not much better than the use of either of these proteins on their own. However, the use of anti-CD40 in combination with p14 led to a

noticeable increase in cross-presentation (figure 4.9). These data build on the results for heterocellular syncytia and phagocytosis in the previous chapter, which show that anti-CD40 in combination with GALV does not cause increase in cell fusion but causes a noticeable increase in the heterocellular fusions caused by p14. The difference of size in the two fusion proteins could be a possible reason behind the difference in their effect on the impact on cross-presentation when expressed in combination with the anti-CD40 agonist. The differences in the two fusion proteins have been discussed in detail in the previous chapter to explain syncytia formation.

Briefly, the reason that size of proteins could have a potential effect on the way proteins interacted lies in the fact that all of these proteins we used in the study had transmembrane domains in their structure, meaning they would embed in the cell membrane. Having a large protein like GALV that has seven transmembrane domains could potentially take up much more space as compared to the small sized p14 which only has one transmembrane domain embedding in the cell membrane. There is the possibility that stearic hindrances could exist in the way these proteins expressed from the cells, making the larger protein likely to be slower in its action as compared to the smaller molecule. In any case, the use of fusion proteins was aimed at ensuring that the cancer cells and APCs could be fused together. The presence of a shared cytoplasm between the cancer cells and APCs would provide direct access of the cancer antigens to the APC immunoproteasome. Having successfully shown heterocellular fusion and subsequent activation of Jurkats in the cross-presentation assay supports the idea that a cytosolic pathway of antigen cross presentation has occurred in this case. While we have not confirmed the exact molecular pathway of antigen presentation in this study, the data does show evidence of supporting our hypothesis that an increase in heterocellular syncytia between cancer cells and APCs leads to increased cross-presentation.

5. Discussion

5.1 Thesis Synopsis

This thesis aimed at exploring ways to enhance interactions between cancer cells and APCs for improving the immune response against cancer. One of the biggest barriers to successful immunotherapy is the tumour resistance and immune evasion caused by the immunosuppressive environment in the TME. Developing a means to activate, and harness the anti-tumour potential of the immune cells present within the TME was sought as a means to overcoming treatment barriers. A number of existing studies have shown that the use of viral fusion proteins leads to lysis of cancer cells, and release of TAA, which are then presented to the immune cells for generating an anti-cancer immune response. We explored the use of this approach and successfully compared the syncytia forming potential of two viral fusion proteins; GALV and FAST p14.

The homoocellular and heterocellular syncytia-forming potential of the fusion proteins were compared and contrasted. As seen in chapter 3, both; GALV and p14 were successful in syncytia formation, whether it be homocellular (between cancer cells) or heterocellular (between cancer cells and macrophages) syncytia. The different methods employed for exploring syncytia formation were developed and refined from the literature to identify the best possible ways to image and also to quantify fusions caused by each of these proteins. Imaging was carried out after staining the cells with cell tracker dyes or by using stable cell lines expressing fluorescent proteins. As has been shown in the results in chapter 3, the use of cell tracker dyes on their own led to dye leaching and loss of fluorescence, making it difficult to identify two different colours in the same field of view when observed using a confocal microscope.

Moving forward from combinations of cell tracker dyes, the combination of cells stably-expressing fluorescent reporter proteins and cell tracker dyes led to slightly better images (figure 3.5), implying that this was a more reliable approach. Having confirmed the formation of homocellular syncytia through imaging, we explored ways to possibly quantify the extent of syncytia formation by the viral fusion proteins. In this regard, the Tet operator system provided a way forward in that the system works as a regulatory operon for the expression of transgenes. The use of a system that relied on the successful fusion of cell cytoplasms to allow molecular interactions to induce expression of GFP provided a reliable way of quantifying syncytia by means of measuring the integrated intensity of fluorescence observed from the cells present in a well. This system holds the potential of being used further for quantification purposed by refining the method we currently employed.

The heterocellular syncytia formation potential of GALV and p14 were compared through microscopy as well as flow cytometry. It was observed that p14 performed better than GALV when expressed from cancer cells and co-cultured with PBMC derived macrophages. Since the two proteins are quite different in their size as well as method of recruiting cells into syncytia, we did expect to see varying rates of fusion potential. The results are in line with our hypothesis that p14 is better in forming heterocellular syncytia sine it is receptor independent and has a promiscuous binding strategy, which possibly makes it faster in its action and more diverse in the types of cells it binds to as compared to GALV. The aim of generating fusions between cancer cells and APCs was embedded in exploring strategies for cancer vaccination.

Along with the syncytia formation, the use of a membrane-linked CD40 super agonist antibody was also explored with the aims of enhancing the interactions and activation levels of cancer cells and APCs. Our results suggest that the use of the anti-CD40 on its own does lead to an increased interaction between cancer cells and APCs, evidenced by more cell aggregation seen by flow cytometry. Moreover, we also used combinations of the anti-CD40 with GALV or p14

(figure 3.16) to explore the possibility of further increasing the interaction and fusion of cancer cells and APCs. The expression of the anti-CD40 from cancer cells had a two-edged aim; increasing the interaction with APCs, and the subsequent activation of the APCs. Further, adding a syncytium forming protein to the same cancer cell was aimed at enabling higher rates of fusions. This aim was well achieved with the use of p14, but the same was not seen in the case of GALV. Theese results are again in line with our hypothesis that the p14 has an advantage over GALV due to the lack of need of a specific cellular receptor for aiding fusion. Moreover, the GALV being a large sized protein, could possibly have a slower rate of fusion formations when supplemented with another transmembrane protein (membrane anchored anti-CD40), creating the possibility of stearic hindrances in the cell membrane and lower overall syncytia formation in comparison to p14.

The goal of facilitating syncytia formation with the anti-CD40 was to ensure that cancer cells could fuse with APCs such that the TAAs could be in the same cytoplasm as that of the APC after fusion, giving direct access to the APC immunoproteasome and possibly leading to enhanced antigen cross-presentation. Our results (chapter 4) support this hypothesis showing that the use of fusion proteins does indeed facilitate antigen cross-presentation. Moreover, in the case of p14 in particular, addition of the CD40 super agonist led to a significant increase in the antigen cross-presentation, as detected by increased Jurkat activation (GFP expression from the reporter cells).

After exploring the potential of heterocellular fusions, role of anti-CD40, and cross-presentation of antigens, we conclude that our data supports the cytoplasmic route of antigen cross-presentation. The fusion of cancer cells and APCs brings the cytoplasm of the two cell types together, as show through imaging data for heterocellular syncytia. Following fusions, the rate of fusion is also correlated with the extent of cross-presentation by each of the fusion proteins used. Therefore, we conclude that in our experimental setup, the cytoplasmic route of

antigen cross-presentation appears to be functional. While this does not rule out the chance that the vacuolar pathway can also be used, our data leans more towards the cytoplasmic route of antigen cross-presentation being the functional outcome in this study.

5.2 Future Directions

Having explored the heterocellular fusion potential and role of anti-CD40 in cross-presentation, the next steps in utilizing the systems developed and explored here include further refining and testing the pathways explored. Firstly, a molecular analysis for confirming that the presence of tumour antigens in the same cytoplasm as that of an APC indeed leads to stable antigen cross-presentation and not simply cross-priming. Moreover, identifying the true molecular basis of why p14 seems to function better in combination with anti-CD40 as compared to the GALV and anti-CD40 combination.

Further to these studies, the clinical advantages of fusion proteins and the CD40 super agonist can be explored by encoding these constructs in an oncolytic virus. The potential of fusion proteins in helping the spread of viruses in their normal life cycle can potentially be applied in the context of immunotherapy as well. This has been shown to be a successful approach in several studies that have used GALV for achieving better spread of oncolytic viruses (Roulstone et al., 2021; Thomas et al., 2019). The addition of an anti-CD40 along with fusion proteins with the aim of enabling interaction of APCs with the cancer cells could possibly help in overcoming the various treatment barriers posed by the TME. Since the TME already includes APCs, enabling the interaction and activation of those APCs against cancer cells can potentially be useful in generating an anti-tumour response.

References

Barbuto, J. A. M., Ensina, L. F., Neves, A. R., Bergami-Santos, P. C., Leite, K. R., Marques, R., . . . Buzaid, A. C. (2004). Dendritic cell–tumor cell hybrid vaccination for metastatic cancer. *Cancer Immunology, Immunotherapy, 53*, 1111-1118.

Baron, U., & Bujard, H. (2000). Tet repressor-based system for regulated gene expression in eukaryotic cells: principles and advances. In *Methods in enzymology* (Vol. 327, pp. 401-421): Elsevier.

Bernhard, C. A., Ried, C., Kochanek, S., & Brocker, T. (2015). CD169+ macrophages are sufficient for priming of CTLs with specificities left out by cross-priming dendritic cells. *Proceedings of the National Academy of Sciences, 112*(17), 5461-5466.

Bevan, M. J. (1976). Cross-priming for a secondary cytotoxic response to minor H antigens with H-2 congenic cells which do not cross-react in the cytotoxic assay. *The Journal of experimental medicine, 143*(5), 1283-1288.

Boutilier, J., & Duncan, R. (2011). The reovirus fusion-associated small transmembrane (FAST) proteins: virus-encoded cellular fusogens. *Current topics in membranes, 68*, 107-140.

Bray, F., Laversanne, M., Sung, H., Ferlay, J., Siegel, R. L., Soerjomataram, I., & Jemal, A. (2024). Global cancer statistics 2022: GLOBOCAN estimates of incidence and mortality worldwide for 36 cancers in 185 countries. *CA: a cancer journal for clinicians, 74*(3), 229-263.

Brown, C. W., Stephenson, K. B., Hanson, S., Kucharczyk, M., Duncan, R., Bell, J. C., & Lichty, B. D. (2009). The p14 FAST protein of reptilian reovirus increases vesicular stomatitis virus neuropathogenesis. Journal of virology, 83(2), 552-561.

Brown, C. W., Stephenson, K. B., Hanson, S., Kucharczyk, M., Duncan, R., Bell, J. C., & Lichty, B. D. (2009). The p14 FAST protein of reptilian reovirus increases vesicular stomatitis virus neuropathogenesis. *Journal of virology, 83*(2), 552-561.

Burgdorf, S., Kautz, A., Böhnert, V., Knolle, P. A., & Kurts, C. (2007). Distinct pathways of antigen uptake and intracellular routing in CD4 and CD8 T cell activation. *science, 316*(5824), 612-616.

Burgdorf, S., Schuette, V., Semmling, V., Hochheiser, K., Lukacs-Kornek, V., Knolle, P. A., & Kurts, C. (2010). Steady-state cross-presentation of OVA is mannose receptor-dependent but inhibitable by collagen fragments. *Proceedings of the National Academy of Sciences, 107*(13), E48-E49.

Ciechonska, M., Key, T., & Duncan, R. (2014). Efficient reovirus-and measles virus-mediated pore expansion during syncytium formation is dependent on annexin A1 and intracellular calcium. *Journal of virology, 88*(11), 6137-6147.

Charles, J., Chaperot, L., Hannani, D., Bruder Costa, J., Templier, I., Trabelsi, S., . . . Hegelhofer, H. (2020). An innovative plasmacytoid dendritic cell line-based cancer vaccine primes and expands antitumor T-cells in melanoma patients in a first-in-human trial. *Oncoimmunology, 9*(1), 1738812.

Chatterjee, B., Smed-Sörensen, A., Cohn, L., Chalouni, C., Vandlen, R., Lee, B.-C., . . . Mellman, I. (2012). Internalization and endosomal degradation of receptor-bound antigens regulate the efficiency of cross presentation by human dendritic cells. *Blood, The Journal of the American Society of Hematology, 120*(10), 2011-2020.

Cheng, Y. J., Nie, X. Y., Ji, C. C., Lin, X. X., Liu, L. J., Chen, X. M., . . . Wu, S. H. (2017). Long-term cardiovascular risk after radiotherapy in women with breast cancer. *Journal of the American Heart Association, 6*(5), e005633.

Corcoran, J. A., & Duncan, R. (2004). Reptilian reovirus utilizes a small type III protein with an external myristylated amino terminus to mediate cell-cell fusion. *Journal of virology, 78*(8), 4342-4351.

Cohen, F. S., & Melikyan, G. B. (2004). The energetics of membrane fusion from binding, through hemifusion, pore formation, and pore enlargement. *The Journal of membrane biology, 199*(1), 1-14.

De Leeuw, O. S., Koch, G., Hartog, L., Ravenshorst, N., & Peeters, B. P. (2005). Virulence of Newcastle disease virus is determined by the cleavage site of the fusion protein and by both the stem region and globular head of the haemagglutinin–neuraminidase protein. *Journal of General Virology, 86*(6), 1759-1769.

Deronic, A., Nilsson, A., Thagesson, M., Werchau, D., Enell Smith, K., & Ellmark, P. (2021). The human anti-CD40 agonist antibody mitazalimab (ADC-1013; JNJ-64457107) activates antigen-presenting cells, improves expansion of antigen-specific T cells, and enhances anti-tumor efficacy of a model cancer vaccine in vivo. *Cancer Immunology, Immunotherapy, 70*, 3629-3642.

Di Pucchio, T., Chatterjee, B., Smed-Sörensen, A., Clayton, S., Palazzo, A., Montes, M., . . . Connolly, J. E. (2008). Direct proteasome-independent cross-presentation of viral antigen by plasmacytoid dendritic cells on major histocompatibility complex class I. *Nature immunology, 9*(5), 551-557.

Duncan, R., Chen, Z., Walsh, S., & Wu, S. (1996). Avian reovirus-induced syncytium formation is independent of infectious progeny virus production and enhances the rate, but is not essential, for virus-induced cytopathology and virus egress. *Virology*, *224*(2), 453-464.

Duncan, R., & Sullivan, K. (1998). Characterization of two avian reoviruses that exhibit strain-specific quantitative differences in their syncytium-inducing and pathogenic capabilities. Virology, 250(2), 263-272.

Ferlay, J., Soerjomataram, I., Dikshit, R., Eser, S., Mathers, C., Rebelo, M., . . . Bray, F. (2015). Cancer incidence and mortality worldwide: sources, methods and major patterns in GLOBOCAN 2012. *International journal of cancer, 136*(5), E359-E386.

Ferlay, J., Steliarova-Foucher, E., Lortet-Tieulent, J., Rosso, S., Coebergh, J.-W. W., Comber, H., . . . Bray, F. (2013). Cancer incidence and mortality patterns in Europe: estimates for 40 countries in 2012. *European journal of cancer, 49*(6), 1374-1403.

Fielding, A. K., Chapel-Fernandes, S., Chadwick, M. P., Bullough, F. J., Cosset, F.-L., & Russell, S. J. (2000). A hyperfusogenic gibbon ape leukemia envelope glycoprotein: targeting of a cytotoxic gene by ligand display. *Human gene therapy, 11*(6), 817-826.

Gaudin, Y., Ruigrok, R. W., & Brunner, J. (1995). Low-pH induced conformational changes in viral fusion proteins: implications for the fusion mechanism. *Journal of General Virology, 76*(7), 1541-1556.

Guedan, S., Grases, D., Rojas, J., Gros, A., Vilardell, F., Vile, R., . . . Alemany, R. (2012). GALV expression enhances the therapeutic efficacy of an oncolytic adenovirus by inducing cell fusion and enhancing virus distribution. *Gene therapy, 19*(11), 1048-1057.

Harrington, K. J., Puzanov, I., Hecht, J. R., Hodi, F. S., Szabo, Z., Murugappan, S., & Kaufman, H. L. (2015). Clinical development of talimogene laherparepvec (T-VEC): a modified herpes simplex virus type-1–derived oncolytic immunotherapy. *Expert review of anticancer therapy*, *15*(12), 1389-1403.

Hartsock, A., & Nelson, W. J. (2008). Adherens and tight junctions: structure, function and connections to the actin cytoskeleton. *Biochimica et Biophysica Acta (BBA)-Biomembranes*, *1778*(3), 660-669.

Hayes, M. J., Rescher, U., Gerke, V., & Moss, S. E. (2004). Annexin–actin interactions. *Traffic*, *5*(8), 571-576.

Helming, L., & Gordon, S. (2009). Molecular mediators of macrophage fusion. *Trends in cell biology*, *19*(10), 514-522.

Higuchi, H., Bronk, S. F., Bateman, A., Harrington, K., Vile, R. G., & Gores, G. J. (2000). Viral fusogenic membrane glycoprotein expression causes syncytia formation with bioenergetic cell death: implications for gene therapy. *Cancer Research*, *60*(22), 6396-6402.

Hoffmann, T. K., Meidenbauer, N., Müller-Berghaus, J., Storkus, W. J., & Whiteside, T. L. (2001). Proinflammatory cytokines and CD40 ligand enhance cross-presentation and cross-priming capability of human dendritic cells internalizing apoptotic cancer cells. *Journal of Immunotherapy*, *24*(2), 162-171.

Holmström, M. O., Cordua, S., Skov, V., Kjær, L., Pallisgaard, N., Ellervik, C., . . . Andersen, M. H. (2020). Evidence of immune elimination, immuno-editing and immune escape in patients with hematological cancer. *Cancer Immunology, Immunotherapy*, *69*, 315-324.

Huttner, W. B., & Zimmerberg, J. (2001). Implications of lipid microdomains for membrane curvature, budding and fission: Commentary. *Current opinion in cell biology*, *13*(4), 478-484.

Jayasingam, S. D., Citartan, M., Thang, T. H., Mat Zin, A. A., Ang, K. C., & Ch'ng, E. S. (2020). Evaluating the polarization of tumor-associated macrophages into M1 and M2 phenotypes in human cancer tissue: technicalities and challenges in routine clinical practice. *Frontiers in oncology*, *9*, 1512.

Key, T., & Duncan, R. (2014). A compact, multifunctional fusion module directs cholesterol-dependent homomultimerization and syncytiogenic efficiency of reovirus p10 FAST proteins. *PLoS pathogens*, *10*(3).

Koch, A. W., Manzur, K. L., & Shan, W. (2004). Structure-based models of cadherin-mediated cell adhesion: the evolution continues. *Cellular and molecular life sciences*, *61*(15), 1884-1895.

Kratzer, T. B., Bandi, P., Freedman, N. D., Smith, R. A., Travis, W. D., Jemal, A., & Siegel, R. L. (2024). Lung cancer statistics, 2023. *Cancer*, *130*(8), 1330-1348.

Krueger, C., Danke, C., Pfleiderer, K., Schuh, W., Jäck, H. M., Lochner, S., . . . Berens, C. (2006). A gene regulation system with four distinct expression levels. *The Journal of Gene Medicine: A cross-disciplinary journal for research on the science of gene transfer and its clinical applications*, *8*(8), 1037-1047.

Lauring, A. S., Anderson, M. M., & Overbaugh, J. (2001). Specificity in receptor usage by T-cell-tropic feline leukemia viruses: implications for the in vivo tropism of immunodeficiency-inducing variants. *Journal of virology, 75*(19), 8888-8898.

Le Boeuf, F., Gebremeskel, S., McMullen, N., He, H., Greenshields, A. L., Hoskin, D. W., ... & Duncan, R. (2017). Reovirus FAST protein enhances vesicular stomatitis virus oncolytic virotherapy in primary and metastatic tumor models. *Molecular Therapy-Oncolytics*, *6*, 80-89.

Le Gall, C. M., Cammarata, A., de Haas, L., Ramos-Tomillero, I., Cuenca-Escalona, J., Wijfjes, Z., . . . Figdor, C. G. (2021). Efficient targeting of NY-ESO-1 tumor antigen to human cDC1s by lymphotactin results in cross-presentation and antigen-specific T cell expansion. *bioRxiv*, 2021.2011. 2030.470538

Leifeld, L., Trautwein, C., Dumoulin, F. L., Manns, M. P., Sauerbruch, T., & Spengler, U. (1999). Enhanced expression of CD80 (B7-1), CD86 (B7-2), and CD40 and their ligands CD28 and CD154 in fulminant hepatic failure. *The American journal of pathology, 154*(6), 1711-1720.

Liu, X., Zhang, D., Wang, H., Ren, Q., Li, B., Wang, L., & Zheng, G. (2021). MiR-451a enhances the phagocytosis and affects both M1 and M2 polarization in macrophages. *Cellular Immunology, 365*, 104377.

Lin, E., Salon, C., Brambilla, E., Lavillette, D., Szecsi, J., Cosset, F., & Coll, J. (2010). Fusogenic membrane glycoproteins induce syncytia formation and death in vitro and in vivo: a potential therapy agent for lung cancer. *Cancer Gene Therapy, 17*(4), 256-265.

Lingwood, D., & Simons, K. (2010). Lipid rafts as a membrane-organizing principle. science, 327(5961), 46-50.

Liu, M., & Eiden, M. V. (2011). The receptors for gibbon ape leukemia virus and amphotropic murine leukemia virus are not downregulated in productively infected cells. *Retrovirology, 8*, 1-14.

Marchini, A., Daeffler, L., Pozdeev, V. I., Angelova, A., & Rommelaere, J. (2019). Immune conversion of tumor microenvironment by oncolytic viruses: the protoparvovirus H-1PV case study. *Frontiers in immunology, 10*, 1848.

Marigo, I., Zilio, S., Desantis, G., Mlecnik, B., Agnellini, A. H., Ugel, S., . . . Zanovello, P. (2016). T cell cancer therapy requires CD40-CD40L activation of tumor necrosis factor and inducible nitric-oxide-synthase-producing dendritic cells. *Cancer cell, 30*(3), 377-390.

Märten, A., Renoth, S., Heinicke, T., Albers, P., Pauli, A., Mey, U., . . . Von Ruecker, A. (2003). Allogeneic dendritic cells fused with tumor cells: preclinical results and outcome of a clinical phase I/II trial in patients with metastatic renal cell carcinoma. *Human gene therapy, 14*(5), 483-494.

Monu, N., & Trombetta, E. S. (2007). Cross-talk between the endocytic pathway and the endoplasmic reticulum in cross-presentation by MHC class I molecules. *Current opinion in immunology, 19*(1), 66-72.

Narayan, V., Barber-Rotenberg, J. S., Jung, I.-Y., Lacey, S. F., Rech, A. J., Davis, M. M., . . . Maude, S. L. (2022). PSMA-targeting TGFβ-insensitive armored CAR T cells in metastatic castration-resistant prostate cancer: a phase 1 trial. *Nature medicine, 28*(4), 724-734.

Neves, A. R., Ensina, L. F. C., Anselmo, L. B., Leite, K. R., Buzaid, A. C., Câmara-Lopes, L. H., & Barbuto, J. A. M. (2005). Dendritic cells derived from metastatic cancer patients vaccinated with allogeneic dendritic cell–autologous tumor cell hybrids express more

CD86 and induce higher levels of interferon-gamma in mixed lymphocyte reactions. *Cancer Immunology, Immunotherapy*, *54*, 61-66.

Nieto-Torres, J. L., Verdiá-Báguena, C., Castaño-Rodriguez, C., Aguilella, V. M., & Enjuanes, L. (2015). Relevance of viroporin ion channel activity on viral replication and pathogenesis. *Viruses*, *7*(7), 3552-3573.

Ogueta, S. B., Yao, F., & Marasco, W. A. (2001). Design and in vitro characterization of a single regulatory module for efficient control of gene expression in both plasmid DNA and a self-inactivating lentiviral vector. *Molecular Medicine, 7*, 569-579.

Oliveira, G., & Wu, C. J. (2023). Dynamics and specificities of T cells in cancer immunotherapy. *Nature Reviews Cancer*, *23*(5), 295-316.

Pang, X., Zhang, L., Wu, J., Ma, C., Mu, C., Zhang, G., & Chen, W. (2017). Expression of CD40/CD40L in colon cancer, and its effect on proliferation and apoptosis of SW48 colon cancer cells. *J BUON*, *22*(4), 894-899.

Parmar, H. B., Barry, C., Kai, F., & Duncan, R. (2014). Golgi complex–plasma membrane trafficking directed by an autonomous, tribasic Golgi export signal. *Molecular biology of the cell*, *25*(6), 866-878.

Phan, V., Errington, F., Cheong, S. C., Kottke, T., Gough, M., Altmann, S., . . . Bateman, A. (2003). A new genetic method to generate and isolate small, short-lived but highly potent dendritic cell-tumor cell hybrid vaccines. *Nature medicine*, *9*(9), 1215-1219.

Pilon, C., Levast, B., Meurens, F., Le Vern, Y., Kerboeuf, D., Salmon, H., . . . Baron, C. (2009). CD40 engagement strongly induces CD25 expression on porcine dendritic cells and polarizes the T cell immune response toward Th1. *Molecular immunology*, *46*(3), 437-447.

Pötgens, A., Schmitz, U., Bose, P., Versmold, A., Kaufmann, P., & Frank, H.-G. (2002). Mechanisms of syncytial fusion: a review. *Placenta*, *23*, S107-S113.

Poulin, L. F., Henri, S., de Bovis, B. a., Devilard, E., Kissenpfennig, A., & Malissen, B. (2007). The dermis contains langerin+ dendritic cells that develop and function independently of epidermal Langerhans cells. *The Journal of experimental medicine*, *204*(13), 3119-3131.

Prota, G., Gileadi, U., Rei, M., Lechuga-Vieco, A. V., Chen, J. L., Galiani, S., ... & Cerundolo, V. (2020). Enhanced immunogenicity of mitochondrial-localized proteins in cancer cells. *Cancer Immunology Research*, *8*(5), 685-697.

Ramakrishna, E., Woller, N., Mundt, B., Knocke, S., Gürlevik, E., Saborowski, M., . . . Kühnel, F. (2009). Antitumoral immune response by recruitment and expansion of dendritic cells in tumors infected with telomerase-dependent oncolytic viruses. *Cancer Research*, *69*(4), 1448-1458.

Read, J., Clancy, E. K., Sarker, M., de Antueno, R., Langelaan, D. N., Parmar, H. B., ... & Duncan, R. (2015). Reovirus FAST proteins drive pore formation and syncytiogenesis using a novel helix-loop-helix fusion-inducing lipid packing sensor. *PLoS pathogens*, *11*(6).

Richard, J. P., Leikina, E., Langen, R., Henne, W. M., Popova, M., Balla, T., ... & Chernomordik, L. V. (2011). Intracellular curvature-generating proteins in cell-to-cell fusion. *Biochemical Journal*, *440*(2), 185-193.

Rix, A., Drude, N. I., Mrugalla, A., Baskaya, F., Pak, K. Y., Gray, B., . . . Lederle, W. (2020). Assessment of chemotherapy-induced organ damage with Ga-68 labeled duramycin. *Molecular Imaging and Biology*, *22*, 623-633.

Rock, K. L., & Shen, L. (2005). Cross-presentation: underlying mechanisms and role in immune surveillance. *Immunological reviews, 207*(1), 166-183.

Rossman, J. S., & Lamb, R. A. (2011). Influenza virus assembly and budding. *Virology, 411*(2), 229-236.

Roulstone, V., Kyula, J., Thomas, S., Kuncheria, L., Bommareddy, P. K., Smith, H., . . . Harrington, K. (2021). Immunomodulatory effects of a novel, enhanced potency gibbon ape leukaemia virus (GALV) fusogenic membrane glycoprotein-expressing herpes simplex virus platform with increased efficacy combined with anti PD-1 therapy. *Cancer Research, 81*(13_Supplement), 1917-1917.

Salsman, J., Top, D., Boutilier, J., & Duncan, R. (2005). Extensive syncytium formation mediated by the reovirus FAST proteins triggers apoptosis-induced membrane instability. *Journal of virology, 79*(13), 8090-8100.

Salsman, J., Top, D., Barry, C., & Duncan, R. (2008). A virus-encoded cell–cell fusion machine dependent on surrogate adhesins. *PLoS pathogens, 4*(3).

Sathe, P., Pooley, J., Vremec, D., Mintern, J., Jin, J.-O., Wu, L., . . . Shortman, K. (2011). The acquisition of antigen cross-presentation function by newly formed dendritic cells. *The Journal of Immunology, 186*(9), 5184-5192.

Sengupta, D., Graham, M., Liu, X., & Cresswell, P. (2019). Proteasomal degradation within endocytic organelles mediates antigen cross-presentation. *The EMBO journal, 38*(16), e99266.

Shen, L., & Rock, K. L. (2006). Priming of T cells by exogenous antigen cross-presented on MHC class I molecules. *Current opinion in immunology, 18*(1), 85-91.

Shmulevitz, M., Corcoran, J., Salsman, J., & Duncan, R. (2004). Cell-cell fusion induced by the avian reovirus membrane fusion protein is regulated by protein degradation. *Journal of virology, 78*(11), 5996-6004.

Shmulevitz, M., Salsman, J., & Duncan, R. (2003). Palmitoylation, membrane-proximal basic residues, and transmembrane glycine residues in the reovirus p10 protein are essential for syncytium formation. *Journal of virology, 77*(18), 9769-9779.

Tacken, P. J., Ginter, W., Berod, L., Cruz, L. J., Joosten, B., Sparwasser, T., . . . Cambi, A. (2011). Targeting DC-SIGN via its neck region leads to prolonged antigen residence in early endosomes, delayed lysosomal degradation, and cross-presentation. *Blood, The Journal of the American Society of Hematology, 118*(15), 4111-4119.

Torrisi, J. M., Schwartz, L. H., Gollub, M. J., Ginsberg, M. S., Bosl, G. J., & Hricak, H. (2011). CT findings of chemotherapy-induced toxicity: what radiologists need to know about the clinical and radiologic manifestations of chemotherapy toxicity. *Radiology, 258*(1), 41-56.

Top, D., de Antueno, R., Salsman, J., Corcoran, J., Mader, J., Hoskin, D., ... & Duncan, R. (2005). Liposome reconstitution of a minimal protein-mediated membrane fusion machine. *The EMBO journal, 24*(17), 2980-2988.

Tseng, D., Volkmer, J.-P., Willingham, S. B., Contreras-Trujillo, H., Fathman, J. W., Fernhoff, N. B., . . . Miyanishi, M. (2013). Anti-CD47 antibody–mediated phagocytosis of cancer by macrophages primes an effective antitumor T-cell response. *Proceedings of the National Academy of Sciences, 110*(27), 11103-11108.

Uno, T., Takeda, K., Kojima, Y., Yoshizawa, H., Akiba, H., Mittler, R. S., . . . Smyth, M. J. (2006). Eradication of established tumors in mice by a combination antibody-based therapy. *Nature medicine, 12*(6), 693-698.

Uversky, V. N. (2011). Intrinsically disordered proteins from A to Z. *The international journal of biochemistry & cell biology, 43*(8), 1090-1103.

Wang, H.-F., Xiang, W., Xue, B.-Z., Wang, Y.-H., Yi, D.-Y., Jiang, X.-B., . . . Fu, P. (2021). Cell fusion in cancer hallmarks: Current research status and future indications. *Oncology letters, 22*(1), 1-9.

White, J., Kielian, M., & Helenius, A. (1983). Membrane fusion proteins of enveloped animal viruses. *Quarterly Reviews of Biophysics, 16*(2), 151-195.

Wiener, F., Klein, G., & Harris, H. (1971). The analysis of malignancy by cell fusion: III. hybrids between diploid fibroblasts and other tumour cells. *Journal of Cell Science, 8*(3), 681-692.

Wong, C. M., Poulin, K. L., Tong, G., Christou, C., Kennedy, M. A., Falls, T., . . . Parks, R. J. (2016). Adenovirus-mediated expression of the p14 fusion-associated small transmembrane protein promotes cancer cell fusion and apoptosis in vitro but does not provide therapeutic efficacy in a xenograft mouse model of cancer. *PLoS One, 11*(3), e0151516.

Yan, Y., Zhang, L., Zuo, Y., Qian, H., & Liu, C. (2020). Immune checkpoint blockade in cancer immunotherapy: mechanisms, clinical outcomes, and safety profiles of PD-1/PD-L1 inhibitors. *Archivum Immunologiae et Therapiae Experimentalis, 68*(6), 36.

Yang, S. T., Kiessling, V., Simmons, J. A., White, J. M., & Tamm, L. K. (2015). HIV gp41–mediated membrane fusion occurs at edges of cholesterol-rich lipid domains. *Nature chemical biology, 11*(6), 424.

Yun, T., Yu, B., Ni, Z., Ye, W., Chen, L., Hua, J., & Zhang, C. (2014). Genomic characteristics of a novel reovirus from Muscovy duckling in China. *Veterinary microbiology, 168*(2-4), 261-271.

Yunna, C., Mengru, H., Lei, W., & Weidong, C. (2020). Macrophage M1/M2 polarization. *European journal of pharmacology, 877*, 173090.

Zhu, B., Yang, J.-r., Fu, X.-p., & Jiang, Y.-q. (2014). Anti-tumor effects of gene therapy with GALV membrane fusion glycoprotein in lung adenocarcinoma. *Cell Biochemistry and Biophysics, 69*, 577-582.

Zugazagoitia, J., Guedes, C., Ponce, S., Ferrer, I., Molina-Pinelo, S., & Paz-Ares, L. (2016). Current challenges in cancer treatment. *Clinical therapeutics, 38*(7), 1551-1566.

APPENDIX

GALV DNA sequence

ATGGTATTGCTGCCTGGGTCCATGCTTCTCACCTCAAACCTGCACCACCTTCGGC
ACCAGATGAGTCCTGGGAGCTGGAAAAGACTGATCATCCTCTTAAGCTGCGTATT
CGGCGGCGGCGGGACGAGTCTGCAAAATAAGAACCCCCACCAGCCCATGACCCT
CACTTGGCAGGTACTGTCCCAAACTGGAGACGTTGTCTGGGATACAAAGGCAGT
CCAGCCCCCTTGGACTTGGTGGCCCACACTTAAACCTGATGTATGTGCCTTGGCG
GCTAGTCTTGAGTCCTGGGATATCCCGGGAACCGATGTCTCGTCCTCTAAACGAG
TCAGACCTCCGGACTCAGACTATACTGCCGCTTATAAGCAAATCACCTGGGGAGC
CATAGGGTGCAGCTACCCTCGGGCTAGGACTAGAATGGCAAGCTCTACCTTCTAC
GTATGTCCCCGGGATGGCCGGACCCTTTCAGAAGCTAGAAGGTGCGGGGGGCTA
GAATCCCTATACTGTAAAGAATGGGATTGTGAGACCACGGGGACCGGTTATTGG
CTATCTAAATCCTCAAAAGACCTCATAACTGTAAAATGGGACCAAAATAGCGAA
TGGACTCAAAAATTTCAACAGTGTCACCAGACCGGCTGGTGTAACCCCCTTAAAA
TAGATTTCACAGACAAAGGAAAATTATCCAAGGACTGGATAACGGGAAAAACCT
GGGGATTAAGATTCTATGTGTCTGGACATCCAGGCGTACAGTTCACCATTCGCTT
AAAAATCACCAACATGCCAGCTGTGGCAGTAGGTCCTGACCTCGTCCTTGTGGAA
CAAGGACCTCCTAGAACGTCCCTCGCTCTCCCACCTCCTCTTCCCCCAAGGGAAG
CGCCACCGCCATCTCTCCCCGACTCTAACTCCACAGCCCTGGCGACTAGTGCACA
AACTCCCACGGTGAGAAAAACAATTGTTACCCTAAACACTCCGCCTCCCACCACA
GGCGACAGACTTTTTGATCTTGTGCAGGGGGCCTTCCTAACCTTAAATGCTACCA
ACCCAGGGGCCACTGAGTCTTGCTGGCTTTGTTTGGCCATGGGCCCCCCTTATTA
TGAAGCAATAGCCTCATCAGGAGAGGTCGCCTACTCCACCGACCTTGACCGGTG
CCGCTGGGGGACCCAAGGAAAGCTCACCCTCACTGAGGTCTCAGGACACGGGTT
GTGCATAGGAAAGGTGCCCTTTACCCATCAGCATCTCTGCAATCAGACCCTATCC
ATCAATTCCTCCGGAGACCATCAGTATCTGCTCCCCTCCAACCATAGCTGGTGGG
CTTGCAGCACTGGCCTCACCCCTTGCCTCTCCACCTCAGTTTTTAATCAGACTAGA
GATTTCTGTATCCAGGTCCAGCTGATTCCTCGCATCTATTACTATCCTGAAGAAGT
TTTGTTACAGGCCTATGACAATTCTCACCCCAGGACTAAAAGAGAGGCTGTCTCA
CTTACCCTAGCTGTTTTACTGGGGTTGGGAATCACGGCGGGAATAGGTACTGGTT
CAACTGCCTTAATTAAAGGACCTATAGACCTCCAGCAAGGCCTGACAAGCCTCC
AGATCGCCATAGATGCTGACCTCCGGGCCCTCCAAGACTCAGTCAGCAAGTTAG
AGGACTCACTGACTTCCCTGTCCGAGGTAGTGCTCCAAAATAGGAGAGGCCTTG
ACTTGCTGTTTCTAAAAGAAGGTGGCCTCTGTGCGGCCCTAAAGGAAGAGTGCTG
TTTTTACATAGACCACTCAGGTGCAGTACGGGACTCCATGAAAAAACTCAAAGA
AAAACTGGATAAAAGACAGTTAGAGCGCCAGAAAAGCCAAAACTGGTATGAAG
GATGGTTCAATAACTCCCCTTGGTTCACTACCCTGCTATCAACCATCGCTGGGCC
CCTATTACTCCTCCTTCTGTTGCTCATCCTCGGGCCATGCATCATCAATAAGTTAG
TTCAATTCATCAATGATAGGATAAGTGCATGT

FAST p14 DNA sequence

ATGGTATTGCTGCCTGGGTCCATGCTTCTCACCTCAAACCTGCACCACCTTCGGC
ACCAGATGAGTCCTGGGAGCTGGAAAAGACTGATCATCCTCTTAAGCTGCGTATT
CGGCGGCGGCGGGACGAGTCTGCAAAATAAGAACCCCCACCAGCCCATGACCCT
CACTTGGCAGGTACTGTCCCAAACTGGAGACGTTGTCTGGGATACAAAGGCAGT
CCAGCCCCCTTGGACTTGGTGGCCCACACTTAAACCTGATGTATGTGCCTTGGCG
GCTAGTCTTGAGTCCTGGGATATCCCGGGAACCGATGTCTCGTCCTCTAAACGAG
TCAGACCTCCGGACTCAGACTATACTGCCGCTTATAAGCAAATCACCTGGGGAGC
CATAGGGTGCAGCTACCCTCGGGCTAGGACTAGAATGGCAAGCTCTACCTTCTAC
GTATGTCCCCGGGATGGCCGGACCCTTTCAGAAGCTAGAAGGTGCGGGGGGCTA
GAATCCCTATACTGTAAAGAATGGGATTGTGAGACCACGGGGACCGGTTATTGG
CTATCTAAATCCTCAAAAGACCTCATAACTGTAAAATGGGACCAAAATAGCGAA
TGGACTCAAAAATTTCAACAGTGTCACCAGACCGGCTGGTGTAACCCCCTTAAAA
TAGATTTCACAGACAAAGGAAAATTATCCAAGGACTGGATAACGGGAAAAACCT
GGGGATTAAGATTCTATGTGTCTGGACATCCAGGCGTACAGTTCACCATTCGCTT
AAAAATCACCAACATGCCAGCTGTGGCAGTAGGTCCTGACCTCGTCCTTGTGGAA
CAAGGACCTCCTAGAACGTCCCTCGCTCTCCCACCTCCTCTTCCCCCAAGGGAAG
CGCCACCGCCATCTCTCCCCGACTCTAACTCCACAGCCCTGGCGACTAGTGCACA
AACTCCCACGGTGAGAAAAACAATTGTTACCCTAAACACTCCGCCTCCCACCACA
GGCGACAGACTTTTTGATCTTGTGCAGGGGGCCTTCCTAACCTTAAATGCTACCA
ACCCAGGGGCCACTGAGTCTTGCTGGCTTTGTTTGGCCATGGGCCCCCCTTATTA
TGAAGCAATAGCCTCATCAGGAGAGGTCGCCTACTCCACCGACCTTGACCGGTG
CCGCTGGGGGACCCAAGGAAAGCTCACCCTCACTGAGGTCTCAGGACACGGGTT
GTGCATAGGAAAGGTGCCCTTTACCCATCAGCATCTCTGCAATCAGACCCTATCC
ATCAATTCCTCCGGAGACCATCAGTATCTGCTCCCCTCCAACCATAGCTGGTGGG
CTTGCAGCACTGGCCTCACCCCTTGCCTCTCCACCTCAGTTTTTAATCAGACTAGA
GATTTCTGTATCCAGGTCCAGCTGATTCCTCGCATCTATTACTATCCTGAAGAAGT
TTTGTTACAGGCCTATGACAATTCTCACCCCAGGACTAAAAGAGAGGCTGTCTCA
CTTACCCTAGCTGTTTTACTGGGGTTGGGAATCACGGCGGGAATAGGTACTGGTT
CAACTGCCTTAATTAAAGGACCTATAGACCTCCAGCAAGGCCTGACAAGCCTCC
AGATCGCCATAGATGCTGACCTCCGGGCCCTCCAAGACTCAGTCAGCAAGTTAG
AGGACTCACTGACTTCCCTGTCCGAGGTAGTGCTCCAAAATAGGAGAGGCCTTG
ACTTGCTGTTTCTAAAAGAAGGTGGCCTCTGTGCGGCCCTAAAGGAAGAGTGCTG
TTTTTACATAGACCACTCAGGTGCAGTACGGGACTCCATGAAAAAACTCAAAGA
AAAACTGGATAAAAGACAGTTAGAGCGCCAGAAAAGCCAAAACTGGTATGAAG
GATGGTTCAATAACTCCCCTTGGTTCACTACCCTGCTATCAACCATCGCTGGGCC
CCTATTACTCCTCCTTCTGTTGCTCATCCTCGGGCCATGCATCATCAATAAGTTAG
TTCAATTCATCAATGATAGGATAAGTGCATGT

Anti-CD40 sequence

ACGACTCACTATAGGAGGAGGTACCCACCATGGATTGGACATGGAGAATTCTCT
TCCTGGTCGCCGCAGCCACTGGTGCACACAGTCAAGTCCAATTAGTCCAGAGCG
GTGCCGAAGTTAAAAAGCCTGGCGCCAGTGTTAAGGTTTCCTGTAAAGCCTCAG
GATATACGTTCACGGGGTACTATATGCATTGGGTCCGACAAGCCCCAGGTCAAG

GCTTAGAGTGGATGGGCTGGATTAACCCCGATTCAGGAGGCACTAACTATGCTC
AGAAATTCCAGGGGAGAGTCACCATGACTCGCGATACCTCTATTAGCACGGCTT
ATATGGAACTCAATAGGTTGCGCAGTGACGATACGGCAGTCTATTACTGTGCCAG
AGATCAGCCTCTCGGATATTGTACTAATGGCGTCTGCAGCTATTTTGATTATTGG
GGACAGGGTACCCTCGTGACAGTCAGCTCCGGAGGGGGTGGAAGTGGTGGCGGT
GGGTCCGGCGGAGGGGGCAGTGATATTCAAATGACACAAAGCCCTTCTTCAGTC
AGTGCTTCTGTTGGTGATAGGGTGACAATTACATGCCGGGCCAGCCAGGGTATAT
ACAGCTGGTTGGCCTGGTACCAACAGAAACCCGGTAAAGCTCCAAATCTGTTGA
TCTACACAGCCAGTACGCTTCAAAGTGGAGTTCCCAGCAGATTTAGTGGATCTGG
AAGTGGCACTGATTTTACACTCACCATTTCCAGTCTTCAGCCCGAGGACTTTGCC
ACATATTACTGTCAACAGGCTAATATATTCCCTCTGACCTTTGGAGGGGGTACAA
AAGTCGAAATTAAGCGCGGATCCGACTACAAAGACGACGACGATAAAAATGCTG
TGGGCCAGGACACGCAGGAGGTCATCGTGGTGCCACACTCCTTGCCCTTTAAGGT
GGTGGTGATCTCAGCCATCCTGGCCCTGGTGGTGCTCACCATCATCTCCCTTATC
ATCCTCATCATGCTTTGGCAGAAGAAGCCACGTCGGCGGAAGAGAGGCTCCGGC
GCTACCAACTTTTCTCTGCTGAAGCAAGCCGGAGATGTCGAGGAGAATCCCGGA
CCCATGGTATTGCTGCCT

Primers for anti-CD40 cloning

forward: ATGGTATTGCTGCCTGGG
reverse: CCTATAGTGAGTCGTATTAATTTCG